GEOLOGIC SETTING OF THE CENTRAL ALASKAN HOT SPRINGS BELT: IMPLICATIONS FOR GEOTHERMAL RESOURCE CAPACITY AND SUSTAINABLE ENERGY PRODUCTION

A

THESIS

Presented to the Faculty

of the University of Alaska Fairbanks

in Partial Fulfillment of the Requirements

for the Degree of

DOCTOR OF PHILOSOPHY

By

Amanda M. Kolker, B.A.

Fairbanks, Alaska

December 2008

Abstract

The Central Alaskan Hot Springs Belt (CAHSB) is a vast stretch of low-temperature hydrothermal systems that has the potential to be a geothermal energy resource for remote communities in Alaska. Little exploration has occurred in the CAHSB and the resource is poorly understood. A geothermal power plant was installed in 2006 at Chena Hot Springs (CHS), one of the 30-plus hot springs in the CAHSB. This, in addition to the multiple direct use projects at CHS, could serve as a model for geothermal development elsewhere in the CAHSB. This dissertation evaluates the geologic setting of the CAHSB and explores the implications for resource capacity and sustainable energy production. The local geology and geochemical characteristics of CHS are characterized, with a focus on identifying ultimate heat source responsible for the hot springs. A radiogenic heat source model is proposed and tested for the entire CAHSB, wherein the anomalously radioactive plutons that are associated with nearly every hot spring are providing the source of heat driving the geothermal activity. This model appears to be feasible mechanism for the observed heat transfer. This implies that CAHSB "reservoir" fluids are probably low-temperature. It also suggests that individual hydrothermal systems are small-scale and localized features, unlike the types of hydrothermal systems that are conventionally exploited for energy (i.e., those that derive their heat from magmatic or deep crustal sources, which have higher reservoir temperatures and larger spatial extent). In this context, the individual capacity of several CAHSB resources close to communities is assessed, and a preliminary evaluation of the sustainability of the power production

scheme at CHS is given. As another approach to the question of sustainability, this dissertation explores the ways in which external benefits of geothermal energy can influence the economics of a project. In sum, producing geothermal energy from CAHSB resources is somewhat risky at the present time, though it may be less risky than continued use of diesel fuel. The risks of geothermal development could be greatly reduced by rapid and immediate exploration efforts to collect much-needed data about CAHSB geothermal resources.

Table of Contents

Page

Page

Page

Page

Page

Page

List of Figures

Page

Page

List of Tables

Page

Page

List of Appendices

Page

Introduction

Problem statement

Geothermal energy has long been considered a viable resource in Alaska. It is better distributed and less environmentally costly than fossil fuels. However, geothermal resources in Alaska remain largely unexploited due to a combination of factors: cheap fossil fuel resources, high development risk, high capital costs of geothermal development, and scattered energy demand centers. Each of these barriers to development is weakening.

In 2007, energy production in rural Alaska is almost invariably produced by diesel generators. This is a serious problem economically, environmentally, and socio-politically. It is unsustainable over the long-term, especially as the costs of fossil resources continue to increase. Geothermal and other renewable energy supplies now make both economic and environmental sense, reducing and stabilizing energy costs, stimulating local economic development, reducing fuel spills, and decreasing pollution and emissions (Chen et al., 2007; Herzog et al., 2001). Over the past three years in particular, rising fuel costs coupled with recent technological advances have significantly reduced the risk of developing geothermal power plants in Alaska.

Substantial improvements in utilizing low-temperature geothermal fluids for electricity production have brought many of Alaska's lower-temperature resources to the front burner. The Central Alaska Hot Springs Belt (CAHSB) is a vast low temperature system, with many of its 30-plus known hot springs located in relatively close proximity to population centers. Chena Hot Springs, in the eastern part of the CAHSB, installed the

first geothermal power plant in Alaska in 2006. It is the lowest temperature geothermal resource ever tapped for power generation in the world. This has opened up many possibilities in utilizing Alaska's low-temperature resources, which were previously eliminated as potential sites for power generation.

This study evaluates the geologic setting of the poorly understood geothermal resource regime of the CAHSB, and investigates the implications for geothermal resource capacity and sustainable energy production for proximal communities.

Hydrothermal systems

Heat energy in earth's crust is transferred by convection (volcanic activity, hydrothermal systems) and conduction (heat stored in bedrock). Geothermal heat is usually exploited for energy via hydrothermal systems. In these types of systems, geothermal heat is transferred to groundwater, and then transported via convection to earth's surface. Geothermal heat can be from magma or from hot rocks deeper in the crust. Hence, hydrothermal systems have three components: (1) a heat source; (2) circulating groundwater; and (3) a 'plumbing system' of closely-spaced, sub-vertical fractures that enable groundwater to efficiently convect through or around the heat source. The heat source can be shallow (magma or shallow hot rock) or deep (crustal depths of 4 km or greater). Heat is primarily transferred via convection, though some conductive heat transfer can occur (Duffield and Sass, 2003). In high-temperature systems, almost all of the heat transfer is convective. However, the relative importance of convection vs. conduction is more complex for low-temperature systems (Rybach, 1981).

H_2O in hydrothermal systems occurs as fluid or vapor or both, depending on pressure and temperature conditions. Vapor dominated geothermal systems are created when surface waters penetrate into a high temperature region and flash to steam as they rise towards the surface and the pressure drops. The steam continues up to the surface and is discharged as fumaroles. More common, however, are fluid dominated systems. In these systems, meteoric water circulates through lower-temperature and/or higher pressure thermal anomalies and is not heated enough to turn to steam upon rising. These hot waters commonly contain high concentrations of total dissolved solids (TDS) due to the enhanced solubility of silicate minerals at elevated temperature (Nicholson, 1993).

The process of hydrothermal convection happens in 5 steps, which correspond to identifiable zones: (1) the recharge zone, where the major surface recharge of meteoric water occurs. Recharge can occur over a large area and the overall flow path may only allow seepage at low rates through a large volume of rock; (2) the inflow zone, that is, the path meteoric water takes to get to the geothermal reservoir; (3) the hydrothermal reservoir; (4) the outflow zone; that is, the path the geothermal water takes in the subsurface before it rises to the surface; and (5) the upflow zone or discharge end of the flow path, where hot water and/or steam is discharged at (or near) the surface. In contrast to the recharge and inflow zones, flow in the upflow zone must be of sufficient volume and rate to transport the heat upward without losing most of the heat by conduction to the surrounding rock. That is, the process of convection or advective heat transfer must overwhelm the process of conductive heat transfer in the upflow portion (Garg and Kassoy, 1981).

Producing geothermal energy from hydrothermal systems

Geothermal energy can be used for a range of applications, from indirect use (electric power generation) to direct use (heat applications). In this section of my thesis I will review current technologies used to extract power from geothermal energy. Three technologies are currently being used by geothermal power plants to generate electricity from hydrothermal fluids: (a) dry steam, (b) flash, and (c) binary cycle systems. In dry steam power plants, steam from the geothermal reservoir is tapped and routed directly through turbine/generator units to produce electricity. The Geysers in California is a 1,100 MWe-capacity power plant that utilizes this technology. Flash steam plants use water at temperatures greater than 182 °C that is delivered under high pressure to the surface. The water then flashes to steam, which is used to drive turbines. Most geothermal areas, however, contain water below 182 °C. Energy is extracted from these fluids via binary-cycle power plants, where geothermal fluid and a secondary ("binary") fluid with a boiling point lower than water pass through a heat exchanger. Heat from the geothermal fluid causes the secondary fluid to flash to vapor, which then drives the turbines. Before Chena Hot Springs installed their power plant, the minimum temperature of 80°C was required for a binary system (http://www.eere.energy.gov/geothermal/). In all cases, spent fluid is reinjected into the system to maintain reservoir integrity. Besides technological improvements, other factors affecting minimum resource temperature for use in a binary system include the available condensing temperature and the local cost of power generation.

"Direct use" is the oldest and most common use of geothermal heat. The many uses of geothermal heating known as 'direct-use' include any application that does not involve electricity generation. Geothermal heat is widely used for residential, industrial, commercial, and recreational uses. Some uses are: district heating systems, commercial greenhouses, aquaculture, food processing facilities, and recreational bathing. Spent fluids from electric plants can be also be used for direct use (Barbier 2002).

Sustainability and geothermal energy production

Sustainability is and must be a vague concept (Solow, 1991). Before sustainability can be defined, we must understand the context of its origins and intentions. The concept of sustainability has arisen from the context of environmental degradation and widespread recognition of resource limitation. This context challenges the continued legitimacy of unlimited resource exploitation as overriding principles or paradigms. Challenges of resource conservation, resource management, and adaptation to changing and declining resources have supplanted challenges such as exploitation efficiency and access to resources. The concept of sustainability aims to provide a new set of guiding principles, ones that would guide us away from presumably harmful behavior while equipping us to handle the challenges of this new context. The concept of sustainability, then, is vague due to the enormity of its intended scope, and because at the same time it must be somewhat achievable. Because the concept was deliberately inserted into the mainstream by those who wish to shape a new paradigm, it is constantly evolving.

Sustainability is defined many ways. A sustainable system can simply be defined as one that persists for a given amount of time (Costanza, 1995), but this quality can only be assessed in retrospect. Most popular definitions involve recognizing the need to preserve environmental quality while still meeting society's needs and/or quality of life. To practice sustainability, then, the first step is an assessment of present and future needs of society; the second step is assessing the ability of natural resources to provide those needs across some defined temporal scale.

In order to obtain sustainable production from an energy resource, that resource has to be renewable. In the context of geothermal energy, sustainable energy production ensures the renewability of the energy resource. Geothermal resource renewability is dependent on energy recharge rate. In sustainably produced geothermal systems, conditions are such that the action of extracting energy from the natural process does not influence the overall process of energy circulation (Stefansson, 2000). Production declines in geothermal fields, such as at Mutnovsky, Russia, the Geysers, California, and Larderello, Italy, have been attributed to unsustainable energy production (overproduction and/or improper re-injection).

The geothermal production at Chena Hot Springs (CHS) is a case study in the sustainability of small-scale geothermal production in the CAHSB. This study assesses the sustainability of energy production by asking the following questions: has the resource remained stable or has its temperatures and/or pressures changed since production began? How much energy has it produced since inception, and has the system fully displaced all diesel use for the community? What are the direct uses of geothermal

heat at CHS, and how much water and heat does that extract from the system? What are the environmental impacts of geothermal production?

Geothermal resources of Alaska

Alaska's active volcanism and tectonic setting suggests the presence of major geothermal resources. There are over 108 known hot springs in the state of Alaska (Motyka et al., 1983). Most exploratory geothermal work in Alaska occurred during the period 1970-1985, driven in large part by the energy crisis of the 1970's and funded primarily by the US Department of Energy. During this period, Alaska's Division of Geological and Geophysical Surveys (ADGGS) catalogued and sampled all known surface expressions of geothermal systems in the state. This work is summarized in the Geothermal resources of Alaska 1:2,500,000 scale map (Motyka et al., 1983). Preliminary exploration studies were conducted in Southeast Alaska, Western Alaska, and the Aleutian arc during this period. Geothermal drilling occurred at three sites: Makushin, Mt. Adagdak, and Pilgrim Hot Springs. Preliminary exploration studies were started for Interior Alaska but never completed. Many of the Aleutian resources close to population centers are protected by National Parks and Preserves, thereby closed to exploration and development.

There are four predominant geothermal resource regimes in the state of Alaska: 1) The Aleutian Volcanic Arc: 2) The Central Alaskan Hot Springs Belt (CAHSB); 3) The Wrangell Volcanoes; and 4) The Southeast Panhandle.

The Aleutian Volcanic Arc, which includes the Aleutian islands as well as the Alaska peninsula, is Alaska's most promising setting for geothermal energy. However, with some exceptions, most geothermal sites in the Aleutians are too remote to be economically viable. Volcanism in the Aleutian arc results from active subduction of the Pacific plate beneath the North American plate. The arc contains 89 Quaternary volcanoes, 44 of which have been historically active. Subduction-related volcanoes are good candidates for hosting geothermal systems due to the high silica concentration of arc magmas, which because of its high viscosity tends to accumulate in large shallow magma bodies. The Aleutian volcanic front is also associated with deep faults and fractures related to subduction. The combination of these two factors – shallow magma bodies and deep faulting – creates a regional setting conducive to the formation of hydrothermal systems. 56 geothermal systems with surface expressions have been identified; many more likely exist but remain unknown due to poor surface expression (Motyka et al., 1983). Evidence of active hydrothermal systems may lie in the volumes of intense shallow seismicity under Aleutian volcanoes (De Angelis and McNutt, 2005). Most exploratory work in the Aleutian volcanic chain has occurred at three sites: Mt. Adagdak, Makushin Volcano and Akutan Island. Makushin is considered a "Known Geothermal Resource" because temperatures close to 200 °C were encountered in exploratory drilling at depths of ~400 m (Motyka et al., 1993).

A diffuse belt of moderate-temperature geothermal activity runs east-west across central Alaska. I will refer to this phenomenon as the Central Alaska Hot Springs Belt (CAHSB). Thermal springs in the CAHSB have temperatures between 30 and 88 °C

(average ~55 °C) of alkali-chloride type waters. Most of the sites lie within zones of discontinuous permafrost, and most occur as elongate zones of springs and seeps. The CAHSB stretches from the Seward Peninsula to the Yukon Territory. The geologic setting of most CAHSB sites is poorly constrained. Due to lack of data, the heat source driving the geothermal activity in Interior Alaska has not been established. Geothermal activity may be from deep circulation on back-arc faults, radioactive decay of elements within nearby plutons, concealed magma bodies, or some combination of those factors. None of the Interior CAHSB hot springs show any relation to recent volcanism, and the accepted tectonic model for Interior Alaska is not consistent with significant recent magmatic activity (Wes Wallace, pers. comm.; Page and Plafker, 1995).

The Wrangell Volcanic Cluster is another potential geothermal resource in Alaska. Though less extensive than the Aleutians, the Wrangells represent another subduction-related active volcanic regime in Alaska but differ in many ways from Aleutian volcanoes. They are fed by higher-silica magmas, and are extremely large in size with a shield-like geomorphology. They are not associated with deep faulting; in fact, there is little to no evidence for structural control on the Wrangell volcanic cluster (Motyka et al., 1986). There are few thermal springs associated with the Wrangell volcanic complex, and only Mt. Wrangell itself has an active thermal area. The Eastern Copper River Basin (ECRB), close to the western extent of the Wrangell volcanoes, has been the subject of geothermal exploration because it contains mud volcanoes. These are unusual features associated with pressurized groundwater or hydrothermal aquifers. Detailed geochemical and geophysical studies supported the possibility of an intrusive

body underlying the ECRB; however, they give no unequivocal confirmation of a hydrothermal resource (Motyka et al., 1986).

Several hot springs sites are located along the southeast panhandle of Alaska. Most of the hot springs do not occur in close proximity to volcanic centers and are thought to be fault-related rather than volcanic (Motyka and Moorman, 1987; Motyka et al., 1983). Minor, isolated episodes of Quaternary volcanism occur near Mt. Edgecumbe and at small vents on the south end of Revillagigedo Island.

References

Barbier, E., 2002. Geothermal energy technology and current status: an overview. Renewable and Sustainable Energy Reviews, 6 (1-2): 3-65.

Chen, C., Wiser, R., and Bolinger, M., 2007. Weighing the Costs and Benefits of State Renewables Portfolio Standards: A Comparative Analysis of State-Level Policy Impact Projections. Lawrence Berkeley National Laboratory, Environmental Energy Technologies Division, Report No. LBNL-61580.

Costanza, R. 1997. Introduction to Ecological Economics. St. Lucie Press, Boca Raton, FL., 288 pp.

De Angelis, S., and McNutt, S.R., 2005. Degassing and hydrothermal activity at Mt. Spurr, Alaska during the summer of 2004 inferred from the complex frequencies of long-period events. Geophysical Research Letters, 32: L12312, doi:10.1029/2005GL022618, 4 pp.

Duffield, W. and Sass, J., 2003. Geothermal Energy – Clean Power from the Earth's Heat. USGS Circular 1249.

Garg, S.K. and Kassoy, D.R., 1981. Convective Heat and Mass Transfer in Hydrothermal Systems. In: L. Rybach and L. J. P. Muffler (Editors), Geothermal Systems: Principles and Case Histories. Wiley & Sons, New York, pp. 37-68.

Herzog, A. V., Lipman, T. E., Edwards, J. L., and Kammen, D. M., 2001. Renewable Energy: A Viable Choice. Environment, 43 (10): 17 pp.

Motyka, R.J., Moorman, M.A., and Liss, S.A., 1983. Geothermal resources of Alaska. Alaska Division of Geological and Geophysical Surveys (ADGGS) Miscellaneous Publication 8, 1 sheet, scale 1:2,500,000.

Motyka, R.J., Hawkins, D.B., Poreda, R.J., and Jeffries, A., 1986. Geochemistry, isotopic composition, and origin of fluids emanating from mud volcanoes in the Copper River Basin, Alaska. ADGGS Public Data File 86-34.

Motyka, R.J., and Moorman, M.A., 1987. Geothermal resources of southeast Alaska. ADGGS Professional Report 93, 1:1,000,000 map, 1 sheet.

Motyka, R.J., Liss, S.A., Nye, C.J., Moorman, M.A., 1993. Geothermal Resources of the Aleutian Arc. ADGGS Professional Report 114, 17p., 1:1,000,000.map, 4 sheets.

Nicholson, K., 1993. Geothermal Fluids: Chemistry and Exploration Techniques. Springer-Verlag, New York, 223 pp.

Page, R.A., and Plafker, G., 1995. Block rotation in east-central Alaska: A framework for evaluating earthquake potential? Geology, 23: 629-632.

Rybach, L., 1981. Geothermal Systems, Conductive Heat Flow, Geothermal Anomalies. In: L. Rybach and L. J. P. Muffler (Editors), Geothermal Systems: Principles and Case Histories. Wiley & Sons, New York, pp. 3-31.

Solow, 1991. Sustainability: An Economists' Perspective. In: Stavins, R.N. (Editor), Economics of the Environment: Selected Readings. 4th ed. New York: W.W. Norton, 2000, 659 pp.

Stefansson, V., 2000. The Renewability of Geothermal Energy. Proceedings: World Geothermal Congress, Kyushu, Japan, pp. 2671-2676.

CHAPTER 1:

Geologic Setting of Chena Hot Springs, Alaska: A Fault-controlled Geothermal System Hosted by an Anomalously Radioactive Pluton[1]

Abstract

Chena Hot Springs (CHS) is one of over 30 low- to moderate-temperature hot springs that occur in a diffuse belt of geothermal activity running east-west across central Alaska. The geologic mechanism driving the geothermal activity is unknown. The hot springs are located within the Chena pluton. $^{40}Ar/^{39}Ar$ step heat analyses provide evidence that the Chena pluton is a composite of three or more episodes of intrusive activity, spanning from Cretaceous to early Tertiary times. Older plutonic phases consist of granite, granodiorite, and tonalite. A highly evolved younger phase is enriched in U, Th, Rb, F, B and Li; it therefore appears to be of mid-plate origins similar to early Tertiary intrusions in interior Alaska. A propylitic alteration assemblage, widespread in the older plutonic rocks, is probably associated with the intrusion of the younger pluton in the early Tertiary. Geothermal fluids contain elevated concentrations of F, B, and Li, indicating fluid interaction with the Tertiary granite. Hence, though it is poorly exposed at the surface, Tertiary granite probably underlies much of the CHS area. Radioactive decay of K, U and Th within the Tertiary granite may be causing the heat anomaly responsible driving the geothermal activity at CHS. The source ("reservoir") fluids at CHS appear to be 120 °C or cooler, based on three separate pieces of evidence: (1) hydrothermal

[1] Submitted to the Journal of Volcanology and Geothermal Research.

alteration mineral assemblages in well rocks (heulandite, smectite, cryptocrystalline $Si0_2$ and sulfides); (2) SiO_2 and Na-K chemical geothermometry; (3) homogenization temperatures measured in fluid inclusions in quartz from well cuttings. Upwelling of geothermal fluids occurs along a NW-trending fault zone identified by synthesizing a variety of new geochemical, geophysical, and borehole data. In sum, the CHS geothermal system appears to be a low-temperature convective system driven by a high heat producing granite and structurally controlled by a NW-trending fault zone.

Keywords: geothermal, geochemistry, igneous petrology, $^{40}Ar/^{39}Ar$ geochronology

1.1. Introduction

Chena Hot Springs (CHS) is located approximately 60 miles (96 km) northeast of Fairbanks (Fig. 1.1). The surface temperature of the hot springs is 63° C. The community of Chena Hot Springs is semi-remote, accessed year round via a paved road but 33 miles (53 km) from the closest power grid. The springs were "discovered" by gold miners in 1905 and the area has since been run as a resort. Prior to 2006, the resort was powered by diesel generators and consumed over 200,000 gallons of diesel fuel per year. In 2006, the resort proprietors commissioned two 200kW Organic Rankine Cycle (ORC) geothermal power plants, for a total generating capacity of 400kW. The ORC power generation system in use at CHS uses inexpensive, mass produced air conditioning and refrigeration equipment, dramatically reducing the costs of installation. The system, designed by United Technologies Corporation, was originally designed to produce power off of waste heat from industrial applications. The CHS plant is the first geothermal power plant installed in the state of Alaska.

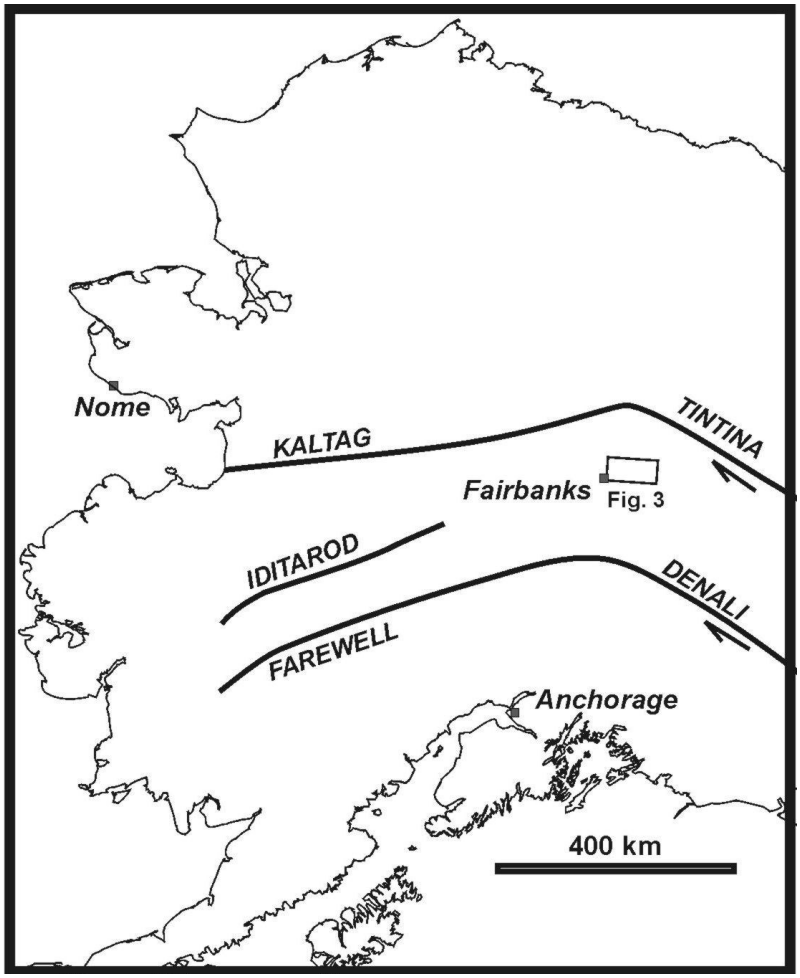

Figure 1.1. Location map of Chena Hot Springs, Alaska. Rectangle indicates study area. Black lines indicate major strike-slip faults, with arrows indicating direction of motion.

Chena Hot Springs is one of more than 30 geothermal occurrences (hot springs) in central Alaska that may have the potential to be similarly developed. Until recently, hot springs such as CHS were not considered suitable for power generation due to the moderate temperature of the surface expression (average 55° C). The heat source for these occurrences is unknown, but they are generally far from any Quaternary volcanic center and display no evidence for magmatic input (Miller et al., 1973). This precludes

any realistic estimates of the resource capacities of the hot springs areas (Miller et al., 1973; Economides et al., 1982).

Hot springs waters from CHS were first analyzed by the U.S. Department of Agriculture (Waring, 1917). Preliminary geological studies were conducted at CHS by Biggar (1973). This study included geologic mapping, petrography and age determinations of the plutonic and metamorphic rocks, a ground temperature survey, a geomagnetic survey, and geothermometry calculations from existing geochemical data. Further exploration work was carried out 1979-1980 to better characterize the geothermal resource at CHS and analyze its potential for power production (Wescott and Turner, 1981). This study included a ground and water conductivity survey, a resistivity survey, a seismic survey, heat flow studies, and helium and mercury soil sampling. The study concluded that the site was unsuitable for power generation given the available technology. Between 1998 and 2005, five shallow (< 100 m) wells were drilled in the immediate hot springs area.

This study was carried out between 2005 and 2007 as part of a D.O.E.-funded Geothermal Resource Evaluation and Definitions program (GRED III) study of the CHS geothermal resource. The GRED III project was designed to assess the resource for power generation, specifically to determine whether the CHS resource has the capacity to sustainably generate enough power to justify the costs of a transmission line to Fairbanks. Our evaluation of CHS may provide a model for other similar low to moderate temperature geothermal occurrences elsewhere. Geologic investigations, thermal gradient drilling, fluid geochemistry, airborne and ground-based geophysics, hydrology, reservoir

engineering and remote sensing studies were all conducted as part of the GRED III study. Additionally, a series of shallow temperature gradient holes were drilled (to depths of up to 300m) to determine the relationship between the shallow geothermal system and the deeper geothermal reservoir. The focus of this study is geologic, geochemical, and petrologic investigations of surface and subsurface rocks from the immediate CHS area.

1.2. Regional Setting

A diffuse belt of geothermal activity runs from the Seward Peninsula to the Yukon Territory of Canada. There are more than 30 hot springs areas within this belt. Though the belt spans numerous different geologic provinces, hot springs are similar in temperature (between 30 and 88 °C) and composition (alkali-chloride type waters; Miller et al., 1973). Due to lack of data, the local geology of most hot springs sites is poorly constrained. While none of the Interior hot springs show any relation to recent volcanism, the extreme western part of Alaska may be an active rift zone, which implies high crustal heat flow and the possible presence of shallow magma (Turner and Swanson, 1981). Like at CHS, Most of the hot springs are located in or near granitic bodies. Several of the bodies are known to contain anomalously high concentrations of the radioactive elements U and Th (Miller and Bunker, 1975; Newberry, 2000). A linear geothermal gradient of 33 C/km was measured from a deep drill hole 55 km southwest of CHS (Biggar, 1973), suggesting relatively normal regional heat flow.

Interior Alaska is structurally bound between two major, active, strike-slip fault systems and contains numerous NE-trending zones of broadly distributed seismicity

(Ratchkovski & Hansen, 2002: Figs. 1.1 and 1.2). Due to the limited distribution of seismic stations, epicenters are not well located outside of the major road corridors. No single fault has been identified as the source of any seismic zones, but rather a network of NE-trending, high-angle faults with sinistral and normal displacements are known from detailed-scale mapping in selected areas (Newberry et al., 1996). Page and Plafker (1995) suggested a block-rotation model for Interior Alaska, wherein crustal blocks rotate clockwise as a result of dextral movement on the Denali and Tintina fault systems combined with sinistral movement on the NE-trending conjugate faults. Three major NNE-trending seismic zones have been identified. One of these zones is located immediately south of the CHS area (Fig. 1.2).

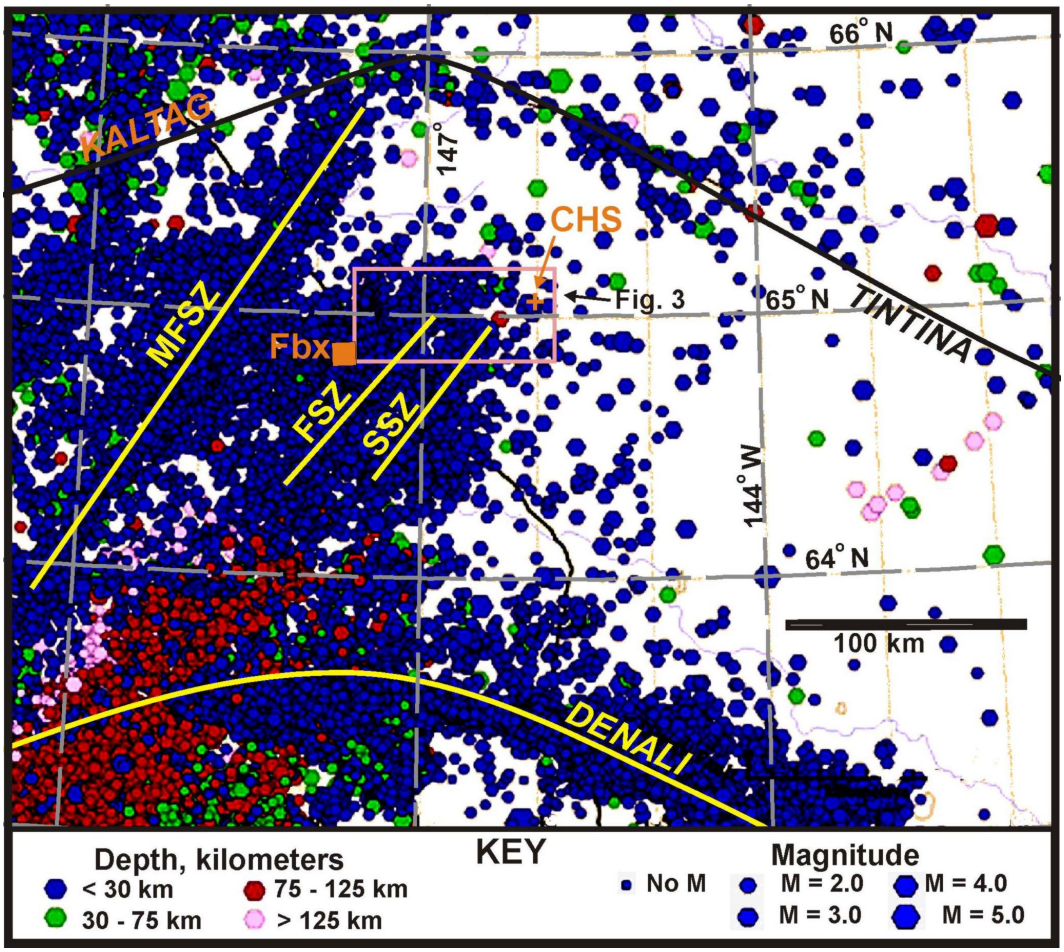

Figure 1.2. Seismicity map of Interior Alaska, modified from Ratchkovski and Hansen, 2002. Black line indicates the Tintina and Kaltag fault systems, yellow lines indicate the Denali fault and associated NE-trending seismic zones: Minto Flats seismic zone (MFSZ), Fairbanks seismic zone (FSZ), and the Salcha seismic zone (SSZ). Purple rectangle indicates Chena Hot Springs (CHS) study area.

Despite high regional seismicity, CHS lies in a relatively quiet zone compared to other locations in Interior Alaska. No faults of significance have been mapped in the immediate CHS region (Fig. 1.3), based on 1:250,000 reconnaissance scale mapping (Wilson et al., 1998). Biggar (1973) suggested two deformational events in the CHS region, recorded as southeast- and northwest-trending faults, fractures, and shear zones. That study postulated that the geothermal activity at CHS is related to circulation of

waters along the northwest-trending fractures and faults. Wescott and Turner (1981) also preliminarily concluded that the springs discharge from a southeast-trending fault or fault zone in the Chena pluton. However, neither study was able to give an exact location of the fault. Rock exposure is poor in the Spring Creek valley (the presumed fault zone).

CHS is located inside of a pluton with a surface exposure of 40 km^2 (Fig. 1.3).

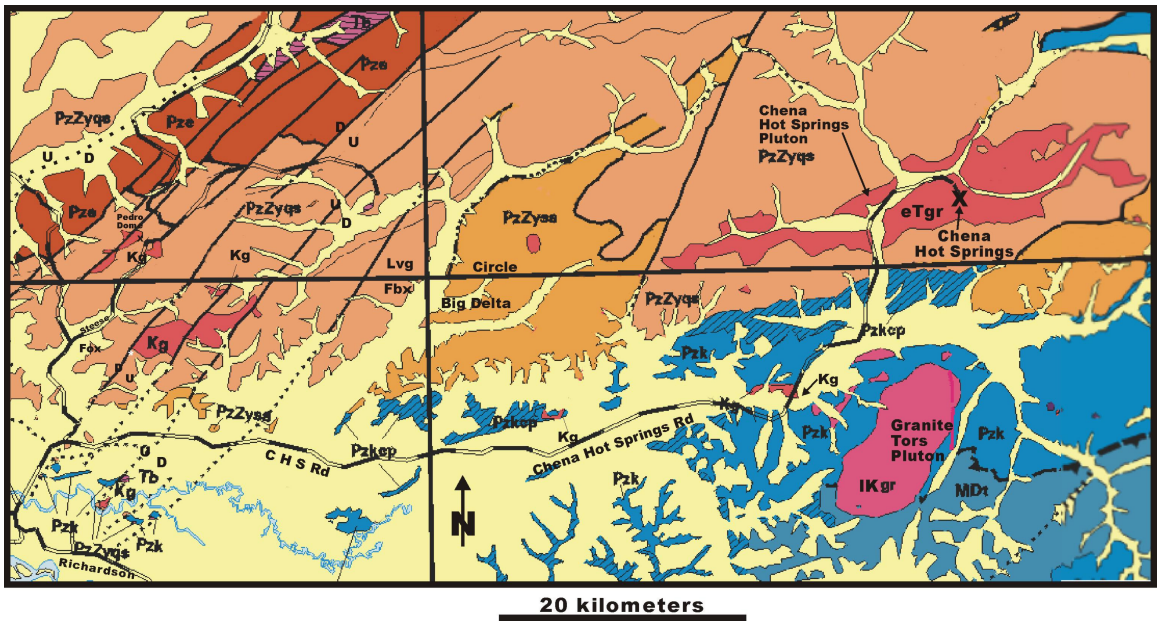

Figure 1.3. Generalized geologic map of CHS and vicinity; modified from Wilson et al. (1998). eTgr, Kgr = granitic bodies of mid-Cretaceous to early Tertiary age; Tb = early Tertiary basalt, Pz units = Paleozoic to late Precambrian metamorphic rocks; all others = quaternary sediments.

Biggar (1973) described the CHS pluton as a biotite-quartz monzonite with minor quartz diorite and granite variations. Three intrusive phases were recognized based on grain size and mineral content: 1) coarse-grained biotite-quartz monzonite; 2) fine-grained biotite-quartz monzonite; and 3) fine-grained hornblende-quartz monzonite. No crosscutting relationships were noted, but such relationships are difficult to recognize due to poor exposure. The coarse-grained biotite-quartz monzonite phase is the dominant rock

type in the CHS area, exhibiting hydrothermal alteration and mechanical deformation to varying degrees. This phase also displays abundant mafic inclusions. Biotite from the fine-grained biotite-quartz monzonite yielded an age of 58.2 ±1.7 my by the ^{40}K-^{40}Ar method. An age of 58.9 ±2.7 my was determined for sphene from the same rock by the fission-track method. Mafic and felsic dikes were mapped in the study area, with the dominant dike rock being a fine-grained dacite to rhyolite porphyry. The thickness of these dikes ranges from 2 cm to 2 m. The Chena pluton is surrounded by Paleozoic metamorphic rocks that have undergone multiple episodes of deformation and regional metamorphism and cooled to below biotite blocking temperatures by about 100 Ma (Newberry et al., 1996). The metamorphic rocks are pelitic schists and micaceous quartzites, with subordinate calc-magnesian and feldspathic schists. The thermal aureole around the Chena pluton was estimated to be 0.5 km wide (Biggar, 1973).

Thermal waters flow from alluvial fill underlain by the Chena pluton. CHS is effluent at ten springs, with a combined flow of 850 L/min and maximum temperature of 63 C. The surface thermal anomaly at CHS is elongated in an east-southeast direction along the south side of Spring Creek valley, parallel to a dominant joint set in the Chena pluton (Fig. 1.4). Prior to modification by man, most of the hot springs issued from the channel of Spring Creek. Since the 1970's, however, the creek has been diverted by a ditch, and the larger hot springs now flow into man-made pools. The length of the thermally anomalous zone is approximately 300 m and 100 m wide. Based on quartz and Na-K geothermometry after White (1970), CHS reservoir temperatures were estimated at 130 to 145 C (Biggar, 1973).

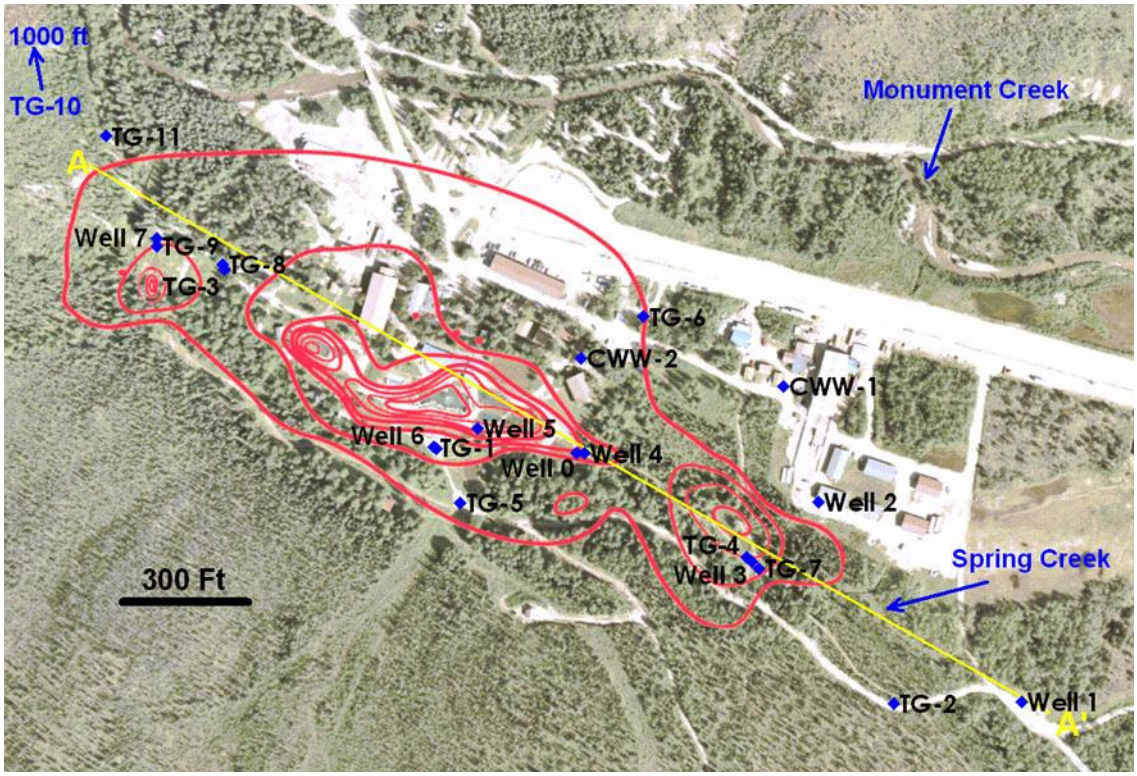

Figure 1.4. Geothermal anomaly and geothermal well locations, superimposed on an areal photograph of the Chena Hot Springs area. Geothermal anomaly expressed as isothermal contours, identified by temperature survey conducted by Wescott & Turner, 1981 Modified from Erkan et al, 2007.

Between 1917 and 2005 water samples were collected from 9 geothermal wells (either from flowing wells or bailed out of static wells). Analyses were conducted in 2005 by Thermochem, Inc. and Desert Research Institute; all others were conducted by the U.S. Geological Survey (USGS; Table 1.1.).

Table 1.1. CHS geothermal fluid chemistry and geothermometers.

SAMPLE	Temp (°C)	pH	TDS	Na	K	Ca	Mg	Li	HCO3	SO4	F
Well 1 T B	<6.7	6.6	97.4	6.9	1.0	17.9	2.0	0.0	645.0	3.8	0.7
Well 2 T B	-	9.2	289.0	96.2	3.0	3.2	0.1	0.3	129.0	33.5	15.1
Well 2 DRI B	-	8.2	-	90.2	2.7	3.5	0.1	0.3	102.0	39.2	17.0
Well 3 T B	<56.1	9.0	282.0	86.8	2.3	2.7	0.0	0.3	122.0	40.4	15.6
TG7 DRI F	68.9	9.0	-	78.2	1.9	2.5	0.0	0.2	98.3	29.2	13.5
Well 0 T F	-	8.8	330.0	102.0	2.7	3.1	0.2	0.3	116.0	64.5	17.7
Well 4 T F	63.9	9.0	330.0	103.0	2.9	2.9	0.0	0.3	122.0	58.5	18.6
Well 5 T F	73.9	9.0	339.0	105.0	2.9	2.6	0.0	0.3	122.0	61.3	18.8
TG1 T F	73.9	8.9	341.0	109.0	3.0	2.5	0.0	0.3	123.0	59.8	18.5
TG8 DRI F	77.8	9.0	-	108.0	2.8	2.6	0.0	0.3	92.0	62.9	19.3
spring2 F	-	-	-	107.0	2.8	2.8	0.0	0.3	131.0	65.7	21.0
spring6 F	-	-	-	112.0	2.7	3.6	0.0	0.3	132.0	66.7	20.0
spring11 F	-	-	-	120.0	2.8	3.6	0.1	0.3	125.0	71.0	20.5
1972 USGS	56.7	9.1	-	110.0	3.3	1.3	0.1	0.3	114.7	68.0	18.6
1917 USGS	65.0		388.0	94.0	2.3	1.2			118.0	78.0	-
1912 USGS	51.0		363.0	107.0	tr	2.9	0.2	tr	116.0	89.0	-

Chemistry data from Holdmann et al. (2006). Units in ppm. T = Analysis by Thermochem, Inc.; DRI = Analyses by Desert Research Institute. B = bailed sample from static geothermal well; F = flowing well sample. USGS = analysis of spring water by the U.S. Geological Survey. TDS = total dissolved solids.

1.3. Materials and Methods

Field mapping focused on the plutonic rocks and major structures in the general CHS area. Geologic mapping, conducted intermittently between 2005 and 2007, included collection of several hundred hand samples. Cuttings were collected from 10 to 20-foot intervals for 11 geothermal wells drilled 2005-2006; and from unlocated intervals for wells W1-W5, which were drilled prior to 2005. Well locations are shown in Fig.1.4. All cuttings were examined with hand lens and binocular microscope. 40 samples were thin sectioned and examined petrographically in transmitted and reflected light.

Fugro, Inc. conducted a 937 km^2 airborne geophysical survey via DIGHEM (Digital Helicopter ElectroMagnetics); specifications described by Pritchard (2005), including apparent gamma radiometry (measured counts per second divided into Total,

U, Th, and K components), magnetics (total field, nT and vertical derivative), and electromagnetic (900, 7, 200 and 56,000 Hz coplanar data). These maps served as a base for our geologic maps.

Six granitic samples were crushed, washed, sieved, and hand picked for datable mineral phases in preparation for $^{40}Ar/^{39}Ar$ dating. The samples were irradiated in an uranium enriched research reactor for 20 megawatt-hours, and subsequently mounted individually, then heated step-wise *in vacuo*, using a 6-watt argon-ion laser, and analyzed in a VG-3600 mass spectrometer. Layer (2000) describes details of the procedures. Measurement of argon isotopes followed procedures outlined in McDougall and Harrison (1999). All ages are quoted to the $\pm$ 1 sigma level and calculated using the constants of Steiger and Jaeger (1977).

More than 100 hand samples were analyzed for major and trace elements using X-ray fluorescence spectroscopy (XRF). Samples were pulverized and prepared as standard pressed-powder pellets, followed by analysis with a Panalytical 4 kW Wavelength Dispersive Axios Spectrometer in the UAF Advanced Instrumentation Laboratory. Instrument conditions included count times of 10 seconds for major elements and 40-100 seconds for trace elements, accelerating voltage of 32 kV for light elements and 60 kV for heavy elements, and beam current of 66 mA for light elements and 125 mA for heavy elements. Calibrations were done on Natural International Rock Standards. Precision, based on replicate analyses, is <1% of the amount present. Accuracy is approximately $\pm$5% for concentrations >20 ppm and $\pm$1-2% for concentrations >0.5%.

Electron Microprobe analyses were carried out on 8 polished thin sections using a Cameca SX-50 electron microprobe with four wavelength dispersive spectrometers (WDS) and an Edax energy dispersive spectrometer (EDS). We targeted accessory allanite grains, which are known to host U and Th. Analytical conditions included 20kV voltage, 10nA beam current, a 1 m beam diameter, and a ZAF correction procedure.

Hydrothermal alteration mineralogical data was collected using standard optical petrography and X-ray diffraction (XRD). For XRD, X-ray reflections were collected using a Rigaku X-ray Diffractometer in the 2-theta range from 2 to 60 degrees. For clay separates, samples prepared and analyzed following the methods described in Moore and Reynolds (1989).

Geothermometry calculations were performed following the methods described by Fournier (1981) and modifications given in Truesdell (1984).

Fluid inclusion homogenization temperature measurements were performed on samples of vein quartz and epidote from geothermal wells TG1 and TG2. Analyzes were performed at the Energy & Geoscience Institute, in Salt Lake City, UT. Doubly polished crystals were heated using a Linkham THSMG 600 heating and freezing stage calibrated with synthetic fluid inclusions. The precision of the measurements is approximately $\pm 0.1^{\circ}C$ at $0.0^{\circ}C$ and $\pm 0.3^{\circ}C$ at $374^{\circ}C$.

1.4. Results

1.4.1. $^{40}Ar/^{39}Ar$ dating of the Chena pluton

$^{40}Ar/^{39}Ar$ step heat analyses of six samples yielded complex results. All six of the samples contained biotite (Table 1.2), three had biotite and hornblende (Table 1.3). All of the biotites show similar behavior, with flat plateaus for more than 80% release and less than 4% argon loss due to reset. The oldest 4 plateau ages have an average age of 60.4 ± 0.1 Ma. The three hornblendes show similar, but unexpected results. The spectra consist of three distinct parts. The first, constituting the first ~10% of gas release is characterized by down-stepping ages, low Ca/K ratios and low Cl/K ratios. Isochron ages from these fractions are consistent between samples and with the biotite ages at ~60 Ma. These fractions are most likely due to biotite contamination in the hornblende. The second part of the release is characterized by Ca/K ratios that increase to a consistent value of ~5 and high Cl/K ratios (characteristics of hornblende). Ages for these fractions are the oldest, with weighted mean ages of up to 81 Ma. The last ~20% of gas release is characterized by lower Cl/K ratios, variable Ca/K ratios and younger ages, probably reflecting other inclusion mineral phases in the hornblende that do not retain argon as well as the hornblende. The original age of the hornblende is almost completely lost, but it must be older than 80 Ma. Given hornblende's closure temperature of ~550 C and given that the hornblende was not completely reset but the biotite was, the rocks probably last re-equilibrated at temperatures of 400 – 500 C at ~60 Ma.

Table 1.2. $^{40}Ar/^{39}Ar$ results for biotite grains.

Sample	Integrated Age (Ma)	Plateau Age (Ma)
008	58.8 ± 0.3	60.2 ± 0.4
030A	60.2 ± 0.3	60.4 ± 0.3
049	60.0 ± 0.3	60.6 ± 0.3
A6	58.9 ± 0.2	60.4 ± 0.2
D3	58.6 ± 0.2	59.0 ± 0.3
E6	59.3 ± 0.2	59.4 ± 0.2

Table 1.3. $^{40}Ar/^{39}Ar$ results for hornblende grains.

Sample	Integrated Age (Ma)	Low Temp. Isochron age (Ma)	High Temp. Weighted Age (Ma)
030A	80.7 ± 0.3	60.8 ± 2.3	81.0 ± 0.7
049	74.0 ± 0.3	58.0 ± 1.1	76.7 ± 0.4
E6	78.2 ± 0.3	59.2 ± 1.4	80.3 ± 0.5

1.4.2. Rock types and igneous petrology of the Chena pluton

1.4.2.1. Plutonic rocks

The dominant rock type in the 4 km^2 immediate CHS area is coarse-grained monzogranite. However, intermediate composition plutonic bodies, mafic dikes, and metamorphic xenoliths (1-100m^2) also occur within the area. The monzogranite is typically coarse-grained, porphyritic (quartz, feldspar and biotite phenocrysts up to 2 cm^2 in a 1-5 mm groundmass) but is locally fine-grained and equigranular. Biotite is the only mafic mineral observed in the monzogranite, with trace amounts of apatite, sphene, allanite, zircon, rutile, and small amounts of primary oxides. The granodiorite is invariably fine-grained and sub-equigranular (grain sizes 1-5mm). Hornblende is typically present, along with the minerals seen in the monzogranite. Allanite occurs as a

primary accessory mineral in all of these rock types, but is particularly abundant in the hornblende-bearing rocks. Monzogranites often display graphic/myrmekitic intergrowths of quartz and feldspar.

Texturally and mineralogically distinct granites occur in the eastern and southern margins of the pluton. They are highly evolved (in that they contain nearly no mafic minerals, high Rb and low Sr concentrations) and variably occur in close proximity to quartz-feldspar±tourmaline pegmatites. They are equigranular and contain muscovite and minor garnet. These are true granites that are compositionally distinct from monzogranite and granodiorite. Moreover, they do not display the propylitic alteration that is common in the rocks described above.

A third type of granite occurs only in the northern margin of the pluton. This granite is strongly peraluminous (muscovite-bearing, but lacking garnet), medium-grained, and weakly foliated. It contains disseminated and vein tourmaline in the vicinity of fine-grained, equigranular granite dikes that cut across the foliation.

To better quantify the character of the igneous rocks, major and trace element analyses were obtained by XRF. An accepted means of converting a chemical analysis of a plutonic rock into an IUGS name is the R1-R2 method of De la Roche et al. (1980). The major element data confirm the variety of and general rock types identified in the field (Fig. 1.5). The bulk of the samples appear to represent of a uni-modal suite ranging from diorite to granite, with no obvious chemical discontinuities between rock types. In contrast, the tourmaline-garnet-muscovite-bearing granite from the pluton margins and

the mafic dikes are chemically inconsistent. These appear to represent two or three different suites.

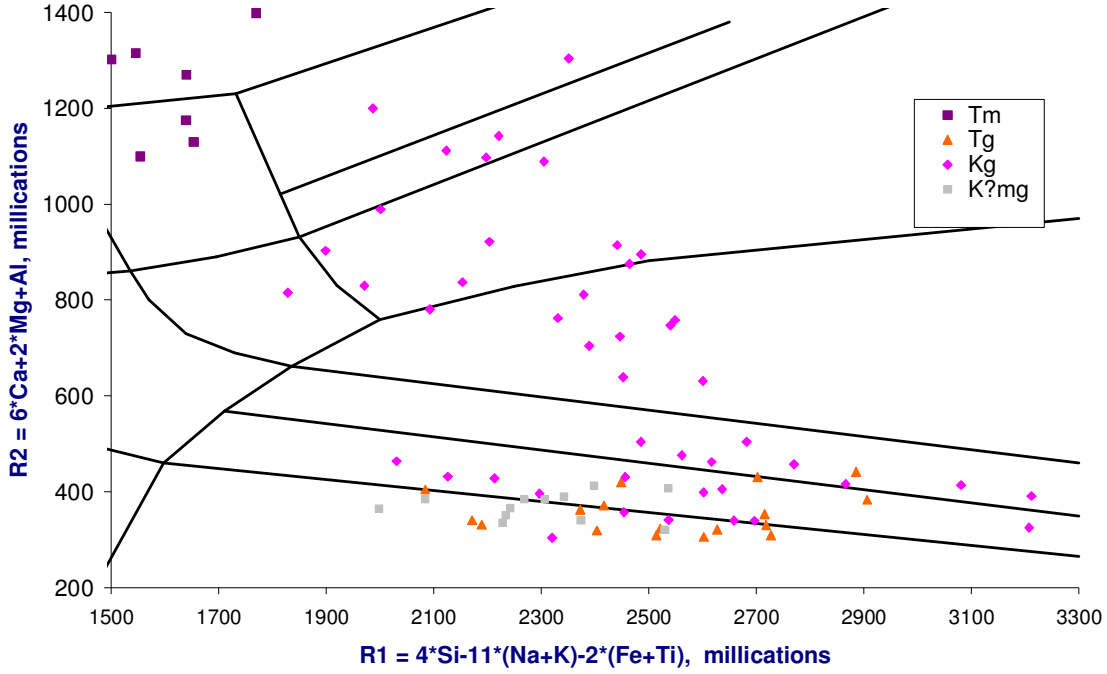

Figure 1.5. Rock types in the Chena pluton by major-element composition, after De la Roche et al. (1980). Tm = mafic dikes of likely early Tertiary age; Tg = granitic rocks of likely early Tertiary age; Kg = granitic rocks of Cretaceous age or older; K?mg = metamorphosed granitic rocks of likely Cretaceous age or older.

Pearce at al (1984) distinguish between plutonic rocks of within-plate, collisional, and volcanic arc origins based on the relative concentrations of Rb, Nb and Y. In the geologic provinces that constitute Interior Alaska, early Tertiary granites invariably display 'within-plate' characteristics, while mid-Cretaceous granitoids show 'volcanic arc' characteristics, and older granitiods (Early Cretaceous) have compositions characteristic of syn-collisional origins (Newberry, 2000). Trace element compositions of CHS rocks display all three characteristics (Fig. 1.6).

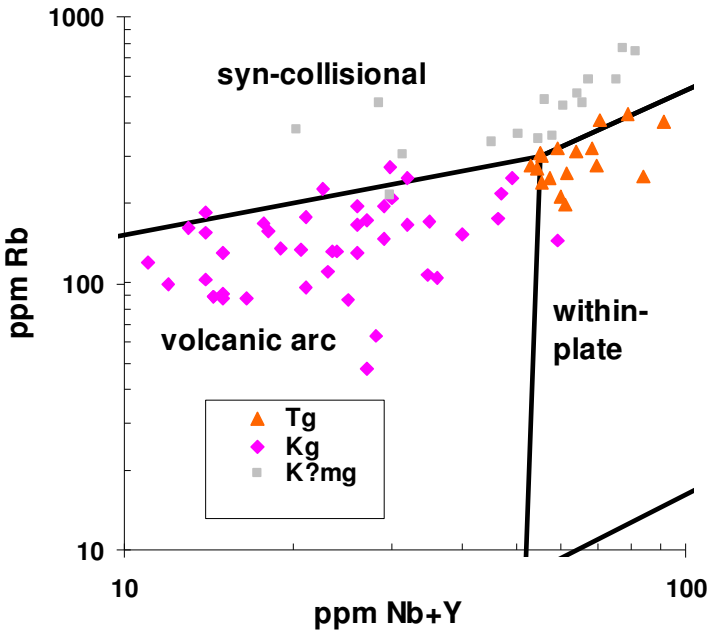

Figure 1.6. Granitoid discriminant diagram for rocks from the Chena pluton, after Pearce et al. (1984). Tg = granitic rocks of likely early Tertiary age; Kg = granitic rocks of Cretaceous age or older; K?mg = metamorphosed granitic rocks of likely Cretaceous age or older.

The U and Th concentrations in suspected early Tertiary granites have anomalously high U and Th concentrations (Fig. 1.7), as well as F (up to 0.3%), Sn (to 75 ppm), and Cs (to 150 ppm; see Appendix 1.A for supplementary data).

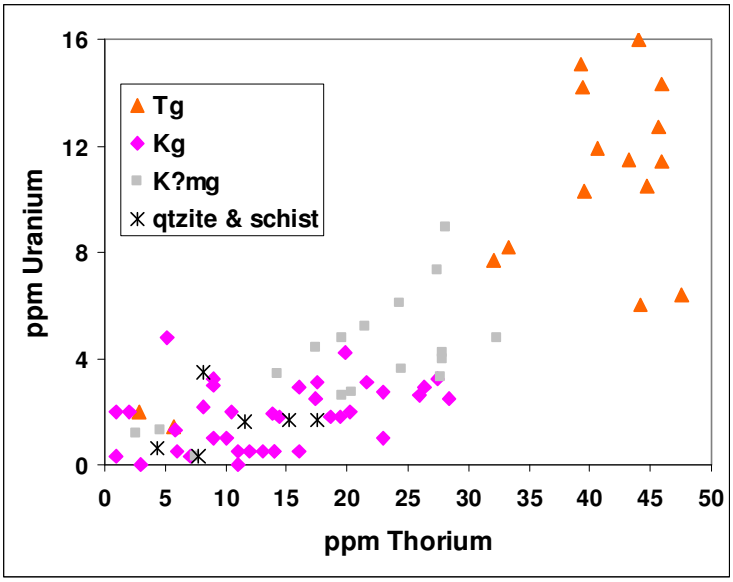

Figure 1.7. Uranium and Thorium concentrations in rocks from Chena pluton. Tg = granitic rocks of likely early Tertiary age; Kg = granitic rocks of Cretaceous age or older; K?mg = metamorphosed granitic rocks of likely Cretaceous age or older; qtzite&schist = Paleozoic quartzites and schists.

Th also occurs in Cretaceous rocks, but only as secondary alteration in primary allanite grains. Secondary U and Th occur as thorite ($(Th,U)SiO_4$) and bastnasite ($(Th,REE)(CO_3)F$) in association with pyrite, based on back-scattered electron images and energy dispersive spectrometry.

1.4.2.2. Propylitic alteration

The first group of plutonic rocks at CHS (the monzogranite - granodiorite suite that occurs in the immediate hot springs area) have been variably affected by propylitic alteration. Epidote and high-Fe (dark green) chlorite occur as disseminated replacements of primary minerals. Biotite is partially or fully replaced by chlorite; hornblende by chlorite $\pm$ epidote; and plagioclase by sericite $\pm$ clinozoisite. Epidote and high-Fe chlorite

also occur in microfractures and veins, where they are frequently associated with quartz, feldspar, ±pyrite. Epidote-containing veins typically fill low-angle fractures. Epidote-chlorite veins are often observed in sheared and microbrecciated rocks, but euhedral epidote is common in fractures where shearing has not occurred. Secondary albite, while rare, can be seen in some mineralized veins, especially if the rock has undergone intense microbrecciation. Whether alteration occurs as disseminated replacements or as fracture fill appears to be related to the grain size of the pluton (occurring primarily as veins in fine-grained rocks; and primarily as disseminated replacements in coarse-grained rocks). Psuedomorphic replacement of biotite by muscovite was observed in some samples. Secondary Th-silicates (thorite) and Th-carbonates (bastnasite) occur as alteration products in primary allanite grains.

1.4.2.3. Low-temperature alteration

Low-temperature hydrothermal alteration minerals, identified by XRD, occur as precipitates and fracture fill on well cuttings. These include smectite, heulandite (a Ca-Na-K zeolite), euhedral pyrite, low-Fe chlorite, and rare calcite.

Cross-cutting relationships of the observed minerals are given in Table 1.4. Based on these observations, minerals are grouped into three assemblages, each representing a separate alteration episode. These assemblages are: “magmatic,” related to syn-intrusive processes; “propylitic,” related to widespread hydrothermal fluid circulation sometime post-instrusion but significantly prior to the present time; and “late,” resulting from low-temperature hydrothermal fluid circulation related to present-day hydrothermal activity.

Table 1.4. Alteration mineral assemblages observed in CHS plutonic rocks.

Mineral	Method	Relative timing based on cross-cutting relationships *Early*----------→ *Late*	Alteration episode
Albite	Pet.	– –	Magmatic
Muscovite	Pet.	– –	Magmatic
Epidote	Pet.	– – –	Propylitic
High Fe chlorite	Pet.	– – –	Propylitic
Thorite	Probe	– – –	Propylitic
Bastnasite	Probe	– – –	Propylitic
Pyrite	Pet.	– – – –	Late
Chalcedony	XRD	– – – –	Late
Fluorite	Pet.	– – – –	Late
Calcite	Pet.	– – – –	Late
Mixed-layer chl.-smectite	XRD	– – –	Late
Low Fe chlorite	XRD	– – –	Late
Smectite	XRD	– – –	Late
Heulandite	XRD	– – –	Late

Methods: Pet. = petrographic; XRD = X-ray diffractometry; Probe = Electron Microprobe (energy dispersive spectrometry).

1.4.2.4. Lithologies encountered in geothermal boreholes

Geothermal boreholes were drilled almost entirely within the thermal anomaly at CHS (Fig. 1.4). Lithologies encountered in boreholes were mostly plutonic rock of variable composition and texture, ranging from fine-grained granodiorite and quartz diorite to coarse-grained granite. Alluvium was encountered only within the top 2-15 m of the boreholes and consists of undifferentiated stream gravels, alluvium, and colluvium. While the rock encountered in boreholes is exclusively plutonic, the inability to clearly correlate plutonic lithologies, mineralogies, and veins between wells – even those only 10 feet apart – is striking. It is uncertain where the fault traces extend beneath the surface in this region, and at what dip angle.

Cuttings display both types of alteration described above, Samples from most wells contain chlorite, epidote, clays, and pyrite; however, many depth intervals contained unaltered rocks. Cuttings also display mineralized veins and evidence for shearing**.** Two microbreccia units were encountered in geothermal wells. The first breccia is a white-green, powdery breccia with a clay matrix and rare calcite. It occurs at the contact between alluvium and plutonic rocks, or in layers between mineralized veins. The thickness of these breccia intervals is difficult to determine as it occurs as coatings on alluvium or vein fragments. The second breccia, a cryptocrystalline $Si0_2$-cemented microbreccia, occurs with tiny (~0.1mm) disseminated pyrite crystals, pyrite veins, and fluorite mineralization. Breccia clasts consist of 0.1-1mm-sized crystal (quartz and feldspar) fragments, granite clasts, clasts of quartz-epidote veins, and rare clasts of re-annealed brecciated material. It is cemented by a cristobalite and/or chalcedony matrix (both polymorphs were identified by XRD). Granite clasts within SiO_2 breccias contain chloritized biotites, sericitized plagioclase, and heavily strained quartz grains with undulose extinction patterns and sheared edges. Sulfides occur as precipitates on surfaces and as disseminated grains within the matrix. The SiO_2 breccia occurs at present-day production zones of fluid as hot as ~80^o C. Many of the chalcedony cuttings from production zones displayed mineralized slickensides. These zones range in thickness from 1-2 cm to ~8 m. Cryptocrystalline SiO_2 also occurs as coatings on well cuttings.

1.4.3. Structure

A poorly exposed northwest-trending fault zone appears to underlie the major creek valleys in the CHS area (Fig. 1.8). This fault zone contains at least three distinct splays. The fault zone was identified by 1) Lithologic discontinuities across valleys; 2) Intense shearing and microbrecciation in well rocks within the fault zone; 3) Resistivity and lithologic patterns indentified from DIGHEM airborne geophysical surveys (Pritchard, 2005); 4) Slickensides on outcrop faces in the northern section of the northwest -trending fault zone.

A prominent fluid upflow zone connecting three geothermal wells (TG10, TG9, and TG8) correlates with the southernmost of the NW-trending fault splays. The dip of the fluid-filled fault is approximately 80 °NE. The northwest -trending fault zone is apparently truncated by a series of northeast-trending faults. The latter set of faults is consistent with regional patterns (see Fig. 1.3). These faults display left-lateral strike slip motion as well as vertical motion.

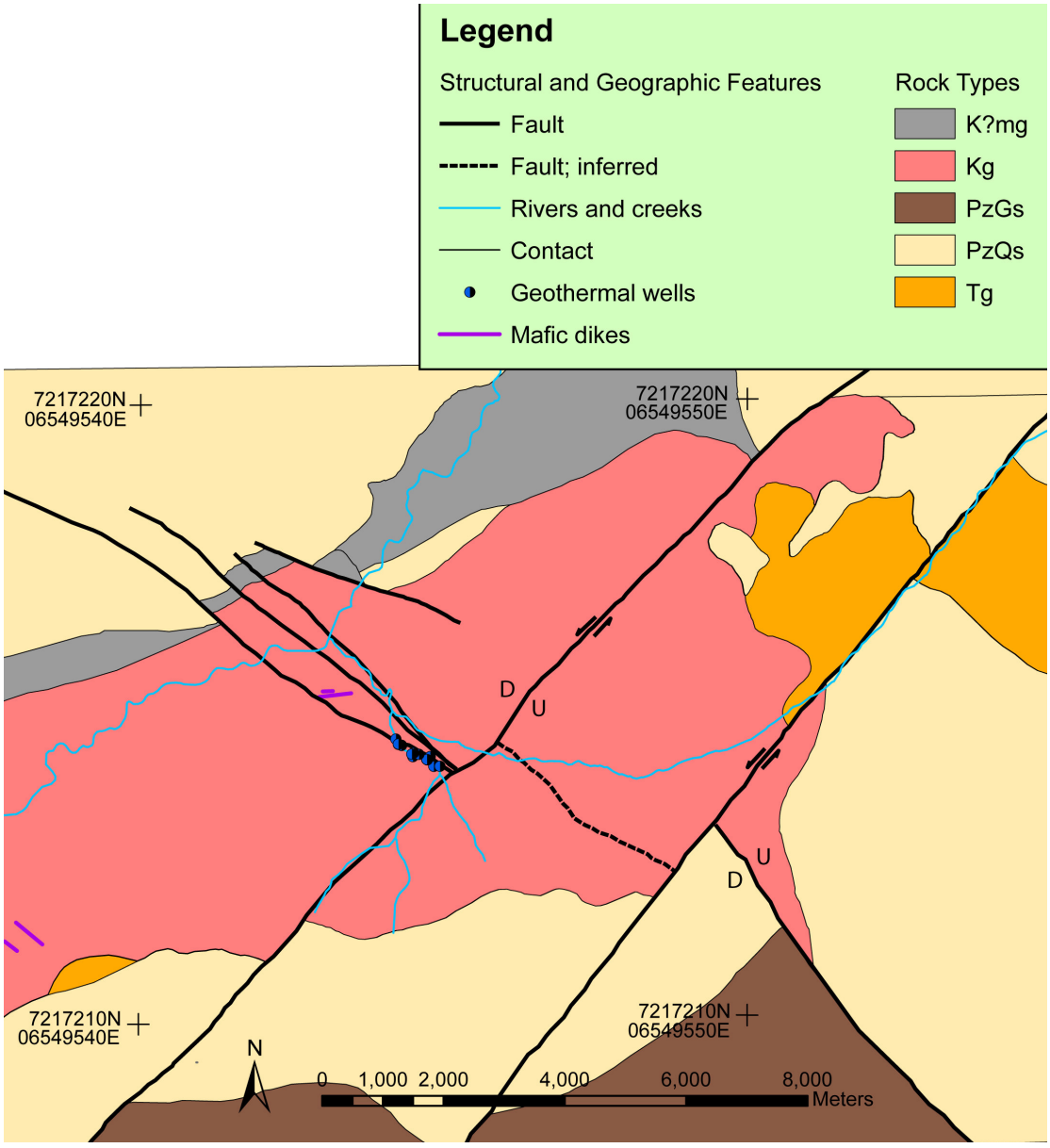

Figure. 1.8. Geologic map of CHS area based on airborne geophysical data (radiometrics, resistivity), ground traverses, rock microscopy and compositional data, and previous maps (Biggar, 1973; Wilson et al., 1998; see Fig. 1.3). K?mg = metagranite of likely Cretaceous age; Kg = undifferentiated Cretaceous granitoids; PzGs = Paleozoic graphitic schist; PzQs = Paleozoic quartzite schist; Tg = Tertiary granite (see text for detailed description of units).

Joints, veins, and dikes in the immediate CHS area display similar orientations. The dominant orientations are approximately 100° (ESE), 130° (NW), and to a lesser extent, 20° (NNE). Joints with 100° (ESE) azimuth have an average dip of 75-85 ° S. Joints with 130° (NW) azimuth have an average dip of 65-85 SW and ~45 ° NE (Fig. 1.9).

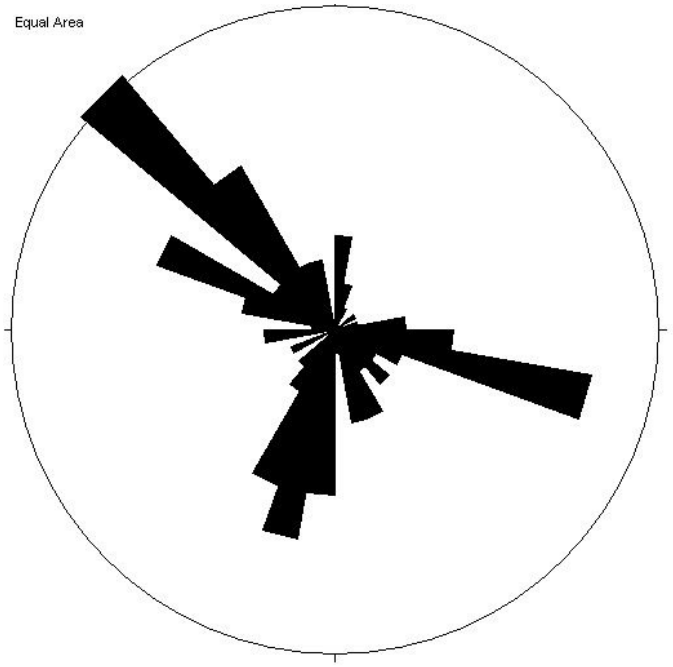

Figure 1.9. Rose diagram showing joint orientations near CHS. n=124. Figure created by Elliot Thorum.

1.4.4. Fluid inclusions, fluid chemistry, and chemical geothermometry

Quartz-hosted fluid inclusions from geothermal well TG1, at 60-66 feet, contain two distinct populations of fluid inclusions. Population 1 gives fluid homogenization temperatures of 295-303 °C and freezing point measurements of –0.9°C; whereas population 2 gives fluid homogenization temperatures of 72-120 °C and ice melting measurements of 0.0 °C.

All of the geothermal wells at CHS appear to be fairly uniform in chemistry (Table 1.1). CHS geothermal fluids are dilute alkali-chloride type waters, with a pH of 9 and total dissolved solids concentration (TDS) between 282 and 388 ppm. All of the geothermal fluids are notably enriched in B, Li, and F. Elements likely to be of deep thermal origin (Si, F, B, Li, and Cl) are spatially zoned around the highest-temperature wells.

Na-K, Na-Ca-K, and SiO_2 (quartz) geothermometers give reservoir temperatures of ~120-130 °C, but chalcedony geothermometers give temperatures of ~100 °C (Fig. 1.10). At temperatures of less than 190 °C, it is sometimes found that silica contents reflect equilibrium with chalcedony rather than with quartz (Henley et al., 1984). The relatively low temperature of the CAHSB hot springs, coupled with the observation of chalcedony in geothermal well cuttings from Chena Hot Springs, both imply that the chalcedony geothermometer is probably more appropriate for CAHSB systems. Additionally, the Na-K-Ca and Na-K geothermometers assume that the critical feldspar-mica assemblage is present in the reservoir. However, Ca is relatively absent in the felsic plutonic host rocks at CHS, and K is relatively high. Hence, chalcedony may be the only geothermometer that accurately predicts reservoir temperatures at CHS.

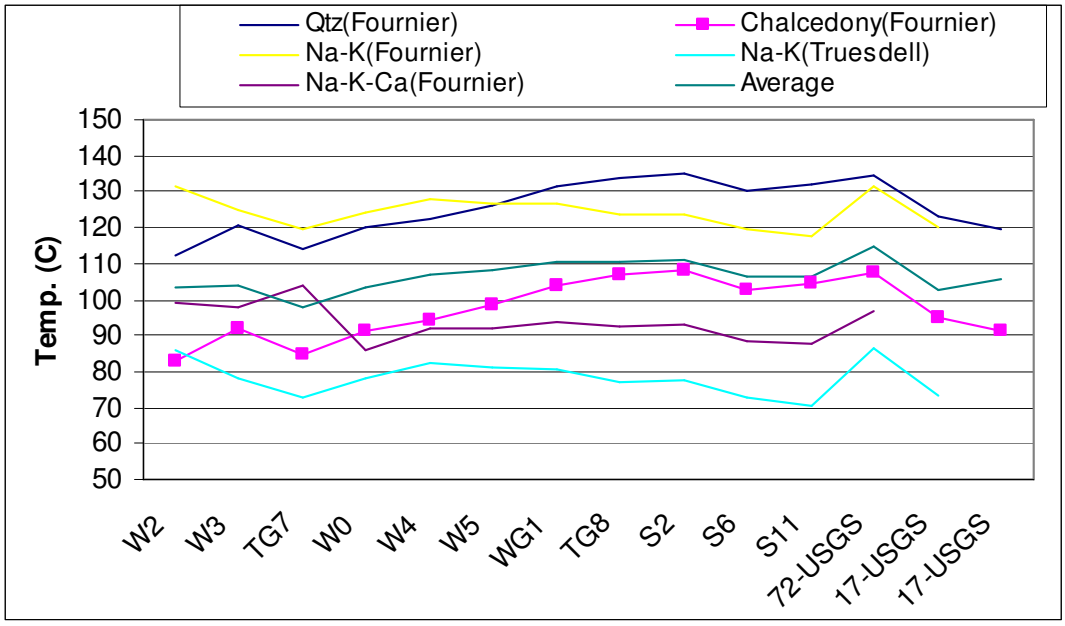

Figure 1.10. Chemical geothermometers applied to CHS fluids, after Fournier (1981) and Truesdell (1984). W and TG = well fluids; S, 71, 17 = spring fluids.

1.5. Discussion

1.5.1. Geology of the Chena pluton

Hornblende $^{40}Ar/^{39}Ar$ spectra suggest that the previously reported 60 Ma age for the exposed Chena plutonic rocks is not the true age, but rather represents a thermal reset age. The original age must be older than 81 Ma, and is most likely mid-Cretaceous (ca. 90 Ma). Moreover, these rocks are much more similar to other interior Alaska mid-Cretaceous than to early Tertiary plutons in terms of rock type, trace element geochemistry, and mineralogy (Newberry, 2000; Figs. 1.2-1.4). The likely cause for the thermal reset is an intrusion by a very large Tertiary igneous body. Since such a body is not obviously present at the surface, it is most likely under the exposed mid-Cretaceous

pluton. Further, the geothermal water at CHS is notably enriched in B, Li, and F, so rocks rich in these elements must be present below the surface. Enrichments in these elements are characteristic of the early Tertiary granites of Interior Alaska (Newberry, 2000). Hence, we propose that an early Tertiary granite similar to that seen at the northern and northeastern edge of the body sits below the hot springs. This body reset the K-Ar systematics in Cretaceous biotites to yield a Tertiary age. The depth of the Tertiary granite beneath the hot springs area is unknown, but must be deeper than ~300 m as it was not penetrated by any of the geothermal wells (all well rocks are weakly to strongly altered, characteristic of the older suites of plutonic rocks). The metamorphosed granite is compositionally and texturally similar to a weakly foliated granite body ~30 km east of Chena Hot Springs (Werdon et al., 2004). That granite was determined to be of Early Cretaceous age by $^{40}Ar/^{39}Ar$ techniques, so we suspect it is also Early Cretaceous. Hence, the Chena pluton appears to be a composite of three distinct phases: one emplaced in the Early Cretaceous, one in the mid-Cretaceous, and one in the early Tertiary.

An analogous situation occurs at Circle Hot Springs, where mid-Cretaceous and early Tertiary granitic rocks are present in a composite body. The first K-Ar date of ~70 Ma was determined from a biotite in the Cretaceous portion, ~5 km from the contact with Tertiary granite. Subsequent mapping showed compositionally different parts of the body. $^{40}Ar/^{39}Ar$ dating in the Cretaceous part yielded ages between 55 and 90 Ma, depending on proximity to Tertiary bodies (McCoy et al., 1997). The Tertiary rocks are also more enriched in U than the Cretaceous rocks (Fig. 1.11).

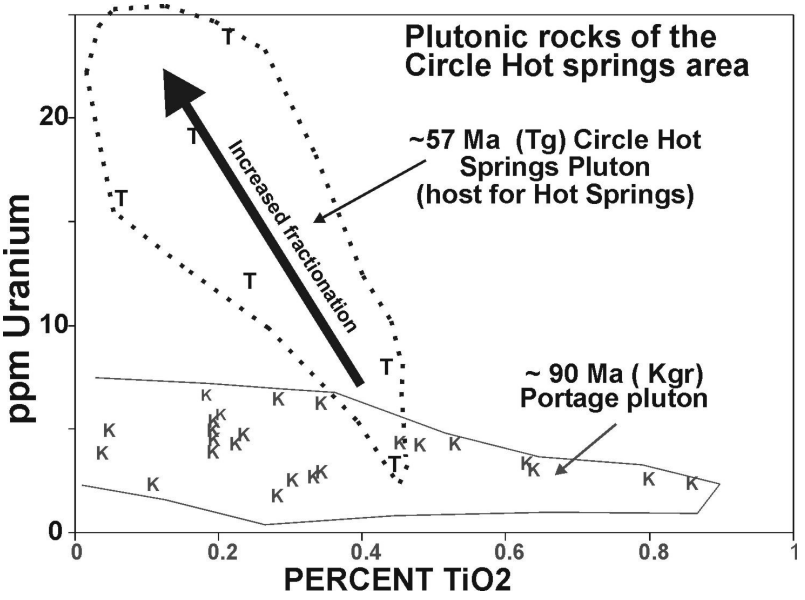

Figure 1.11. U concentrations in rocks from Circle Hot Springs, Alaska. Tertiary granites have significantly greater U concentrations (from Newberry et al., 2000).

1.5.2. Heat production calculation based on U and Th concentrations

Based on airborne radiometric data, U concentrations in well-exposed parts of the eastern edge of the Chena pluton are approximately 5 times and Th 2-3 times as in the central part of the pluton. These count rate differences are consistent with the XRF-determined values for U and Th in the main portions and the east margin of the Chena pluton. A method for calculating radiogenic heat production (A) from plutonic rocks is given by Rybach (1981):

$$A\ (\ W/m^3) = 10^{-5}\rho\ (9.52c_U + 2.56c_K + 3.48c_{Th} \qquad \textbf{[Eq. 1.1]}$$

where c is the concentration of the radioactive elements U and Th in ppm, and K in % and ρ is the rock density. In the Chena Hot Springs Tertiary granite, the average c_U = 12 ppm; the average c_K = 4.4%; and the average c_{Th} = 44 ppm. $\rho_{granite}$ = 2670 kg/m^3 (see

Appendix for data). Calculating the heat production from radioelement concentrations in the Tertiary pluton (after Rybach, 1981) yields an anomalously high heat production value (A) of 7.44 Wm^{-3}. Hence, radioactive decay of U, Th, and K within a mostly-concealed Tertiary pluton could be causing a local elevation of the geothermal gradient, producing a small heat anomaly at relatively shallow crustal levels.

1.5.3. Hydrothermal alteration and fluid-rock interactions

At least two distinct episodes of hydrothermal activity are evidenced by alteration assemblage patterns and fluid inclusion analyses. Within the well cuttings, the brecciated and re-annealed rocks contain clasts of epidote-chlorite-altered granite, indicating that propylitic alteration occurred before brecciation. Multiply brecciated and multiply re-annealed rocks show evidence of both propylitic and lower-temperature alteration, so some shearing and (or) brecciation activity must have continued after initiation of the lower-temperature alteration. These multiply brecciated and re-annealed rocks indicate either multiple episodes of faulting in the CHS area and/or rapid expansion accompanying repeated boiling of geothermal fluids causing brecciation and deposition of fine-grained silica. In the absence of any other evidence for boiling in the CHS system, it is more likely that these breccias reflect faulting activity.

The fluid inclusions show two populations, based on different episodes of alteration. Inclusion population 1, with homogenization temperatures of 295 -303 °C, correlates with widespread propylitic alteration (epidote, high-Fe chlorite, albite, local pyrite), stable at such temperatures. Such alteration is especially intense along mafic

dikes that have trace and major element compositions similar to early Tertiary mafic dikes in the western part of the Chena pluton . This observation, coupled with the lack of spatial correlation between propylitic alteration and present-day geothermal activity, suggest that this alteration episode is not associated with the present-day geothermal system. Consequently, the propylitic alteration is probably syn- or post-early Tertiary. If the bulk of plutonic rocks in the immediate CHS area are of mid-Cretaceous age, their unusually high degree of propylitic alteration could be due to hydrothermal circulation following both mid-Cretaceous emplacement and intrusion of early Tertiary bodies.

Different, younger, and lower-temperature alteration (minerals) was only observed in areas of present-day geothermal activity. Maximum stability temperatures for this assemblage depend on fluid composition, but they are compatible with temperatures of 80 – 120 °C given by fluid inclusion population 2. This hydrothermal alteration is associated with present-day geothermal fluids. Together with fluid geothermometry, these observations provide a strong set of evidence that the present-day hydrothermal reservoir is ~ 120 °C. Erkan et al. (2007) predicted that 120 °C waters should lie at about 500-1000 m depth in the upwelling zone, based on temperature gradient studies of existing wells and assumptions about conductive temperature-depth behavior.

Systematic variations in Si, F, B, Li, and Cl concentrations in well fluids indicate that these elements originate in deep thermal fluids and are diluted by mixing with near-surface groundwater. 15 samples analyzed by Southern Methodist University for stable isotopes, including waters from local creeks and snow, show that the CHS geothermal waters are within 0.5 per mil of the local meteoric water line (Holdmann et al., 2006).

The very small degree of isotopic difference between the hottest geothermal fluids and the local meteoric waters suggests argues that the geothermal fluids are derived from local meteoric waters under present day climatic conditions (Holdmann et al., 2006).

1.5.4. Relationship between hot springs and structural features

The upwelling at CHS appears to be controlled by a NW-trending subvertical fault zone. Linear conductivity zones identified by airborne resistivity maps; microbrecciation in well cuttings; slickensides on outcrops and well cuttings; and lithologic discontinuities across Monument Creek; all provide indirect evidence for a poorly exposed NW-trending fault zone. The inability to clearly correlate units between wells further supports the placement of faults bounding the immediate hot springs area, indicating that the plutonic rocks are likely offset in the zone between mapped faults. As is common for steeply-dipping faults, these postulated faults are present in major stream valleys and are not exposed at the surface. This fault zone may be exploiting a crustal weakness at a subsurface contact zone between the early Tertiary and the mid-Cretaceous pluton bodies. Based on temperature and pressure data, Erkan et al. (2007) argue that Chena Hot Springs is a "typical fault/fracture driven geothermal system." In the Erkan et al. model, deep thermal waters enter the shallow system at the west end of the geothermal anomaly, ~500 m west of the natural hot springs area. These waters flow east and mix with cold groundwater to form a shallow convective flow pattern in the main hot springs area. Soil helium levels are also highest in the western end of the thermal anomaly

(Wescott & Turner, 1981), corroborating the hypothesis that thermal fluids enter the system from the west.

1.6. Conclusions

The Chena pluton appears to be a composite body of three distinct intrusive phases. The youngest of the three bodies is highly evolved and appears to be anomalously radioactive due to elevated concentrations of K, U and Th. This body probably makes up the bulk of the subsurface rocks but is poorly exposed at the surface. Radioactive decay of elements within this body could partially explain the heat anomaly responsible for CHS and other hot springs in Central Alaska. This heat anomaly may be locally elevating the geothermal gradient, producing a small hydrothermal system at relatively shallow crustal levels. The geothermal fluids at CHS have circulated primarily within the anomalously radioactive pluton.

A section of a poorly exposed NW-trending fault zone appears to be the main upwelling zone for the hydrothermal fluids. Due to the chemical homogeneity of 'parent' geothermal fluids at CHS, they appear to originate from a single source. However, substantial fluid movement also occurs along fractures within the plutonic rock, as evidenced by mineralized veins and the orientation of the hot springs along a prominent joint set. Geothermal fluids enter the shallow subsurface at the west end of the geothermal anomaly, and undergo substantial mixing with cold groundwater as they flow eastward. The maximum temperature of the geothermal fluids beneath Chena Hot Springs appears to be ~120 °C. These reservoir fluids are of meteoric origin. Deep geophysical

studies and/or deep drilling in the upflow zone would help verify the source and the nature of the deep geothermal reservoir at CHS.

1.7. Acknowledgements

Thanks to Paul Layer and Jeff Drake for providing the $^{40}Ar/^{39}Ar$ analyses and for aiding in interpretation. This work was supported by the U.S. Department of Energy GRED III program under award DE-FC36-04GO14347; and by a graduate research fellowship from the Inland Northwest Research Alliance. The authors kindly thank Gwen Holdmann, Joe Moore, John Eichelberger, Dick Benoit, David Blackwell, Elliot Thorum, Louise Spann, Joe LaFleur, Wes Wallace, Bernie Karl, and Dan Brotherton for their feedback and contributions. Thanks to Lena Krutikov, Dave West, Bill Witte, and June Champlin for technical advice and support. Thanks also to Rusty Foraker, Kelly Hansen, Jim Altieri, Dayton Dove, and Hannah Clilverd for their assistance in the field.

1.8. References

Biggar, N., 1973. A Geological and Geophysical Study of Chena Hot Springs, Alaska, Master's Thesis, University of Alaska Fairbanks, Fairbanks, Alaska.

De la Roche, H., Leterrier, J., Grand Claude, P. and Marchal, M., 1980. A classification of volcanic and plutonic rocks using R1-R2 diagrams and major element analyses - its relationships with current nomenclature. Chemical Geology, 29: 183-210.

Economides, M.J., Ansari, J., Arce, G.N. and Reeder, J.W., 1982. Engineering and geological analyses of the geothermal energy potential of selected sites in the state of Alaska, Proceedings of the 8th Stanford Geothermal Reservoir Engineering Workshop, Stanford University, Stanford, CA, pp. 31-37.

Erkan, K., Holdmann, G., Blackwell., D. and Benoit, W., 2007. Thermal Characteristics of the Chena Hot Springs Alaska Geothermal System, Stanford 32nd Workshop on Geothermal Reservoir Engineering, Stanford University, California, pp. 117-124.

Fournier, R.O., 1981. Application of water geochemistry to geothermal exploration and reservoir engineering. In: L. Rybach and L. J. P Muffler (Editors), Geothermal Systems: Principles and Case Histories. Wiley & Sons, NY, pp. 3-31.

Henley, R.W., Truesdell, A.H. and Barton, P.B.J., 1984. Chemical Geothermometers for Geothermal Exploration. Reviews in Economic Geology, 1: 31-43.

Holdmann, G., Blackwell., D. and Benoit, W., 2006. Chena Hot Springs GRED III Project: Phase 1 Report. Unpublished report to USDOE. Chena Hot Springs, AK.

Layer, P.W., 2000. Argon-40/argon-39 age of the El'gygytgyn impact event, Chukotka, Russia. Meterotics and Planetary Science, 35: 591-599.

McCoy, D., Newberry, R. J., Layer, P., DiMarchi, J. J., Bakke, A., Masterman, S., Minehane, D.L. (Editor), 1997. Plutonic-related gold deposits of Interior Alaska. Economic Geology Monograph: Mineral deposits of Alaska., 9: 50 pp.

McDougall, I., & Harrison, T. M., 1999. Geochronology and Thermochronology by the 40Ar/39Ar method. Oxford University Press, NY, 269 pp.

Miller, T.P., Barnes, I. and Patton, W.W., 1973. Geologic Setting and Chemical Characteristics of Hot Springs in Central and Western Alaska. USGS Open-file Report No. 575.

Miller, T.P. and Bunker, C.M., 1975. U, Th, and K Analyses of Selected Plutonic Rocks from West-Central Alaska. ADGGS Open-file Report No. 75-216.

Moore, D.M. and Reynolds, R.C., 1989, X-ray diffraction and the identification and analysis of clay minerals, Oxford University Press, NY, 322 pp.

Newberry, R.J., Bundtzen, T. K., Clautice, K. H., Combellick, R. A., Douglas, T., Laird, G. M., Liss, S. A., Pinney, D. S., Reifenstuhl, R. R., and Solie, D. N., 1996. Preliminary geologic map of the Fairbanks mining district, Alaska. Alaska Division of Geological & Geophysical Surveys (ADGGS) Report No. 96-16, 1:63,360 map.

Newberry, R.J., 2000. Mineral deposits and Associated Mesozoic and Tertiary Igneous Rocks within the Interior Alaska and adjacent Yukon portions of the 'Tintina Gold Belt': A Progress Report. University of Alaska, Fairbanks, Fairbanks, AK.

Page, R.A., and Plafker, G., 1995. Block rotation in east-central Alaska: A framework for evaluating earthquake potential? Geology, 23: 629-632.

Pearce, J.A., Harris, N.B.W., and Tindle, A.G., 1984. Trace element discrimination diagrams for the tectonic interpretation of granitic rocks. Journal of Petrology, 25: 956-983.

Pritchard, R., 2005. DIGHEM Survey for Chena Hot Springs Resort, Big Delta Quads D-4 and D-5, Circle Quads A-4 and A-5.

Ratchkovski, N. and Hansen, R., 2002. New Constraints on Tectonics of Interior Alaska: Earthquake Locations, Source Mechanisms, and Stress Regime. Bulletin of the Seismological Society of America, 92 (3): 998-1014.

Rybach, L., 1981. Geothermal Systems, Conductive Heat Flow, Geothermal Anomalies. In: L. Rybach and L. J. P. Muffler (Editors), Geothermal Systems: Principles and Case Histories. Wiley & Sons, New York, pp. 3-31.

Steiger, R.H. and Jaeger, E., 1977. Subcommission on geochronology: Convention on the use of decay constants in geo and cosmochronology. Earth and Planetary Science Letters, 36 (4): 359-363.

Truesdell, 1984. Fluid-mineral equilibria in hydrothermal systems. In: Henley, R.W., Truesdell, A.H. and Barton, P.B.J., (eds.) 1984. Chemical Geothermometers for Geothermal Exploration. Reviews in Economic Geology, 1: 31-43.

Turner, D., L. and Swanson, S. E., 1981. Continental Rifting - A New Tectonic Model for the Central Seward Peninsula.

Waring, G. A. 1917. Mineral Springs of Alaska. USGS Water Supply Paper 418, 114 pp.

Werdon, M.B., Newberry, R.J., Athey, J.E., Szumigala, D.J., 2004, Bedrock geologic map of the Salcha River-Pogo area, Big Delta Quadrangle, Alaska. ADGGS Report No. 2004-1b, 1:63,360 map, 1 sheet.

Wescott, E., and Turner, D., 1981. A Geological and Geophysical Study of the Chena Hot Springs Geothermal Area, Alaska., University of Alaska Fairbanks, Geophysical Institute Report No. UAG-R-268.

Wilson, F.H., Dover, J. H., Bradley, D. C., Weber, F. R., Bundtzen, T. K., and Haeussler, P. J., 1998. Geologic Map of Central (Interior) Alaska. 1:63,360 map, 1 sheet.

Appendix 1.A: geochemical data from the Chena pluton

SAMPLE	SiO2	TiO2	Al2O3	Fe2O3	MnO	MgO	CaO	Na2O	K2O	P2O5	Total
Younger (early T?) equigranular granite											
056	76.4	0.03	13.6	0.7	0.08	0.08	0.33	3.6	5.1	0.01	100.0
CHS056D	75.0	0.03	14.0	0.8	0.07	0.06	0.41	3.4	5.1	0.02	98.9
057-CHS	77.3	0.05	12.7	0.9	0.05	0.05	0.54	3.6	4.8	0.01	100.0
CHS057D	74.0	0.05	15.0	0.9	0.05	0.08	0.61	4.1	4.7	0.01	99.5
058-CHS	73.6	0.05	15.6	0.8	0.09	0.10	0.20	4.3	5.0	0.01	99.8
CHS058D	73.0	0.05	16.0	1.0	0.09	0.11	0.20	4.1	5.2	0.02	99.8
061-CHS	73.8	0.13	14.4	1.3	0.09	0.18	0.75	3.4	5.4	0.03	99.5
CHS061D	74.0	0.13	15.0	1.4	0.10	0.17	1.10	3.3	5.3	0.03	100.5
06CHS058B	76.1	0.02	13.8	0.4	0.07	0.06	0.47	3.9	4.9	0.02	99.8
07NO41B	76.9	0.04	13.2	0.6	0.11	0.06	0.64	3.9	4.4	0.01	99.8
CHS062A	75.0	0.07	14.0	1.4	0.09	0.13	1.40	3.1	4.9	0.02	100.1
94rn05	75.0	0.10	13.1	1.3	0.06	0.22	1.08	2.9	4.6	0.02	99.0
94rn06	74.4	0.10	13.2	1.5	0.06	0.27	1.58	2.9	4.5	0.03	99.3
07RN644A	75.7	0.01	14.2	0.3	0.07	0.05	0.36	4.8	4.0	0.09	99.6
07RN637B	76.7	0.02	13.4	0.3	0.06	0.03	0.42	4.2	4.6	0.06	99.9
mg gr	76.1	0.03	14.3	0.5	0.03	0.22	0.58	4.3	3.6	0.15	99.7
Younger felsic dikes											
07RN184C	71.4	0.36	14.6	2.1	0.07	0.26	1.31	3.48	5.7	0.15	99.4
07AK75	72.1	0.37	14.4	2.4	0.06	0.24	1.03	3.39	5.4	0.13	99.6
Younger (early T) mafic dikes											
CHS-DIKE	52.7	2.7	13.3	13.2	0.17	4.7	5.9	2.7	2.7	0.83	99.0
05CH26B	52.7	2.8	13.4	11.8	0.14	4.2	5.9	2.9	3.1	0.94	97.8
05CH26A	52.3	2.9	12.8	12.5	0.17	4.4	6.6	3.1	2.2	0.92	97.9
03RN238A	52.3	3.1	15.3	12.0	0.17	3.8	7.3	3.3	1.6	1.02	99.9
07RN184B	53.0	2.6	15.0	11.0	0.18	3.7	7.7	4.1	1.4	1.0	99.7
056B	53.8	1.4	13.3	8.2	0.25	7.2	8.0	2.5	1.6	0.65	97.0
94rn6b	48.4	3.4	14.3	12.9	0.20	4.7	7.5	2.9	1.3	0.85	99.1
Mid-K(?) foliated granite											
065N	73.1	0.14	15.3	1.2	0.06	0.16	0.5	4.0	5.1	0.07	99.7
066	75.2	0.09	13.8	0.9	0.05	0.11	0.5	4.2	5.3	0.37	100.6
067A	73.2	0.14	14.7	0.9	0.05	0.12	0.5	3.3	6.3	0.09	99.4
067C	72.1	0.05	15.9	0.6	0.04	0.08	0.5	3.3	6.9	0.16	99.7
068R	74.0	0.08	12.7	0.6	0.05	0.09	1.2	2.9	7.6	0.81	100.2
65	75.9	0.02	14.5	0.5	0.07	0.01	0.4	6.2	2.3	0.27	
64	75.8	0.16	12.6	1.7	0.08	0.31	1.3	2.7	5.1	0.04	
07RN634A	74.3	0.09	14.9	1.0	0.04	0.10	0.4	3.9	5.1	0.07	99.9
07RN636B	76.2	0.03	13.7	0.5	0.01	0.04	0.5	4.1	4.7	0.05	99.8
07RN638A	72.5	0.22	15.7	2.0	0.06	0.22	0.8	3.4	4.5	0.11	99.5
07RN639A	72.8	0.18	15.5	1.6	0.06	0.18	0.7	3.8	5.0	0.08	99.8
07RN640A	72.5	0.22	15.5	1.5	0.04	0.20	0.7	3.6	5.4	0.10	99.7

SAMPLE	SiO2	TiO2	Al2O3	Fe2O3T	MnO	MgO	CaO	Na2O	K2O	P2O5	Total
07RN641A	72.8	0.15	15.6	1.4	0.04	0.14	0.7	3.6	5.1	0.10	99.7
07RN643A	73.0	0.20	15.0	1.6	0.04	0.19	1.0	3.4	5.2	0.08	99.7
CHS-A-4	56.8	1.2	18.0	7.9	0.14	2.2	6.9	3.2	2.1	0.6	99.0
05CH-P6?	57.1	1.6	16.7	8.0	0.11	3.1	7.7	2.0	2.4	0.6	99.3
05AKCH-044B	57.4	1.2	16.6	9.0	0.13	1.9	6.4	2.9	2.1	0.6	98.0
05CH30D1	58.0	0.7	17.0	6.8	0.14	2.7	6.0	2.7	3.0	0.4	97.5
05CH-E3	58.5	1.1	17.7	7.4	0.12	2.0	6.5	2.8	2.3	0.5	98.9
Mid-K granitic rocks--Diorite and Quartz Diorite											
05CH19D	61.3	0.90	17.8	6.4	0.12	1.5	6.2	3.0	2.4	0.48	100.0
05CHS27	62.8	0.56	17.5	4.1	0.09	0.9	4.8	4.0	3.5	0.38	98.6
05CHS23	63.1	0.58	16.7	3.5	0.06	1.6	3.9	4.4	3.0	0.26	97.1
05AKCH-42	63.6	0.68	15.5	5.3	0.08	1.0	4.0	3.2	4.1	0.42	97.9
fg 'grd'	63.6	0.84	16.3	5.4	0.10	1.4	5.0	3.6	2.8	0.43	99.4
FG tn	63.9	0.76	15.0	5.4	0.10	2.0	4.5	2.6	3.4	0.31	98.1
05CH23	64.0	0.62	18.0	4.2	0.06	1.3	3.9	3.7	3.1	0.20	99.1
05CH29B	64.5	0.61	17.8	3.4	0.05	0.9	3.9	3.2	3.4	0.24	98.0
05CH29	64.8	0.71	18.1	3.4	0.05	1.0	4.8	3.4	2.7	0.27	99.1
05CHS29	64.8	0.71	17.1	3.4	0.05	1.0	4.8	3.4	2.7	0.27	98.1
05CH27	65.0	0.56	17.4	4.0	0.08	0.9	4.0	4.0	4.1	0.38	100.4
Mid-K granitic rocks -- tonalite											
05CH31A	65.8	0.52	16.2	3.6	0.06	0.9	3.8	3.3	3.7	0.29	98.1
79aws89	66.3	0.53	16.2	4.2	0.05	1.3	3.4	3.0	3.4	0.28	98.6
05AKCH-19	66.8	0.28	14.4	2.8	0.05	0.5	1.8	3.1	3.8	0.14	93.8
05CH31B	67.0	0.53	15.3	3.3	0.06	0.8	3.9	3.3	3.2	0.30	97.7
05AKCH-6	67.1	0.10	13.4	1.0	0.02	0.2	0.6	2.7	5.5	0.05	90.7
CHS-D4	66.0	0.30	16.0	3.2	0.10	0.8	1.6	8.4	0.4	0.10	96.9
53	68.7	0.22	16.4	1.3	0.02	0.4	0.8	2.8	8.3	0.12	99.3
05AKCH-8	67.2	0.55	14.5	3.3	0.04	0.8	2.9	3.0	3.9	0.23	96.3
CHS-W-4M	67.8	0.76	15.7	3.2	0.06	1.1	0.9	3.8	4.8	0.38	98.6
CHS-A-6	68.3	0.73	15.4	3.3	0.05	1.0	3.5	3.1	4.0	0.27	99.7
05CHS28	68.5	0.40	16.3	2.1	0.05	0.6	3.3	3.5	4.0	0.16	98.8
CHS-W-5	68.9	0.57	15.7	2.8	0.08	0.9	2.7	3.4	3.8	0.30	99.2
CHS-E6	69.0	0.25	13.6	1.7	0.02	0.4	1.6	3.3	3.9	0.10	93.8
Mid-K granitic rocks -- granodiorite											
05AKCH-21	70.3	0.38	14.4	3.9	0.07	0.75	0.4	5.0	2.1	0.14	97.4
05AKCH-33	71.6	0.20	12.6	2.2	0.03	0.39	0.4	5.5	2.9	0.06	95.7
05CH4	72.0	0.17	14.7	1.3	0.03	0.22	1.2	3.6	6.0	0.07	99.3
07BM26	73.2	0.14	14.8	1.1	0.02	0.15	1.9	3.6	4.6	0.06	99.6
05CH14	73.5	0.23	14.0	1.8	0.05	0.40	1.6	2.4	5.9	0.03	99.9
05CH13B2	74.1	0.04	14.3	0.7	0.11	0.09	1.4	3.2	5.7	0.04	99.7
05CH13B	74.2	0.03	14.1	0.6	0.05	0.10	1.4	3.4	6.4	0.05	100.3
05CH18	74.2	0.15	14.8	0.9	0.01	0.19	1.7	3.6	4.5	0.04	100.1
CHS-W-1	74.7	0.20	14.2	1.4	0.01	0.20	0.5	3.3	4.8	0.07	99.3
05CH13	74.8	0.02	14.4	0.3	0.01	0.06	1.0	3.6	6.0	0.03	100.2

SAMPLE	SiO2	TiO2	Al2O3	Fe2O3T	MnO	MgO	CaO	Na2O	K2O	P2O5	Total
05CH-6	75.5	0.08	13.9	0.7	0.01	0.10	1.2	3.6	4.7	0.03	99.8
03RN239A	75.6	0.04	14.2	0.6	0.01	0.10	0.5	3.8	4.9	0.10	99.8
54	75.8	0.17	13.1	1.0	0.02	0.26	1.1	2.6	4.1	0.04	98.6
CHS-E1	76.5	0.19	12.4	0.8	0.01	0.23	1.5	2.6	4.8	0.06	99.0
50	76.8	0.04	13.5	0.4	0.01	0.07	0.8	2.6	4.1	0.04	98.3
05AKCH-44	77.9	0.15	13.6	1.6	0.02	0.17	1.3	3.2	4.4	0.03	102.4
53	78.2	0.09	12.3	0.6	0.01	0.17	0.7	2.1	5.4	0.03	99.7
CHS-A-4	56.8	1.2	18.0	7.9	0.14	2.2	6.9	3.2	2.1	0.6	99.7
05CH11	74.9	0.19	14.4	1.0	0.02	0.22	1.0	3.9	4.2	0.05	99.9
CHS-D1F	75.0	0.24	12.2	1.7	0.02	0.61	0.6	3.4	1.8	0.02	95.6

SAMPLE	Rb	Sr	Y	Nb	Th	U	Zr	Sn
Younger (early T?) equigranular granite								
056	279	75	53	16	40	10	69	3
CHS056D	314	85	51	13	43	12	64	4
057-CHS	302	130	30	25	48	6	37	5
CHS057D	277	114	29	24	44	6	43	3
058-CHS	322	116	43	16	45	11	66	4
CHS058D	310	107	40	15	46	13	57	2
061-CHS	259	132	42	20	41	12	99	6
CHS061D	248	130	39	18	39	14	64	4
06CHS058B	323	48	44	25	46	11	49	3
07NO41B	271	108	42	12	46	14	47	5
CHS062A	238	134	36	20	39	15	59	6
94rn05	211	137	32	28	44	16	70	
94rn06	199	176	34	27			76	
07RN644A	431	13	16	63	3	2	19	8
07RN637B	413	13	29	41	6	1	17	4
mg gr	403	5	48	43	48		37	29
Younger felsic dikes								
07RN184C	252	150	58	26	31	8	287	4
07AK75-CHS F DIKE	236	163	61	33	33	8	420	7
Younger (early T) mafic dikes								
CHS-DIKE	140	450	66	25	8		464	
05CH26B	174	445	65	24	6	<1	442	
05CH26A	142	456	69	27	7	<1	447	
03RN238A	54	440	70	27			375	
07RN184B	132	589	61	22			340	
056B	21	1591	33	15	<1	<1	257	<1
94rn6b	39	383	56	31			412	
Mid-K(?) foliated granite								
065N	466	77	30	31	20	3	121	
066	767	52	46	31	14	3	81	64
067A	585	65	35	32	32	5	152	33
067C	514	23	17	48	20	5	68	34
068R	740	62	45	37	28	9	163	
65	474	16	2	63	3	1	9	50
64	213	260	16	13	28	4	83	5
07RN634A	487	54	29	27	17	4	93	10
07RN636B	378	21	14	6	8	0	11	7
07RN638A	582	59	43	32	24	6	121	41
07RN639A	341	68	21	24	25	4	104	8
07RN640A	363	79	24	27	28	3	132	11
07RN641A	350	63	28	26	22	5	96	12
07RN643A	357	71	31	27	28	4	133	10

SAMPLE	Rb	Sr	Y	Nb	Th	U	Zr	Sn
Mid-K granitic rocks –Diorite and qtz diorite								
CHS-A-4	86	1337	27	30	21		309	
05CH-P6?	64	1236	20	8	3	<1	194	
05AKCH-044B	75	1349	29	32	14	2	401	2
05CH30D1	135	921	18	1	6	1	117	
05CH-E3	87	1416	23	2	11	<1	293	
Mid-K granitic rocks – tonalite								
05CH19D	97	1367	20	1	22	3	282	
05CHS27	132	959	19	6	9		226	1
05CHS23	88	890	12	4	12		181	<5
05AKCH-042	105	856	20	16	9	3	299	2
fg 'grd'	107	1430	18	17			223	
FG tn								
05CH23	88	985	11	4	12	1	181	
05CH29B-sm	120	937	10	1	16	1	221	
05CH29	89	1078	11	4	14	1	219	
05CHS29	89	1078	11	4	14		219	<5
05CH27	132	964	18	6	9	1	226	
Mid-K granitic rocks – granodiorite								
05CH31A	99	1040	11	1	13	1	218	
79aws89								
05AKCH-19	146	573	16	13	20	2	174	3
05CH31B	91	1013	14	1	14	1	198	
05AKCH-006	250	177	34	15	5	5	37	7
CHS-D4	22	393	8	7	16	2	137	5
53	322	507	19	13	24	2	177	14
05AKCH-008	131	696	12	14	28	3	213	2
CHS-W-4M	274	528	14	16	26	3	291	
CHS-A-6	145	676	40	19	21		317	
05CHS28	133	728	14	6	11		113	<5
CHS-W-5	176	892	25	21	19		206	
CHS-E6	157	327	10	8	18	3	158	2
05CH31A	99	1040	11	1	13	1	218	
79aws89								
Mid-K granitic rocks – granite								
05AKCH-021	48	242	9	18	27	3	171	5
05AKCH-033	111	294	11	12	10	2	122	4
05CH4	216	236	37	10	9	3	45	
07BM26	169	276	12	6	23	3	80	2
05CH14	161	416	11	2	23	1	48	
05CH13B2	196	256	20	9	1	2	32	
05CH13B	209	271	21	9	10	1	29	
05CH18	156	319	7	7	7	0	104	
CHS-W-1	194	432	18	8	12		95	

SAMPLE	Rb	Sr	Y	Nb	Th	U	Zr	Sn
05CH13	185	251	7	7	1	0	25	
05CH11	130	356	9	6	11	1	124	
CHS-D1F	104	296	8	6	6	1	164	1
05CH-6	173	164	15	12	2	2	41	
03RN239A	225	85	16	7	19	2	32	5
54	165	286	18	14	26	3	109	6
CHS-E1	167	361	15	11	19	2	130	15
50	171	68	16	19	17	3	27	7
05AKCH-044	179	339	13	8	8	2	108	5
053B	249	269	18	14	20	4	49	3

CHAPTER 2:

The Central Alaskan Hot Springs Belt: Radiogenic Hydrothermal Convection Systems Driven by High Heat Producing Granites[2]

Abstract

The low temperature geothermal resource of the Central Alaska Hot Springs Belt (CAHSB) is poorly understood, and is commonly attributed to deep circulation of meteoric water along faults and fractures. However, the tectonic setting, geologic features, or fluid chemical characteristics of the CAHSB are not consistent with other 'deep circulation' systems elsewhere in the world. This study proposes an alternative heat source model as the driver of geothermal activity in the CAHSB: radiogenic heating from high-heat-producing plutons. This model is supported by anomalously high U, Th and K concentrations in CAHSB plutons and helium isotope signatures of CAHSB fluids that indicate a purely crustal origin (no mantle input). Heat production calculations for CAHSB plutons verify the feasibility of this model; however, the hydrothermal convection systems appear to be relatively small-scale and temporally limited. While they are not the ultimate source of heat for CAHSB fluids, small-scale faults and fractures do provide the permeability pathways necessary for convecting fluids to circulate.

[2] Prepared for submission in Geothermics.

2.1. Introduction

Considerable interest exists in developing Alaska's geothermal renewable energy resources. The Alaska state legislature recently established a renewable energy grant fund, meant to encourage projects such as the geothermal development at Chena Hot Springs (CHS). In 2006, CHS installed the first geothermal power plant in Alaska, utilizing geothermal fluids at about 80 °C to produce about 400 kW of electric power. This has demonstrated the geothermal opportunities in Alaska's low-temperature resources, which were previously eliminated as potential sites for power generation. Additionally, the direct use projects showcased at Chena Hot Springs (district heating, year-round greenhouses, absorption refrigeration, and hydrogen production) have significantly raised the awareness regarding direct use of geothermal heat in Alaska.

CHS is one of over 30 known hot springs in the Central Alaska Hot Springs Belt (CAHSB). The CAHSB is a vast low temperature geothermal regime, and several springs are located relatively close to population centers (Fig. 2.1). The CAHSB geothermal resource is poorly understood, which has precluded realistic estimates of its energy production potential (Miller et al., 1973; Motyka et al., 1983). Hot springs in the CAHSB are unlike most Alaskan hot springs in that they are not related to an active volcanic center. Their origins are unknown. Previous workers have suggested that they are derived from deeply circulating groundwater along faults (e.g., Miller, 1994). This study attempts to identify the heat source driving geothermal activity in the CAHSB.

Geothermal systems have been classified in a variety of ways. Most authors distinguish between "convective" and "conductive/static" types (e.g., Rybach, 1981;

Nicholson, 1993). Static or conductive type systems are characterized by a thermal regime due to conduction alone, either in deep aquifers or sedimentary basins, and usually in a low permeability environment. Convective type systems are classified as "magmatic" (related to abnormal heat flow caused by young intrusives (<1 Ma, Cathles et al., 1997), "deep circulation" (resulting from deep circulation of meteoric water along subvertical fault/fracture zones in regions of high heat flow), and 'others'. Convective type hot springs systems also occur in areas of elevated natural radioactivity (e.g., Pocos de Caldas, Brazil; Ramsar, Iran; Orissa, India; and Paralana, Australia – see Gomes and Hamza, 2005; Ghiassi-Nejad et al., 2005; Brugger et al., 2005; Baranwal et al., 2006), and this type may constitute a variety of 'others'. However, few studies have identified and characterized active geothermal convection systems driven by a radiogenic heat source. This is partially because energy extraction from the low-enthalpy fluids associated with radiogenic heat sources has only recently become economic; it may also be that active radiogenic hydrothermal systems are quite rare in nature. Observations of fossil hydrothermal activity in high heat-producing granites (e.g., Durrance, 1985) suggest that such activity could be cyclic and relatively short-lived.

One source of confusion in distinguishing among these types is that *all* convective hydrothermal systems (magmatic, deep circulation, or radiogenic) require vertical permeability pathways of closely-spaced fractures and/or faults that enable groundwater to efficiently convect through or around the heat source. Hence all geothermal systems are essentially deeply circulating groundwaters, particularly as 'deep' is ambiguous. However, the typical 'deep circulation' geothermal systems are associated with active,

broad-scale (>100 km long surface expression) normal faults in extensional settings for which the heat source is related to an abnormal thermal gradient. This abnormal thermal gradient may, in turn, be generated by a deep mafic intrusion, leading to confusion with the 'magmatic' type.

To minimize confusion caused by these ambiguities, we refer to three types of geothermal systems in this work: radiogenic, volcanic/magmatic, and deep circulation. The predominant geological features of the different types of convective hydrothermal systems, as taken from the literature, are given in Table 2.1.

Table 2.1. Characteristics of geothermal systems derived from volcanic, deep-circulation, and radiogenic heat sources.

Type (reference)	**Tectonic Setting**	**Geologic Features**	**Surface expressions and reservoir temperatures**	**Examples**	**TDS (mg/L)**
Radiogenic (1)	Unspecified	High heat producing (HHP) granitoids + permeable conduits	Low (<90 °C) temperature hot springs, estimated reservoir T's 95-130 °C*	Paralana hot springs, Australia	Low (<5000)
Volcanic / Magmatic (2,3,4,5)	Volcanic settings (subduction zones, rift zones, hot spots)	Young (<1 ma) volcanic fields + fracture/fault permeability, typically associated with silicic volcanism	Fumaroles, boiling springs, geysers, and other high-temperature features, reservoir Ts up to 350°C	Lardarello, Italy	Medium to High (5,000-15,000)
Deep circulation (2,3,6)	Extensional basins, shear zones, and/or large-scale rift zones	*Active*, broad-scale normal faults (>100 km map trace), high regional heat flow (60-100 W/m^3)	Moderate- to high-temperature (90-150 °C) hot springs in topographic lows, reservoir Ts up to 260°C	Dixie Valley, Nevada, USA	High (>10,000)

Sources: (1) Brugger et al., 2005; (2) Rybach, 1981; (3) Nicholson, 1993 (4) Broggi et al., 2003; (5) Batini et al., 2003; (6) Wisian and Blackwell, 2004. *Predicted reservoir temperatures are from chemical geothermometry methods. TDS = total dissolved solids concentrations in geothermal fluids.

This study investigates the feasibility of a radiogenic heat source model for CAHSB geothermal systems. We test the radiogenic heat source model in the following ways: 1) By calculating the heat production from radioelement concentration in CAHSB plutons; 2) By measuring the $^{3}He/^{4}He$ ratio in fluids from Chena Hot Springs to determine the degree of mantle input; 3) By evaluating other CAHSB geological and chemical characteristics in the context of other magmatic, deep circulation, radiogenic geothermal systems.

2.2. Background and Previous Work

2.2.1 Hot springs in the CAHSB

The CAHSB stretches from the Seward Peninsula east toward Canada (Fig. 2.1). Thermal springs in the CAHSB all have alkali-chloride type waters at temperatures between 30 and 88 °C (Miller et al., 1973) (average ~55 °C). Due to their low temperature, little exploratory work has occurred at these hot springs apart from USGS and Alaska state-funded preliminary investigations in 1970-1985. Miller et al. (1973) conducted chemical and isotopic analyses on the CAHSB fluids and classified them into two groups. The bulk of the springs are low-TDS (< 1500 ppm), pH-neutral alkali-chloride type waters. However, most of the Seward Peninsula hot waters are either more saline (2500-4500 ppm) or alkaline (pH >9). Na-K-Ca and quartz geothermometers suggest subsurface temperatures in the general range of 80 °C to 150 °C (Miller et al., 1973).

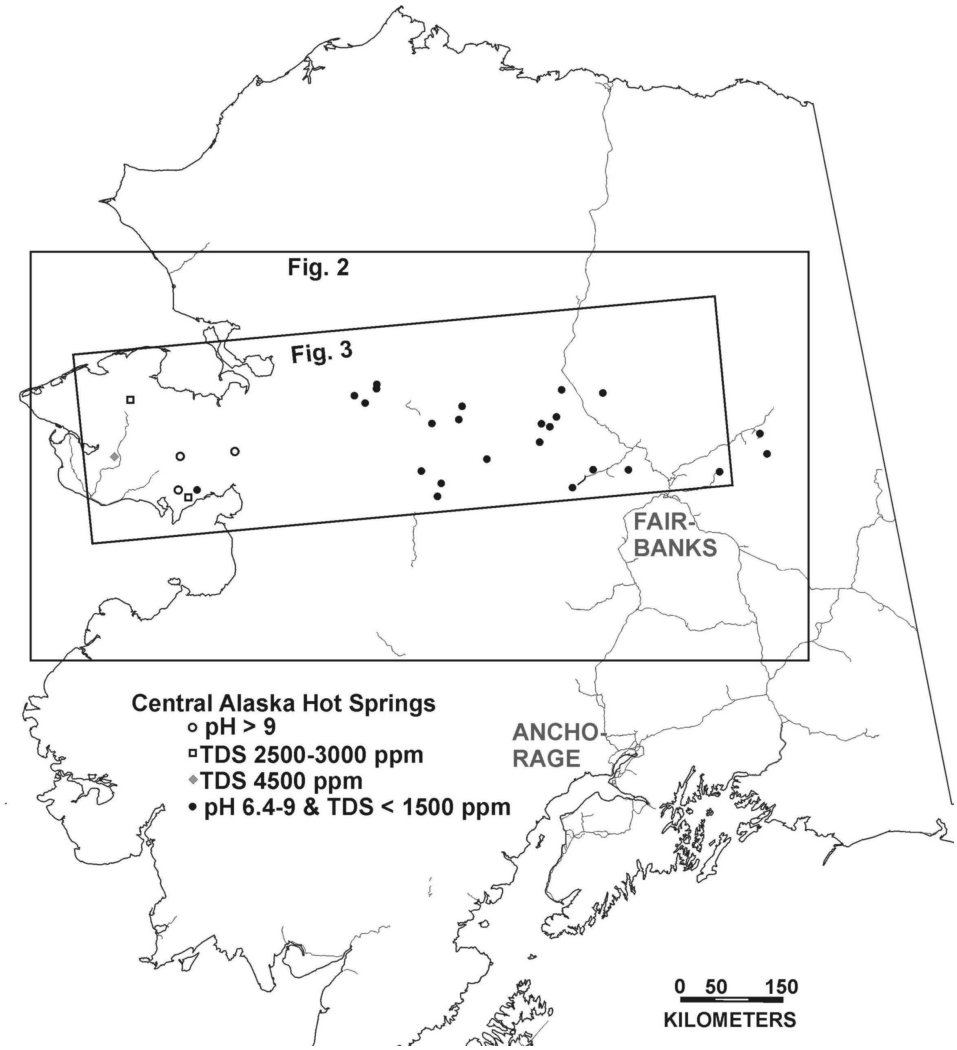

Figure 2.1. Locations and characteristics of hot springs in the Central Alaska belt. Spring locations superimposed on a map of 'mainland' Alaska with major roads. Data from Motyka et al. (1983).

The only hot spring in the CAHSB other than CHS to have been the subject of detailed geothermal exploration is Pilgrim Hot Springs (PHS), north of Nome. The exploration at PHS (1979-1982) included drilling six shallow wells (up to 304 m). Turner and Swanson (1981) concluded that the geothermal activity was fault-related due to rifting in the central part of the Seward Peninsula, and that the PHS is the surface

expression of a cyclic, low-temperature, non-volcanic hydrothermal system. Very limited studies were conducted at Manley Hot Springs (East, 1982) and at CHS (Biggar, 1973; Wescott and Turner, 1981a). Extensive geoscientific studies of the CHS system were carried out during 2005-2006, as part of the power plant installation project. Both the CHS and the Manley studies concluded that thermal fluids circulate along faults and fractures within a granitic pluton until they are heated to temperatures of up to 130 °C.

Previous workers (e.g., Turner and Forbes, 1980; Motyka et al., 1983; Miller, 1994, Erkan et al., 2007) have explained the CAHSB geothermal activity as a result of deep groundwater circulation along subvertical faults and/or fractures under normal geothermal gradient conditions. Unanswered by such a hypothesis are (1) why a few areas contain hot springs and most do not; and (2) the driving mechanism for the geothermal circulation. Thermal gradient measurements for the CAHSB indicate that the regional gradient for the CAHSB province is not anomalous; averaging 30 C/km (Table 2.2, also see Erkan et al., 2007).

Table 2.2. Heat flow and thermal gradient measurements from boreholes in Alaska.

Location	**Closest Hot Springs**	**Distance to hot springs (km)**	**Geothermal gradient (°C/km)**	**Crustal heat flow (W/m^2)**
W. Seward Peninsula	Pilgrim, Serpentine	~120 km	38	-
N. Seward Peninsula	Granite Mtn.	~90 km	30	75-100
Hughes area	Pocohontas, Sun Mtn., T. Lake	~20-30 km	31	-
Eilson	Chena	~80 km	33	80-100
Eagle	Circle, Big Windy	~110 km	26	-
Healy	Manley	~90 km	21	60-79
Ft. Yukon	Circle	~120 km	26	60-79

Data from Galanis and Williams, in preparation.

None of the Interior CAHSB hot springs display a spatial association with young volcanism, but some hot springs in the western part of the CAHSB occur near Quaternary basalt fields (Wood and Keinle, 1990). Nearly all of the hot springs are in or near granitoid plutons of Mesozoic to early Tertiary age. Thermal upwelling in the CAHSB often occurs at pluton-country rock contacts, and many of the hot springs have a linear surface expression, suggesting structural control. However, few significant faults have been identified in the immediate vicinity of any of the hot springs. While intrusive bodies of a variety of types and ages are present along the CAHSB, geothermal activity is restricted to plutons of Late Cretaceous and early Tertiary granite and mid-to Late Cretaceous syenite. Nearly all of these plutons contain anomalous concentrations of U and Th. The possibility that the elevated U and Th present in the igneous rocks are ultimately responsible for the hot springs is the subject of this investigation.

2.2.2. Geologic setting of the CAHSB

The CAHSB spans numerous different geologic provinces, but the local geology of most CAHSB sites is poorly constrained, with geologic mapping rarely more detailed than 1:250,000 scale. From west to east, these provinces are: the Seward Peninsula province, the Yukon-Koyukuk province, and the Yukon-Tanana upland. The present-day structural setting of Interior and Western Alaska is influenced by strike-slip tectonics along the Denali and Tintina- Kaltag fault systems, large-scale arcuate features that girdle central Alaska from west to east and mark a continental-scale crustal boundary. Redfield et al. (2007) proposed an “extrusion tectonics” scenario wherein relatively rigid, fault-

bounded crustal blocks in central Alaska are transported westward along these strike-slip faults.

The Seward Peninsula geologic province is characterized predominantly by metamorphic rocks that are locally intruded by plutons of mid-Cretaceous and early Tertiary age. Quaternary basalt covers large parts of the north-central part of the Peninsula. Thermal springs in the Seward Peninsula province include Serpentine, Pilgrim, Lava Creek, Battleship Mountain, Kwiniuk, and Clear Creek.

The Yukon-Koyukuk geologic province, directly east of the Seward Peninsula, is a large tract of volcanic, metamorphic, and volcanic-sedimentary rocks intruded by an east-west belt of Tertiary and Cretaceous granitic rocks. All of the hot springs are spatially associated with granitic intrusions. Quaternary basalt covers several hundred square kilometers in the western part of the province, also called the Koyuk-Buckland volcanic field. The age of the basalts is unknown, but Wood and Kienle (1990) correlate them with the Imuruk basalt field 100 km to the west. Hot springs in the Yukon-Koyukuk province include Granite Mountain, Purcell Mountain, Divison, Hawk, South, Sun Mountain, Pocohantas, Tunalkten Lake, Dulbai, Melozi, Little Melotzina, and Hornor.

The Yukon-Tanana upland is defined by a northeast-trending sequence of Precambrian to Tertiary sedimentary, metasedimentary, and lesser volcanic and metavolcanic rocks, and intruded by granitoid plutons of Late Triassic to early Tertiary ages (Rinehart et al., 1997). Page and Plafker (1995) suggested a block-rotation model for Interior Alaska, wherein crustal blocks rotate clockwise as a result of dextral movement on the Denali and Tintina fault systems combined with sinistral movement on conjugate

oblique faults. Such regional scale shearing has resulted in a pattern of localized extension and contraction along faults between crustal blocks. Such faults are not known to define CAHSB locations. Hot Springs in this province include Ray River, Dall, Kanuti, Kilo, Ishtalitna, McQuesten, Manley, Tolovana, Hutlinana, Chena, Circle, and Big Windy.

2.2.3. CAHSB plutons

Hot springs in the CAHSB are spatially associated with mid-Cretaceous and (or) early Tertiary plutonic bodies (Fig. 2.2). Additional plutons not associated with hot springs have been omitted from the map. The association is striking, as < 20% of the area is underlain by plutons.

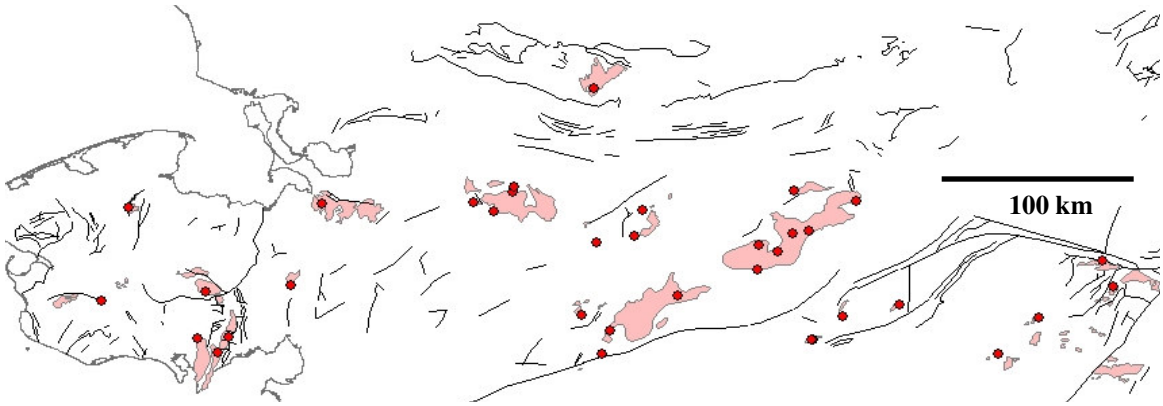

Figure 2.2. Map of CAHSB plutons (pink shapes), hot springs (red circles), and mapped faults (black lines). Adapted from Beikman, 1980. Few of the faults shown on this map are known to be active. Some plutons far from hot springs and (or) not of mid-Cretaceous or early Tertiary age have been omitted from the map.

In particular, 30 out of the 32 CAHSB springs (94%) occur inside or at the margin of a pluton. Of those, 16 hot springs (52%) occur inside or at the center of a pluton, and

14 are located at the margins of the pluton. The two hot springs that do not occur in or near a pluton are Pilgrim hot springs and Hutlinana hot springs, located 15 km and 25 km away, respectively, from the nearest known pluton (Table 2.3).

Table 2.3. Relationship between hot springs and plutons in the CAHSB.

Hot springs name	**Relation to pluton**	**Pluton name (age)**
Big Windy	Margin of pluton	unnamed pluton
Circle	Faulted pluton margin	Circle (eT and mK)
Chena	Center of pluton	Chena (mK & eT)
Tolovana	1.5 km from pluton	Tolovana (lK?)
Hutlinana	No known pluton	None
Manley	Margin of pluton	Manley (eT)
Kilo	In pluton near margin	Ray mtns (Ruby batholith) (K)
Ishtalitna	3 km from pluton	Ray mtns (Ruby bath.) (K)
Upper Ray River	Center of pluton	Ray mtns (Ruby bath.) (K)
Lower Ray River	Center of pluton	Ray mtns (Ruby bath.) (K)
Dall	Center of pluton	Dall mtns (Ruby bath.) (K)
Kanuti	In pluton near margin	Kanuti (Ruby bath.) (K)
Tunalkten lake	4 km from pluton	Indian Mtn.(Hogatza) (K)
Hornor	In pluton near margin	Kokrines Hills (Ruby bath.) (K)
Little Melotzina	Center of pluton	Moran Dome (Ruby bath.) (K)
Pocahontas	3 km from pluton	Indian Mtn.(Hogatza) (K)
Melozi	Center of pluton	Kokrines Hills (Ruby bath.) (K)
Deniktow/Sun Mt.	2.5 km from pluton	Sun Mtn. (age unknown)
Dulbai	1 km from pluton	Dulbatna Mtn. (Ruby bath.) (K)
Purcell Mt./Upper Division	Between 2 plutons (400m & 8 km)	Purcell Mt. (Hogatza) (K)
Lower Division	Between 2 plutons (3 & 6 km)	Purcell Mt./Z. Hills (K)
South	In pluton near margin	Wheeler Ck (Hogatza) (K)
Hawk River	In small pluton	Hawk mtn. (Hogatza) (K)
Granite Mt.	Margin of pluton	Granite Mt. (Hogatza) (K)
Clear Ck.	In pluton near margin	Darby (K)
Kwiniuk/Elim	Center of pluton	Darby (K)
Battleship Mt.	In pluton near margin	Kachauik (K)
Lava Ck.	Margin of pluton	Bendeleben (K)
Serpentine	Center of pluton	Serpentine (lK)
Pilgrim	15 km from pluton	None

Age of plutons given in parentheses: K=Cretaceous; T=Tertiary. Most ages reported from K-Ar studies, with occasional Ar-Ar studies. References: Miller and Bunker, 1975; Miller and Finch, 1976; Miller and Johnson, 1978; Jones and Forbes, 1976; Hudson, 1979; Wilson et al., 1998.

Many of the plutons in the CAHSB are composite bodies, some of multiple ages spanning up to 35 million years (Jones and Forbes, 1976; Wallace, 1979; Kolker et al., 2007). The bulk of the plutonic rocks are biotite-bearing granitoids with lesser amphibole-bearing mafic bodies (Miller and Bunker, 1975). Many contain tourmaline and (or) fluorite as accessory minerals (Jones and Forbes, 1976; Solie et al., 1993c; Kolker et al., in press). Several of the CAHSB-related plutons have anomalously high concentrations of radioactive elements U and Th (Eakins et al., 1977; ; Miller and Johnson, 1978; Reed and Miller, 1980; Newberry, 2000).

Due to the occurrence of uraniferous plutonic rocks, a large part of the western CAHSB is considered a uranium-thorium metallogenic province (Miller and Finch, 1976). Kolker et al. (2007) suggested that an anomalously radioactive body within a composite pluton at Chena Hot Springs was at least partially responsible for the development of hydrothermal convection at that location. All across the CAHSB, there is evidence for anomalous radioactivity in the vicinity of hot springs related to plutons of Cretaceous to Tertiary age. Many studies took place between 1951 and 1975 attempting to locate commercial-grade uranium deposits in the region, primarily in the U, Th-enriched alkaline plutonic rocks of west-central Alaska. Airborne radiometrics surveys found radiometric anomalies associated with CAHSB plutons, especially in the western part of the belt (e.g., Eakins et al., 1977; Miller and Bunker, 1975; Matzco and Freeman, 1955). Mineralogical and petrological studies confirmed that plutonic bodies were the source of the U and Th anomalies (e.g., Wallace, 1979; White et al., 1968; Gault et al., 1953). In general, radioactive elements were found to be disseminated throughout

CAHSB granitic bodies (West, 1948; Wedow and White, 1954; Eakins et al.,1977; Wallace, 1979). More recent investigations showed U concentrations up to 97 ppm and Th up to 2910 ppm in the Zane Hills pluton (Solie et al. 1993b).

The Seward Peninsula contains many small stocks of epizonal biotite granite plutons, including the Serpentine Hot Springs granite (Hudson, 1979). The 'Hogatza plutonic belt' is a large (300 x 35 km) belt of epizonal alkaline potassic rocks extending from Kotzebue sound to Hughes. The Hogatza belt straddles two geologic provinces; the Seward Peninsula province in the west and the Yukon-Koyukuk province in the east (Miller, 1972). It is characterized by uncommon rock types such as malignite, foyaite, juvite, and borolanite, as well as uncommon minerals such as nepheline, black (Ti-rich) garnets, and fluorite. Sixteen separate plutons make up the belt, ranging in area from 5-350 km^2. Interior Alaska experienced three major plutonic episodes in Cretaceous and Tertiary periods. In general, the Tertiary intrusions contain high concentrations of Sn, U, and F (Newberry, 2000), as does the mid-Cretaceous (105–115 ma) Ruby batholith. The Ruby batholith is a northeast-trending body of peraluminous granitic rocks, comprised of more than a dozen individual plutons (Barker, 1991). The early Tertiary igneous rocks in Interior Alaska are bimodal: biotite monzogranite and syenogranite, intruded by aphanitic to diabasic-textured basalt dikes or sills. Minerals in the granitic rocks include smoky quartz, minor biotite, and accessory minerals such as topaz, fluorite, tourmaline, and zinnwaldite (Newberry et al., 1998).

CAHSB hot springs are commonly associated with airborne Th anomalies (Fig. 2.3). Of 32 hot springs located in areas with airborne Th surveys, 22 (2/3) are in areas of high surface Th. However, due to the low flight height (400 ft) and relatively wide flight lines (6 mi), less than 4% of the ground surface was actually sampled in the areas surveyed and the resulting map depends strongly on interpolations. Hence, many of the areas lacking Th anomalies simply lack large Th anomalies. For example, CHS is in an area lacking Th anomalies on Fig. 2.3, but detailed helicopter-based gamma ray surveys show high Th in the CHS area. With this proviso, the correlation between hot springs and Th anomalies is striking.

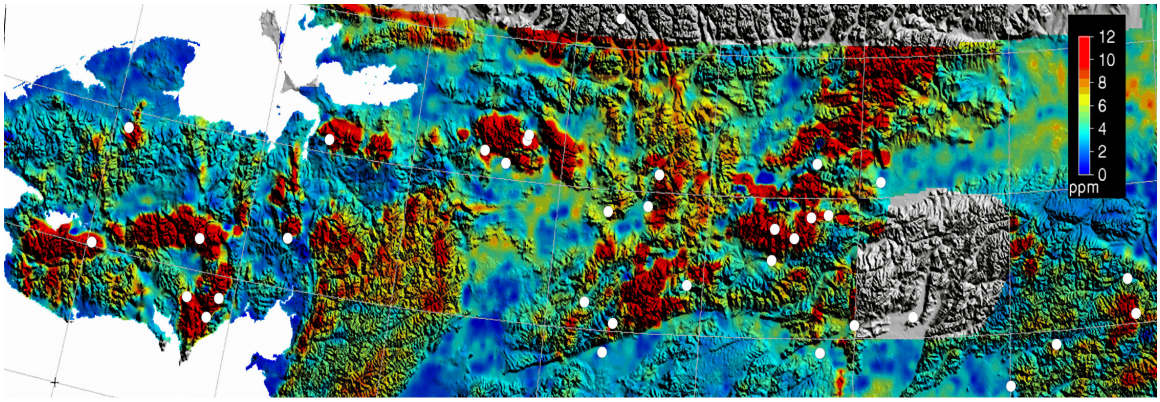

Figure 2.3. CAHSB hot springs (white circles) and surface equivalent Th concentrations (from Saltis, 1999), draped over a shaded Alaskan DEM. Colors represent equivalent Th in parts per million (ppm) averaged over the upper meter of the land surface, from merged airborne gamma-ray surveys with 6 mile spacing (Saltus, 1999). Areas with no data are shown in grey.

2.2.4. Radioactive heat production of granitic rocks

The principal primary source of the radioactive elements U, Th and K are felsic igneous rocks. The average U concentration for felsic igneous rocks is 4 ppm; in Thorium it is 18 ppm. For comparison, the average U concentration for sedimentary rocks it is 1.3-3.2 ppm U; for mafic igneous rocks it is 0.8 ppm U (Eakins et al., 1977). Radioactive heat production in granitic rocks comes from the decay of long half-life radioactive isotopes K^{40}, U^{235}, U^{238}, Th^{232} . Under oxidizing conditions uranium is highly mobile and soluble, but thorium is not. In the western U.S., U concentrations have been found to be abnormally high in Mesozoic and Cenozoic plutonic rocks (Marjaniemi and Basler, 1972).

Anomalous concentrations of radioactive elements in granites of southwest England were shown to cause high heat production and considerable post-magmatic hydrothermal convection (Fehn, 1985). Durrance (1985) suggested that HHP granites go through a several million year cycle of: heating by radioactive decay with minimal conductive heat loss; inflation due to heating; inflation-induced fracturing; convective groundwater circulation; and finally deflation and cooling due to efficient convective cooling. At least 4 such cycles are identified by radiometric dating for granites of Cornwall, England (Stone and Exley, 1985). Additionally, heat production in granites may induce fracturing by thermal expansion (Durrance, 1985), providing the vertical permeability required as circulation pathways for convecting fluids.

There are many radioactive (high heat-producing) plutonic bodies throughout the world in places such as in Brazil, China, Taiwan, India, Canada, Greenland, USA,

Canada, Iran, Uganda, Kenya, and China. The plutons are typically highly evolved, granite, alkali granite, syenite, pegmatite and (or) related rock types. Many of these regions also have low-temperature thermal areas, but only limited studies have shown the correlation between radioactive granitic bodies and active hydrothermal circulation. Brugger et al. (2005) attributed the heat driving the Paralana hot springs (PHS) system, South Australia, to a zone of anomalously high heat flow attributed to high concentrations of radioactive elements in a nearby plutonic body.

2.2.5 Helium isotopes and geothermal systems

Helium isotopes provide unequivocal evidence for the presence of mantle-derived volatiles in geothermal systems, and therefore are an indication of heat source. Hence, helium isotopes may be useful in distinguishing between magmatic, "deep circulation," or radiogenic type geothermal systems. Helium in mid-ocean ridge basalts worldwide is characterized by a $^{3}He/^{4}He$ ratio of 8–9 R_A (where R is the measured sample $^{3}He/^{4}He$ ratio and R_A is the ratio in air), which is generally believed to represent the upper mantle composition (Kennedy and van Soest, 2007). Geothermal fluids from regions of young volcanic/magmatic activity show a clear mantle signature in that they contain elevated ^{3}He concentrations (Oxburgh and O'Nions, 1987). The specific helium isotopic composition of fluids that mine heat from active near surface magmatic systems are typically similar to the composition in the mantle source (e.g. Coso, ~7 R_A, Welhan et al, 1988; Long Valley, ~2-7 R_A, Sorey et al., 1993; The Geysers, ~8-9 R_A, Kennedy and Truesdell, 1996). Helium derived from mantle sources but with no magmatic input (for

instance, in deep circulation / crustal thinning settings) is also enriched in ^{3}He, but characterized by lower ^{3}He/^{4}He ratios than magmatic settings. Therefore, any value higher than 0.1 R_A is considered to have a significant mantle He component (Ballentine et al., 2002). For example, fluids from the Dixie Valley, NV geothermal field range from 0.70 to 0.76 R_A, indicating that 7.5% of the total helium is derived from the mantle (Kennedy and van Soest, 2007). A summary of helium isotope signature from the different types of geothermal systems is given in Table 2.4.

Table 2.4. ^{3}He/^{4}He ratio (R) in geothermal fluids relative to the ^{3}He/^{4}He ratio in air (R_A)

Hot springs type	**He isotope signature (R/R_A)**
Radiogenic (1)	0.02-0.04 (crustal)
Volcanic / Magmatic (2,4,5,6)	2-16 (2)
"Deep circulation" (2,3,5)	~0.70 (3)

Sources: (1) Brugger et al., 2005; (2) Kennedy and van Soest, 2005; (3) Kennedy and van Soest, 2007; (4) Christenson et al., 2002; (5) Ballentine et al., 2002; (6) Poreda et al., 1988.

Helium associated with crustal fluids that have experienced no mantle influence is dominated by radiogenic ^{4}He produced from radioactive decay of U and Th to Pb and is characterized by a ^{3}He/^{4}He ratio of ~0.02 R_A. Hence, hot springs containing low R_A (<0.04) have originated in non-magmatic crustal settings only.

2.3. Methods of study

Geothermal fluid and gas samples were collected from Chena Hot Springs in May 2007 for He isotope analyses. At CHS, the highest He concentrations occur in the northwest of the thermal anomaly (Wescott and Turner, 1981a). This area is interpreted

to be the upwelling area (least mixed) for deep thermal source fluids (Erkan et al., 2007). Hence, He samples were collected from wells in the northwest of the thermal anomaly. For the gas sampling, the wellhead fluids were passed directly through an inverted "Y-shaped" separator, isolating a sample of the free-gas phase for collection. The sampling apparatus was initially filled with the wellhead liquid; the separated gas phase was captured using a water displacement technique. Geothermal well fluid was collected by submerging a tube in the wellhead and pulling water through the sampling apparatus using a peristaltic hand pump. After several volumes of water had passed through the system a sample of the liquid was collected for analysis of the dissolved gases. Both samples were collected at ambient conditions in a Cu-tube cold-welded at each end using bolt-driven clamps. To ensure sample integrity, the clamps remained in place until the sample was ready for analysis and attached to the sample preparation vacuum line, which is in series with the noble gas mass spectrometer. Sample preparation and the noble gas analyses were conducted in the Roving Automated Rare Gas Analysis (RARGA) laboratory at the Lawrence Berkeley National Laboratory. Sample preparation, analytical techniques and the instrumentation used in the RARGA laboratory are similar to those described by Kennedy et al. (1985).

Published U and Th data for CAHSB plutons were compiled and supplemented with additional plutonic rock samples. Additional samples were collected from the field (Kanuti and Tolovana samples) and from the Alaska Division of Geological and Geophysical Surveys (ADGGS) Geologic Materials Center in Eagle River, Alaska (Ray Mts. and Darby pluton samples). A variety of methods were utilized to determine U and

Th concentrations reported herein, including INAA (Instrumental Neutron Activation Analysis); AA (Atomic absorption); DN (Delayed neutron); γS (Gamma ray spectroscopy); and XRF (X-ray fluorescence). For the XRF analyses presented in this study, rock samples were prepared and analyzed at the UAF Advanced Instrumentation Laboratory following procedures described in Kolker et al (2007). Precision, based on replicate analyses, is <1% of the amount present. Accuracy is approximately ±5% for concentrations >20 ppm and ±1-2% for concentrations >0.5%.

2.4. Results

A gas sample from Chena Hot Springs well fluids gives an R_A value of 0.035, and a sample from Chena Hot Springs well fluids gives an R_A value of 0.033 (Table 2.5). These values indicate a purely crustal heat source with little to no mantle or magmatic input into the system.

Table 2.5. R/R_A values, noble gas concentrations and relative abundances for CHS.

Sample	**[^{36}Ar] 10^{-6} cc/ml**	**$(R/R_A)m$**	**+/-**	**$(R/R_A)c$**	**+/-**	**F(^{4}He)**	**+/-**	**F(^{22}Ne)**	**+/-**
CHS water	1.434	0.050	0.005	0.033	0.016	15.6	0.2	0.300	0.004
CHS gas	60.05	0.037	0.005	0.035	0.018	276	4	0.520	0.006
0 ^{o}C	1.754					0.177		0.235	

(R/Ra)m = measured air normalized 3He/4He ratio; (R/Ra)c = measured air normalized 3He/4He ratio corrected for air helium (correction assumes all ^{36}Ar and ^{22}Ne is air derived). F(i) values are ^{36}Ar normalized fractionation factors with respect to air composition [(F(i) = (i/^{36}Ar)sample/(I/^{36}Ar)air]. For comparison, the composition of 0 ^{o}C water in equilibrium with air is also provided (0 ^{o}C ASW). Data from M. B. Kennedy, Center for Isotope Geochemistry, Lawrence Berkeley National Laboratory.

Combining U, Th analytical data for this study and previous work yielded 284 analyses. We grouped the U, Th data into 17 separate groups, each representing one CAHSB pluton or plutonic complex. Datasets for some of these groups came from a single source; other datasets combine data from multiple sources (Table 2.6). The mean U concentration for CAHSB plutons is 24 ppm, with a range from 5 (Tolovana pluton) to 127 (Purcell Mts. Pluton). The mean Th concentration is 87 ppm, with a range from 22 (Indian Mountain pluton) to 454 (Zane Hills pluton) (Table 2.6).

Analytical error was not reported for much of the published data sources, and the variability in the data far exceeds analytical variability for the samples for which this is known. Hence, we report error as ± 1 standard deviation of the mean value for both the U, Th concentration computations. For datasets where the standard deviation exceeded 400%, that dataset was revisited and data from particular sources was eliminated from our computations. For example, Barker (1991) reported extremely high U and Th concentrations for rocks in the Zane Hills area. However, Barker (1991) was deliberately searching for high U, Th rocks in the Zane Hills and his data are deliberately skewed towards high values. These data were consequently excluded from our heat production computations as they are not representative of the pluton as a whole.

Heat production (A) was calculated from radioelement concentration in CAHSB plutons (after Rybach, 1981):

$$\mathbf{A\ (\ W/m^3) = 10^{-5}\rho\ (9.52cU + 2.56cK + 3.48cTh} \quad \mathbf{[Eq.\ 2.1]}$$

Where A = heat production, c = radioelement concentration (U, Th in ppm, K in %), and ρ = rock density. We used a ρ = 2670 kg/m^3, the average for granitic rocks. K concentrations were missing from most datasets, so we used a calculated average of 4.12% for eastern CASHB plutons based on data from the Interior Plutons database (ADGGS, 2008) and 4.97 for western CAHSB plutons based on data from Miller and Bunker (1975).

Table 2.6. U and Th compositions and heat production (HP) of CAHSB plutons.

Hot Spring	**Pluton**	**No. samples**	**Ave U (ppm)**	**Max U (ppm)**	**Ave Th (ppm)**	**Max Th (ppm)**	**K (%)**	**HP (mW/m^3)**
Serpentine	Serpentine (2)	5	26±9	34	48±17	66	5.0	11±3
Granite Mtn	Granite Mtn. (3,4.5)	30	34±66	198	62±46	129	5.0	15±21
Kwiniuk, Clear Ck., Lava Ck.	Darby (1,4,5)	53	8±4	17	48±11	84	5.0	7±2
Battleship Mtn.	Kachauik (4)	5	6±4	12	28±8	36	5.0	5±1
Hawk, South, Division	Purcell Mts. (3)	34	127± 424	2000	177± 852	5000	5.0	49±187
South	Wheeler Ck. (5)	2	14±1	14	49±5	52	5.0	8±1
Division, Sun Mt.	Zane Hills (3)	18	23±28	97	454±855	2910	5.0	48±87
Sun Mtn.	Sun Mt. (3)	9	23±16	39	83±52	160	5.0	14±9
T. Lake, Pocahontas	Indian Mt. (3)	7	11±13	39	22±9	31	4.1	5±4
Dulbai, Melozi	Kokrines Hills (3,6)	10			44±14	70	4.1	7±2
Ray River	Ray Mtns (3)	51	31±20	75	142±96	344	4.1	21±14
Kanuti	Kanuti (1)	24	8±5	20	28±12	51	4.1	5±2
Manley	Manley (7)	4			65±62	165	4.1	11±10
Tolovana	Tolovana (1)	13	5±2	12	19±5	26	4.1	3±1
Chena	Chena (8)	19	12±3	75	37±10	48	4.1	7±1
Circle	Circle (9, 10, 11)	36	16±9	52	50±18	88	4.1	9±4
Average			*24±42*	*179*	*87±137*	*611*		*14*

Sources: (1) This study; (2) Hudson and Arth, 1983; (3) Solie et al., 1993a-d; (4) Miller and Bunker, 1975; (5) Jones and Forbes, 1976; (6) Chapman and Patton, 1978; (7) Liss et al., 1998; (8) Kolker et al., in press; (9) Clautice, 1987; (11) Newberry et al., 1994; (10) Wiltse et al., 1994; *U estimated from Th values and regional U/Th ratios.

Heat production calculations yielded anomalous values for almost all of the CAHSB plutons (Table 2.6). The mean heat production (HP) for CAHSB plutons is 14 W/m^3, with a range of 3±1 (Tolovana pluton) to 49±187 (Purcell Mts. Pluton). The standard deviations from the mean is remarkably high in many cases. When HP values with standard deviations greater than 50% are eliminated, the average HP for CAHSB plutons becomes 9 W/m^3.

Fig. 2.4 compares the U and Th concentrations of CAHSB plutons to the average U and Th concentrations in plutons from elsewhere in the United States. Even when compared with the high-heat producing (HHP) granites of New England, CAHSB plutons contain anomalous concentrations of U and Th.

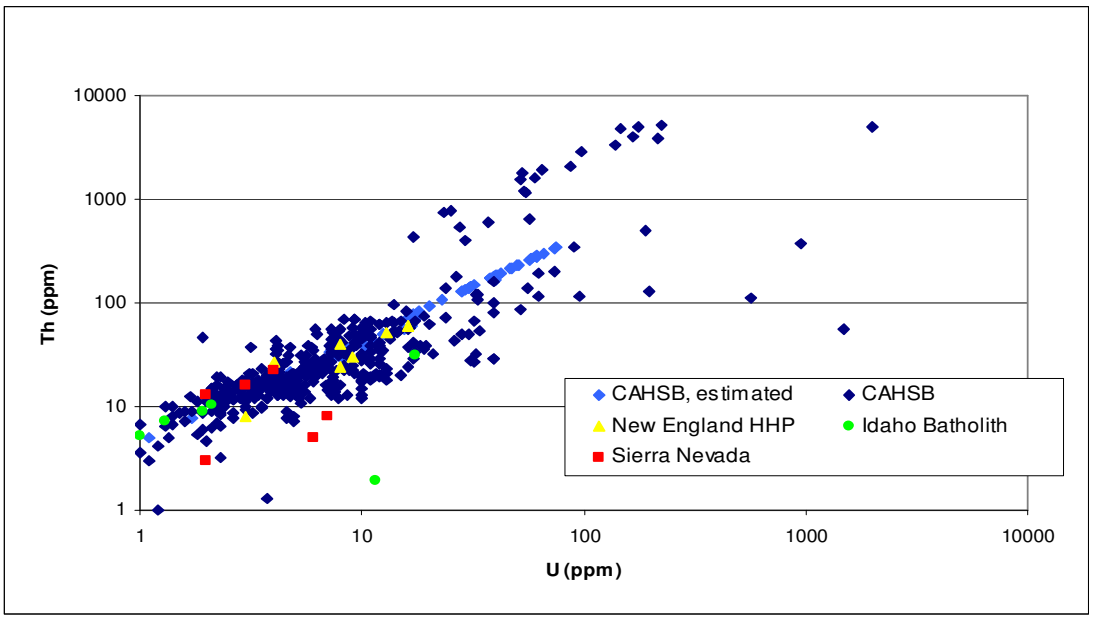

Figure 2.4. U and Th compositions of CAHSB plutons vs. other pluton groups. Data sources for CAHSB plutons are listed in Table 2.6. Data for Idaho batholith plutons from Druschel and Rosenberg, 2001, New England and Sierra Nevada pluton data from and Roy et al., 1968.

2.5. Discussion

2.5.1. Evaluating the deep circulation heat source model

CAHSB fluids are convective (Erkan et al., 2007), which suggests that vertical permeability pathways of closely-spaced fractures and/or faults are present to enable groundwater convection through or around the heat source. However, this does not mean that CAHSB fluids are 'deep-circulation' type. There are several problems with this interpretation. The first problem is that the tectonic setting of Central Alaska – dominated by fault-bounded crustal blocks rotating in response to movement along strike-slip faults – does not provide the same type of deep fault pathways that extensional settings do. There are very few hot springs associated with the large-scale strike-slip faults in the CAHSB. The smaller faults that bound the crustal blocks in Central Alaska are also rarely associated with hot springs. The small-scale fractures and localized faults that are observed in CAHSB plutons and at the pluton-hornfels contacts show no evidence of penetrating to deep crustal levels. Instead, such fractures and faults could be simply a result of intrusive processes and/or post-intrusion thermal expansion from radiogenic heat generation (after Durrance, 1985). High heat production granites throughout the world are associated with block faulting (Plant et al., 1985).

Hence, fractures and faults are clearly providing the vertical permeability required as circulation pathways for convecting fluids – but they may not be the sole phenomenon operating in the CAHSB system. Unfortunately, geologic maps are not available beyond a 1:1,000,000-scale for much of the CAHSB. According to this regional map (see 2.2), 15

out of the 32 hot springs are located on or near mapped faults, though there is no indication of the age of activity of those faults. This number should be considered as a minimum, considering the poor exposure of structural features and lack of field studies in Interior and Western Alaska. In the few areas where detailed maps are available, small-scale faults controlling the geothermal upwelling have been identified. For example, Kolker et al. (2007) argued that the location of Chena Hot Springs is related to a NW-trending strike-slip fault with localized extension, but there is no evidence for recent activity along that fault. The amount of lateral displacement along the Chena Hot Springs fault is <3 km, which is miniscule compared to the faults with tens to hundreds of km displacement in other "deep circulation" systems. At Pilgrim Hot Springs, high-angle faults were identified using gravity surveys and seismic data (Wescott and Turner, 1981b, Lockhart and Kienle, 1981), though those faults appear to control outflow only, as subsequent drilling into those features did not penetrate any deep thermal source.

Moreover, there is little evidence that the small-scale faults in and near CAHSB plutons are active. Active faults are far more important hydraulic conduits than inactive ones (Barton et al., 1995). In geothermal systems, this is even more true due to self-sealing processes from hydrothermal alteration and deposition. In the CAHSB, active faults would have to be held open by shear stresses operating within rotational blocks (Interior Alaska) or by extensional stresses operating within small-scale rift systems (Seward Peninsula). However, the locations of CAHSB hot springs rarely coincide with the zones of seismic activity that mark the boundary of rotational blocks in Interior Alaska (Ratchkovski and Hansen, 2002).

The second problem with the 'deep circulation' hypothesis is that there is no evidence to suggest that the geologic provinces that comprise the CAHSB are necessarily high heat flow provinces, with the possible exception of the extreme western end of the belt. 'Deep circulation' type hot springs typically occur in regions of high heat flow. Thermal gradient measurements indicate relatively normal regional conditions (28-40 °C/km; average ~33 °C/km). However, none of the measured heat flow points are near CAHSB plutons or hot springs (Table 2.6). The highest measured thermal gradients (32-40 °C/km) are from wells at the western end of the Seward Peninsula, in the Purcell Mountains, and at Eilson Air Force Base near Fairbanks – but all are 30 km or farther from the closest hot springs. Thermal gradient measurements from near Chena Hot Springs also indicate a fairly normal gradient in the wells drilled outside of the thermal upwelling zone (28-34 °C/km, Erkan et al., 2007).

While thermal gradient measurements are relatively average for crustal heat flow, heat flow measurements in some parts of the CASHB are higher than average (80-100 mW/m^2; Table 2.6). This discrepancy indicates that there could be substantial local variation and that heat flow could be anomalous in localized areas. Since heat flow is a function of thermal gradient and conductivity, this implies either: (1) the CAHSB has anomalous thermal rock conductivity; or (2) while regional heat flow is average, there are localized sources of anomalous heat flow. The first implication could really only be true if Alaska were a large granitic batholithic terrane. If the second implication is true, then regional extension and/or crustal thinning cannot be the mechanism of heat, since that

would cause a regional widespread heat anomaly. The limited nature of the thermal anomalies argues for a shallow rather than deep source.

2.5.2. U,Th concentrations and heat production of CAHSB plutons.

U and Th concentrations of CAHSB plutons are anomalous when compared to the average U and Th concentrations in plutons from elsewhere in the United States (Fig. 2.4). The New England high-heat producing (HHP) granites shown in Fig. 2.4 were once investigated as a potential source of low-temperature geothermal energy (Costain et al., 1980); however, permeability limitations in this tectonically quiet area preclude the development of hot springs systems. The Idaho batholith is a large complex of Late Cretaceous (100–85 Ma) to early Tertiary granitoid bodies covering approximately 15,400 square miles in central Idaho. The Idaho batholith hosts a number of non-magmatic fracture-controlled hydrothermal systems (Druschel and Rosenburg, 2001), thought to be of the 'deep circulation' type. The Sierra Nevada batholith is a complex of Late Jurassic (160–150 Ma), and Late Cretaceous (100–85 Ma) intrusive bodies. It is not associated with geothermal activity, though unrelated magmatic hydrothermal systems do occur nearby.

The high degree of variability in the U, Th data is probably due to the inhomogeneous distribution of these elements in a given body. A considerable amount of variation in U and Th concentrations within plutons has been documented by most workers (e.g., Herreid, 1969, Jones and Forbes, 1976). Fig. 2.4 shows a near-linear correlation between U and Th in concentrations below 10 and 80 ppm respectively, but at

higher concentrations U and Th behave differently. The two distinct trendlines at high concentrations may reflect post-emplacement U redistribution into quartz veins and other secondary deposits. Another source of variability may be focus of the studies themselves. For example, some studies (e.g., Solie et al., 1993a-d) were seeking geochemical anomalies and therefore would have included vein samples in the analyses; whereas other studies with different aims may have rejected vein samples.

The heat generation of CAHSB plutons ranges from 3 to 49 W/m^3, with an average of 14 W/m^3. If values from plutons with standard deviations >100% are excluded, the average is 9 W/m^3. This is four to six times the average of 2.25 W/m^3 for granitic rocks (Rybach, 1981). Even within the high degree of variability, this places all the CAHSB granites within the category of high-heat-producing (HHP) granites.

2.5.3. Isotope geochemistry and implications for heat source model.

Helium istope ratios are very slightly elevated with respect to those expected for a purely crustal source (CHS R=0.03 R_A; crustal R=0.02 R_A), indicating either that little to no mantle or magmatic helium is present in the CHS geothermal fluids. Little data exists for geothermal systems with a similar crustal signature. The radiogenic geothermal system represented by Paralana hot springs, South Australia, is the only other hot springs with a similar crustal signature. Both magmatic and deep circulation type geothermal systems exhibit at least some degree of mantle input (Table 2.5). This suggests that the primary source of the heat driving the geothermal activity at Chena Hot Springs is

derived neither from active or recently active magmatic activity, nor from circulation along deep fault planes in an extensional setting.

In addition to unusually low helium isotope signatures, CAHSB fluids are also dissimilar to magmatic and deep-circulation type hot springs in terms of fluid chemical characteristics. The low surface temperatures (<90 °C, average 55 °C, near-neutral pH) low concentrations of total dissolved solids (TDS, average <2000), and other characteristics of the CAHSB resembles better the radiogenic Paralana hot springs fluids in South Australia, which are characterized by low-surface temperatures (average 57° C), near-neutral pH (7–8), and average TDS of 1144 mg/L.

Chloride (Cl) concentrations in geothermal fluids are often used in ratios with other elements in the interpretation of water chemistry, the most conservative element in geothermal waters (Nicholson, 1993). In magmatic hydrothermal systems, Cl is thought to be introduced through crystallization of the associated magma, and in deep circulation systems Cl is thought to derive directly from the deep reservoir. Arehart et al. (2003) used Cl/B and Cl/Li ratios in geothermal fluids to distinguish between magmatic-driven and extension-driven ('deep circulation' type) geothermal systems in the Great Basin. Cl/B and Cl/Li ratios of CAHSB fluids resemble neither magmatic nor deep circulation type systems (Fig. 2.5). Cl concentrations in CAHSB fluids are lower than fluids from both other types of systems, but Li and B are lower by several orders of magnitude. This defines a separate trend for CASHB systems, which fits data from the radiogenic geothermal system at PHS. Again, this strongly suggests that the CAHSB represents a different type of geothermal system.

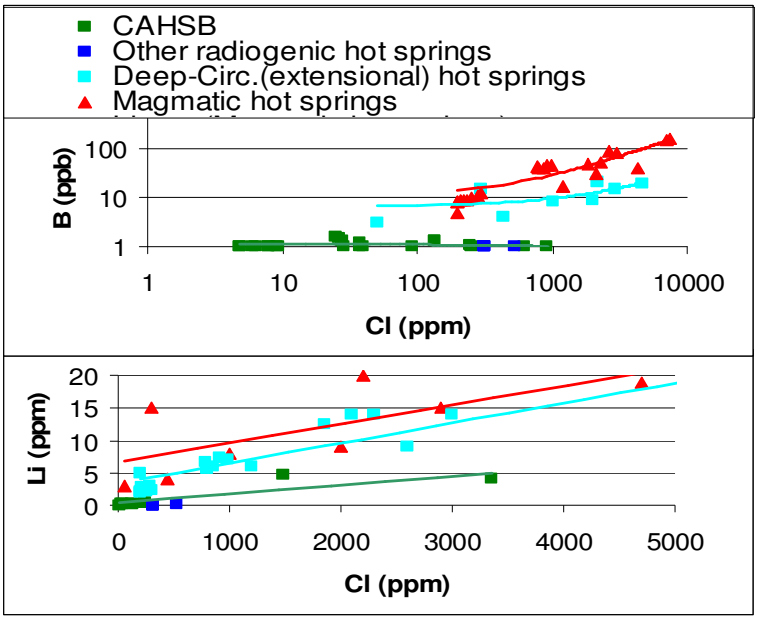

Figures 2.5a and 2.5b. Cl vs. Li and B data from CAHSB hot springs vs. other hot springs. CAHSB data courtesy of Marshall Reed, USGS. Data for other radiogenic hot springs is from the Paralana system (Brugger et al., 2005), data for magmatic hot springs is from magmatic systems in the Great Basin (Arehart et al., 2003); and data for and deep-circulation hot springs is from extensional systems in the Great Basin (Arehart et al., 2003).

Miller et al. (1973) estimated reservoir temperatures utilizing quartz and Na-K-Ca geothermometric methods for some CAHSB fluids. Those estimates ranged from 92 to 136 °C (quartz) and 60 to 167 °C (Na-K-Ca). The equations used in that study are over 30 years old and therefore somewhat outdated, moreover they may be chemically inappropriate for CAHSB fluids. The weakness of the alkali geothermometer (Na-K-Ca) is that it assumes the critical feldspar-mica assemblage is present in the reservoir. However, Ca is relatively absent in the felsic plutonic host rocks at CHS (Kolker et al., in press). This is probably true for most of the other CAHSB host rocks. Hence, alkali geothermometers probably overestimate the reservoir temperatures of CAHSB systems.

Quartz geothermometers may not be appropriate either. The relatively low temperature of the CAHSB hot springs, coupled with the observation of chalcedony in geothermal well cuttings from Chena Hot Springs (Kolker et al., in press), both imply that the chalcedony geothermometer is probably more appropriate for CAHSB systems. At temperatures of less than 190 °C, it is sometimes found that silica contents reflect equilibrium with chalcedony rather than with quartz (Henley et al., 1984). In addition, CAHSB systems have relatively low Ca concentrations due to the absence of available Ca in felsic granitic rocks; therefore the Na-K-Ca geothermometer may also be slightly less accurate than the Na-K geothermometer. Fig. 2.6 presents a plot of temperature estimates for CAHSB reservoir fluids using five separate geothermometers.

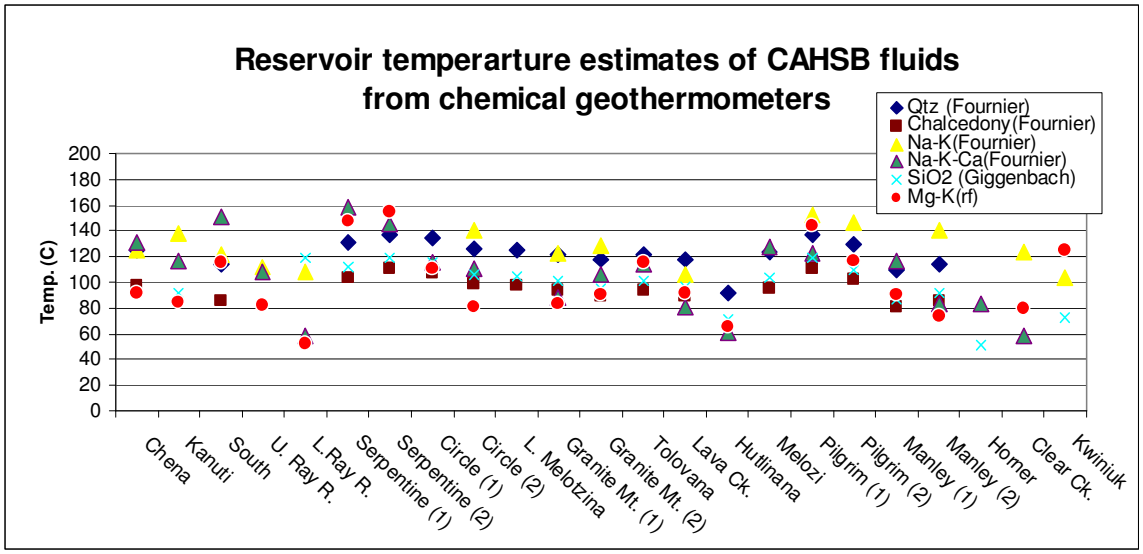

Figure 2.6. Chemical geothermometers for CAHSB fluids. Quartz, chalcedony, Na-K, and Na-K-Ca calculations after Fournier (1981); SiO2 and Mg-K after Giggenbach (1988). Chemical data courtesy of Marshall Reed, USGS.

Fig. 2.6 shows that of the five separate geothermometers, the ones utilized by Miller et al. (1973) represent the highest estimates for reservoir temperatures. The

chalcedony geothermometers, which are more appropriate for CAHSB fluids, give lower estimates. The average reservoir temperature for CAHSB fluids as predicted by the chalcedony geothermometer is ~92 °C. Hence, in this case as well, the CAHSB resemble better the fluids of the Paralana hot springs systems, which give estimated reservoir temperatures of ~95 °C (also based on chalcedony, Brugger et al., 2005).

2.5.4. Feasibility of the radiogenic heat source model

The Paralana hot springs in Southern Australia (PHS) are also thought to be derived from radiogenic heating by buried plutonic bodies (Brugger et al., 2005). Brugger et al. (2005) show that about 4300 tons of the British Empire granite, (average 16 ppm U, 11 ppm Th) or 507 tons of the Paralana gneiss (average 75 ppm U, 288 ppm Th) are sufficient to raise the temperature of 1 kg of water by 65 °C over a year. To test whether radiogenic heat sources can account for *all* of the heat transferred to hot springs in the CAHSB, the following parameters would need to be known:

1) Heat generated by each CAHSB pluton (volume * heat production of plutons).
2) Heat required by CAHSB fluids (volume of water * temperature differential).

For parameter #1, we calculated heat production for as many CAHSB plutons as possible based on our limited dataset of 284 rock samples. To make reasonable assumptions about subsurface pluton geometry, we considered the following factors: (1) intrusive rocks in Alaska are probably vastly more voluminous in the subsurface than their surface outcropping would suggest. Many of the plutons in Interior Alaska are surrounded by contact aureoles of hornfels extending outward for tens of kilometers

(Miller, 1972). In Interior Alaska, Tertiary rocks are thought to be voluminous in the subsurface because of the abundance of Tertiary resets in rocks up to 30 kilometers from known Tertiary igneous rocks; moreover, early Tertiary volcanic rocks rarely occur together with age-equivalent granitoids, hence the early Tertiary thermal event in Alaska appears to be quite widespread (Newberry et al., 1998). Moreover, the "roots" or subsurface depth of CAHSB plutons (even small ones such as the Chena pluton) are thought to be greater than our assumed 5 km (Biggar, 1973; Miller, 1972). On the other hand, plutons in general are likely to become more mafic with depth which would imply that U, Th concentrations would decrease with depth. Considering these factors, we estimated the subsurface volume of CAHSB plutons based on surface outcrop area and two different subsurface geometry assumptions (Table 2.7). Volume estimate (1) assumes a partial-sphere-shaped intrusion in which the outcrop surface area represents 2/3 the size of the largest diameter of the sphere. Volume estimate (2) assumes a partial-cone-shaped intrusion in which the outcrop surface area represents a cross section of the cone at ½ the size of the basal cross section of the cone, and the height (depth) is conservatively assumed to be 5 km or 3 miles (after Bott and Smithson, 1967).

For parameter #2, we assumed that the temperatures of CAHSB fluids are greater at depth than at the surface due to conductive cooling and near-surface mixing with shallow groundwater. This is supported by chemical relationships observed in CHS fluids (Kolker et al., in press). Chemical data were collected by Marshall Reed, and are used here for the purpose of running the thermometry calculations.

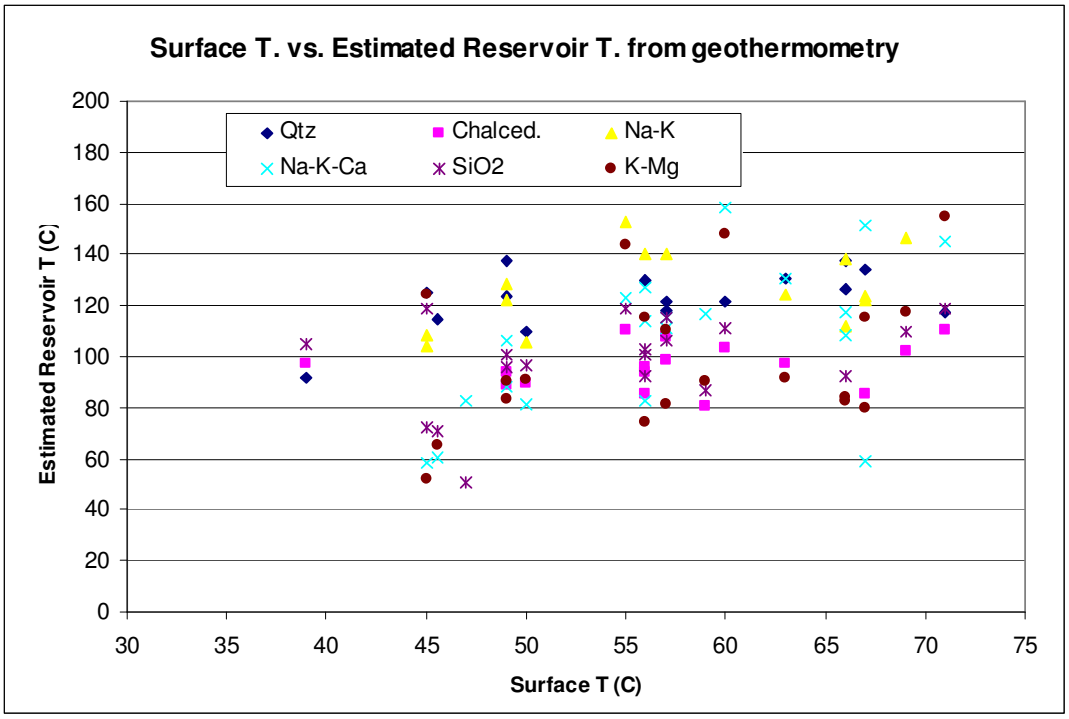

Figure 2.7. Natural surface temperatures vs. estimated reservoir temperatures for CAHSB fluids. Estimated reservoir temperatures calculated from six different geothermometer methods: Quartz, Chalcedony, Na-K, and Mg-corrected Na-K-Ca geothermometers (Fournier, 1981) plus $Si0_2$ and Mg-K geothermometers from Giggenbach (1988).

Due to the poor correlation between surface temperatures and estimated "reservoir" temperatures, we utilized estimated reservoir temperatures rather than surface temperatures to compute the amount of heat required. Our reservoir temperature estimates are from chalcedony geothermometry methods (see above). Where SiO_2 concentration data was unavailable, we used the average reservoir temperature estimate for the CAHSB (92 °C). Hence, the equations are as follows:

$$\mathbf{H_{gen}\,(cal/sec) = Vol_{pluton}\,(m^3) * \; HP_{pluton}(cal/sec/m^3)} \qquad \textbf{[Eq. 2.2]}$$

$$\mathbf{H_{req}\,(cal/sec) = Vol_{fluid}\,(m^3) * \Delta T_{fluid}\,(m^3/sec) * 1cal} \qquad \textbf{[Eq. 2.3]}$$

Where H_{gen} is the amount of heat generated by a pluton; H_{req} = heat required by the geothermal system; ΔT_{fluid} = the change in fluid temperature, calculated as the estimated reservoir temperature (from geothermometry) minus 5 °C (the assumed temperature of meteoric waters); and Vol_{fluid} = measured spring flow (data from Motyka et al., 1983). Calculations assume that 1 calorie raises the temperature of 1 gm of water by 1 ºC. If a pluton was associated with multiple hot springs, the sum of flow rates was used; where no flow rates were given, a flow rate of 400 liters per minute was assumed.

Based on these assumptions, it is unclear whether heat production from HHP granites alone could account for *all* of the heat transfer in the CAHSB (Table 2.7).

Table 2.7. Radiogenic model feasibility results.

Hot spring	**Pluton name**	**Area (km^2)**	**$V1_{pluton}$ (m^3)**	**$V2_{pluton}$ (m^3)**	**ΔT_{fluid} (ºC)**	**Vol_{fluid} (L/s)**	**Ratio ($V1_{pluton}$)**	**Ratio ($V2_{pluton}$)**
Circle	Circle (T.)	67	3.3E+11	1.0E+12	98	25.7	3.0E-01	9.4E-01
Chena	Chena (T.)	67	1.5E+10	1.3E+11	95	13.9	1.9E-02	1.7E-01
Tolovana	Tolovana	8	1.4E+11	5.8E+11	91	19.2	6.5E-02	2.8E-01
Manley	Manley	37	1.0E+11	4.7E+11	83	23.7	1.4E-01	6.5E-01
Various	Ray Mts.	30	1.7E+14	6.6E+13	87	18.2	5.5E+02	2.2E+02
Various	Kokrines	4167	1.2E+14	5.2E+13	87	18.2	9.3E+01	5.8E+01
Kanuti	Kanuti	3333	8.6E+11	2.0E+12	87	42.8	7.9E-01	6.6E-01
Various	Indian Mt.	125	1.0E+12	2.2E+12	91	6.7	2.1E+01	4.5E+00
Sun Mtn.	Sun Mtn.	142	2.7E+11	9.2E+11	87	6.7	9.9E-01	5.4E+00
Division, Purcell	Purcell Mt. / Z. Hills	142	1.1E+14	4.8E+13	81	48.2	5.4E+01	1.5E+02
South	Hawk Mt.	3083	1.5E+10	1.3E+11	81	22.5	1.7E-02	1.5E-01
Hawk	Wheeler	8	5.9E+12	7.1E+12	87	6.7	2.0E+01	2.4E+01
Granite Mt.	Granite Mt.	452	1.9E+11	7.1E+11	86	27.2	9.0E-02	1.1E+00
Various	Darby	45	1.4E+13	1.3E+13	77	22.1	1.4E+01	1.3E+01
Battleship	Kachauik	817	4.0E+12	5.5E+12	*83*	1.2	4.7E+01	6.5E+01
Serpentine	Serpentine	350	3.3E+11	1.0E+12	98	8.7	1.1E+00	3.5E+00

Pluton areas taken from geologic map surface outcrops. Map references: Foster et al., 1983; Kolker et al., in press; Wilson et al., 1998; Reifenstuhl et al., 1998; Beikman, 1980; Miller and Bunker, 1975; Miller and Johnson, 1978; Chapman and Patton, 1978; Miller et al., 1972; Sainsbury et al., 1970. Abbreviations: T. = Tertiary pluton; H_{gen} = Heat generated; H_{req} = heat required.

Whether CAHSB plutons generate a sufficient amount of heat to drive the observed geothermal activity depends in part on the assumed volume of the pluton (Fig. 2.8). Depending on the volume assumption, 7-10 of the CAHSB plutons appear to generate heat equal to or in excess of what is required to heat CAHSB fluids to estimated reservoir temperatures; whereas 5-8 CAHSB plutons generate considerably less heat than what is required for a continuously operating hot spring. This seems reasonable considering, for example, the lack of geologic evidence for a continuously present hot spring at CHS for the last 55 million years.

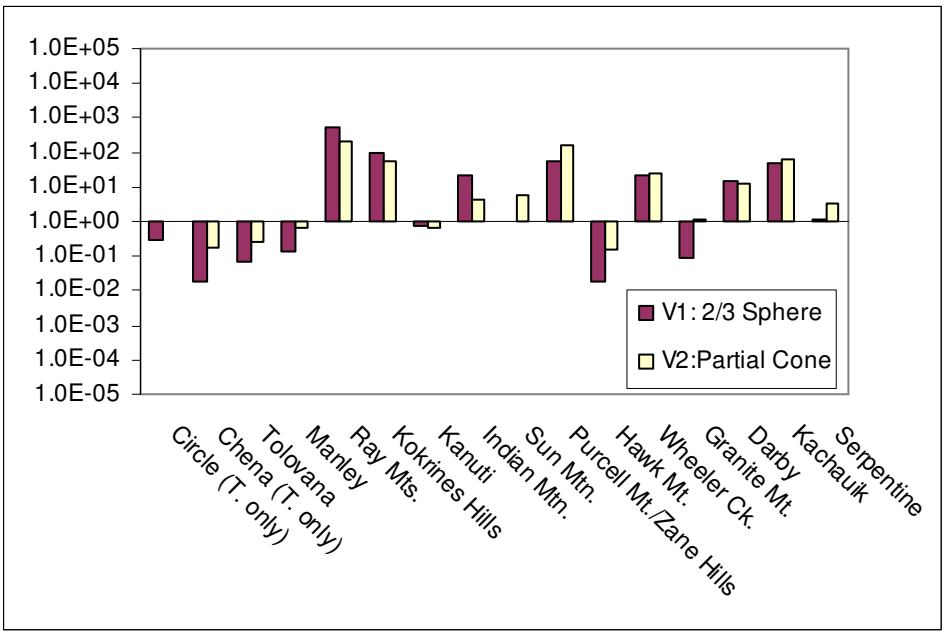

Figure 2.8. Ratio of heat produced/heat required for CAHSB plutons and associated hot springs.

There are two obvious problems with drawing conclusions from our model. First, the U, Th data used as model parameters have a very high degree of uncertainty. Second, the assumptions employed in model parameters change the outcome in 3 out of 14 cases.

Nonetheless, it does appear that the radiogenic heating model is feasible. The fact that some plutons produce sufficient heat to drive the geothermal activity and some do not can be explained by the fact that these systems are likely not steady-state. Indeed, radiogenic hydrothermal systems do not appear to operate continuously in radioactive granite terrains; rather, they occur in discrete pulses when conditions are favorable for circulation and then appear to terminate. For example, ore deposits in SW England, Nigeria, and in the Bohemian massif of Germany, appear to be related to extinct radiogenically-derived hydrothermal systems that were caused by circulation tens of millions of years after intrusions were emplaced (Dill, 1985; Fehn, 1985; Kinnaird, 1985). Durrance (1985) suggested that anomalously radioactive granitic bodies go through a several million year cycle of: heating by radioactive decay with minimal conductive heat loss; inflation due to heating; inflation-induced fracturing; convective groundwater circulation; and finally deflation and cooling due to efficient convective cooling. There are a number of radioactive (HHP) plutonic bodies throughout the world, but not all are associated with present-day hot springs activity. HHP granites buried under "caps" of sedimentary rocks in the northeastern U.S. do appear to have caused anomalous heat flow, but not robust hydrothermal activity (Constain et al., 1980). This could be because permeability in this tectonically quiet region is not sufficient for the development of hydrothermal convective systems. In the CAHSB, it appears that convective hydrothermal systems developed at some point prior to the present time, and the convective heat loss by hydrothermal circulation will presumably continue until it has sufficiently drawn radiogenic heat away from the plutonic body.

Hence, it would appear that in Alaska the combination of high-heat-producing granites of 60-100 Ma and the active structural setting of these plutons create a combination of heat and permeability favorable for the development of low-temperature hot springs at the present time.

The relationship between geothermal activity in the western part of the Seward peninsula and the rest of the CAHSB is unclear. The saline springs at Pilgrim and Serpentine hot springs indicate that the waters either: (a) experienced much more complex water-rock reactions than occurred in the other hot springs; (b) experienced addition of another type of water; or (c) originated in a different geologic setting than the other fluids in the CAHSB (Motyka et al., 1980). These springs are notably hotter than other CAHSB springs. The Seward peninsula may be undergoing incipient crustal rifting (Turner and Swanson, 1981), which suggests high regional crustal heat flow and the possible presence of magma at relatively shallow depths beneath the peninsula. Unlike the other CAHSB springs, there is evidence for deep, near-vertical extensional faults, which could serve as effective hydrothermal conduits (Economides et al., 1982). However, a magmatic or rift-related origin for the Seward peninsula hot springs is complicated by the fact that several of the peninsula springs are also associated with radioactive granitic plutons. Helium isotope studies and heat flow studies in the western part of the CAHSB would help elucidate this issue.

2.6. Conclusions and future work

The accepted 'deep circulation' model for the geothermal activity CAHSB is problematic. The CAHSB does not share many characteristics common to deep circulation systems, such as large-scale extensional features, fluid chemistry indicative of deep circulation and much higher reservoir temperatures at depth, elevated geothermal regional heat flow conditions, and others. Moreover, there is a stronger correlation between hot spring activity and plutons than between hot springs and faults.

We propose an alternative conceptual model for the geologic mechanism and ultimate heat source of the CAHSB geothermal activity: radiogenic heating by high-heat-producing (HHP) granites. Under this model, CAHSB fluids have derived their heat from radioactive decay of radioelements U, Th and K in nearby plutons. CASHB plutons are well-documented as containing elevated concentrations of U, Th and K. This hypothesis is supported by low (crustal) ratios of $^{3}He/^{4}He$ in CAHSB fluids.

Calculated values for radiogenic heat flow indicate that sufficient heat is generated to supply the heat for many of the hot springs in the CAHSB, but not all. This implies that these systems are not steady-state. We conclude that radiogenic heat production appears to be driving the development of small-scale – and temporally limited – hydrothermal convection cells. These cells efficiently transfer heat to the surface without elevating the regional heat flow pattern of Central and Western Alaska. Small-scale fractures and faults within CAHSB plutons provide the permeability pathways necessary for the convecting fluids to circulate.

Hence, the presence of radioactive granites alone is not sufficient to generate hydrothermal convection. Other factors such as permeability, meteoric water recharge, tectonic setting, and surrounding rock characteristics also determine whether hydrothermal convection systems will develop in relation to high-heat-producing granites.

2.7. Acknowledgements

Thanks to Mack Kennedy for providing the helium isotope analyses and aiding with interpretation. Thanks to Colin Williams for heat flow data and other contributions. Thanks so much to Bill Witte, Lena Krutikov and Dave West for technical support. Special thanks to Rusty Foraker, Rebecca Bailey, Sebastien Dos Santos, and John Sandru for their help in the field. Thanks also to and Marshall Reed, Ken Papp, Shirley Liss, Jim Vohden, and Diana Jozwik for assistance in data procurement. Finally, thanks to the Alaska Geological Society and UAF IGERT/RAP for funding support.

2.8. References

Alaska Division of Geologic and Geophysical Surveys (ADGGS), 2008. Interior Plutons Database. [Online]: http://www.dggs.dnr.state.ak.us/webgeochem/index.jsp

Arehart, G.B., Coolbaugh, M.F., and Poulson, S.R., 2003. Evidence for a Magmatic Source of Heat for the Steamboat Springs Geothermal System Using Trace Elements and Gas Geochemistry. Geothermal Resources Council Transactions, 27: 269-274.

Ballentine, C.J., Burgess, R. and Marty, B. 2002. Tracing fluid origin, transport and interaction in the crust. In: D. Porcelli, C.J. Ballentine, and R. Wieler (Editors), Noble Gases in Geochemistry and Cosmochemistry. Mineralogical Society of America, Washington, DC, pp. 47-64.

Barker, J.C., 1991. Investigation of Rare-Earth and Associated Elements, Zane Hills Pluton, Northwestern Alaska. USGS Open-File Report No. 36-91.

Baranwal, V.C., Sharma, S.P., Sengupta, D., Sandilya, M.K., Bhaumi, B.K., Guin, R., and Saha, S.K., 2006. Anewhigh background radiation area in the Geothermal region of Eastern Ghats Mobile Belt (EGMB) of Orissa, India. Radiation Measurements, 41: 602-610.

Barton, C. A., Zoback, M. D, and Moos, D., 1995. Fluid flow along potentially active faults in crystalline rock. Geology, 23 (8): 683-686.

Batini, F., Brogi, A., Lazzarotto, A., Liotta, D., and Pandeli, E., 2003. Geological features of Larderello-Travale and Mt. Amiata geothermal areas (southern Tuscany, Italy) Episodes, 26 (3): 239-244.

Beikman, H.M., compiler, 1980, Geologic Map of Alaska, USGS Map SG0002-1T and 2T. 1:2500000 map, 1 sheet.

Biggar, N., 1973. A Geological and Geophysical Study of Chena Hot Springs, Alaska, Master's Thesis, University of Alaska Fairbanks, Fairbanks, Alaska.

Bott, M. P., and Smithson, S. B., 1967. Gravity Investigations of subsurface shape and mass distributions of granitic batholiths. Bulletin of the Geological Society of America, 78: 859.

Broggi, A., Lazzarotto, A., Liotta, D., and Ranalli, G., 2003. Extensional shear zones as imaged by reflection seismic lines: the Larderello geothermal field (central Italy). Tectonophysics, 363 (1-2): 127-139.

Brugger, J., Long, N., McPhail, D.C., and Plimer, I., 2005. An active amagmatic hydrothermal system: The Paralana hot springs, Northern Flinders Ranges, South Australia. Chemical Geology, 222: 35– 64.

Cathles, L.M., Erendi, A.H., and Barrie, T., 1997. How Long Can A Hydrothermal System Be Sustained by a Single Intrusive Event? Economic Geology, 92: 766-771.

Chapman, R.M., and Patton, W.W. Jr., 1978. Reconnaissance geochemical sampling in the Melozitna Quadrangle, Alaska. ADDGS Open-file Report 78-699.

Christenson, B.W., Mroczek, E.K., Kennedy, B.M., van Soest, M.K., Stewart, M.C., and Lyon, G., 2002. Ohaaki reservoir chemistry: characteristics of an arc-type hydrothermal system in the Taupo Volcanic Zone, New Zealand. Journal of Volcanology and Geothermal Research, 115: 53-82.

Clautice, K.H., 1987. Rock Sample Analyses (1987): Circle, Fairbanks, Healy, and Kantishna Areas. ADDGS Public-data File 87-34.

Costain, J.K., Glover, III, L., and Sinha, A.K., 1980. Low-Temperature Geothermal Resources in the Eastern United States. EOS, 61: 1-4.

Dill, H., 1985, Granite-related and granite-induced ore mineralization on the western edge of the Bohemian Massif. In: High heat production granites, hydrothermal circulation and ore genesis. The Institute of Mining and Metallurgy, London, UK, pp. 55-70.

Durrance E.M., 1985. Hydrothermal circulation and isostasy, with particular reference to the granites of southwest England. In: High heat production granites, hydrothermal circulation and ore genesis. The Institute of Mining and Metallurgy, London, UK, pp. 71-85.

Druschel, G.K., and Rosenberg, P.E., 2001. Non-magmatic fracture-controlled hydrothermal systems in the Idaho Batholith: South Fork Payette geothermal system. Chemical Geology, 173 (4): 271-291.

Eakins, G.R., Jones, B.R., and Forbes, R.B., 1977. Investigation of Alaska's Uranium Potential. ADGGS Open-file Report No. 109.

East, J., 1982. Preliminary Geothermal Investigations at Manley Hot Springs. University of Alaska Fairbanks, Geophysical Institute Report No. UAG R-290.

Economides, M.J., Economides, C.A.E., Kunze, J.F. and Lofgren, B., 1982. A Fieldwide Reservoir Engineering Analysis of the Pilgrim Hot Springs, AK. Proceedings of the 8th Geothermal Reservoir Engineering Workshop, Stanford University, Stanford, CA, pp. 25-30.

Erkan, K., Holdmann, G., Blackwell., D. and Benoit, W., 2007. Thermal Characteristics of the Chena Hot Springs Alaska Geothermal System, Stanford 32nd Workshop on Geothermal Reservoir Engineering, Stanford University, California, pp. 117-124.

Fehn, U., 1985. Post-magmatic convection related to high heat production in granites of Southwest England: a theoretical study. In: High heat production granites, hydrothermal circulation and ore genesis. The Institute of Mining and Metallurgy, London, UK, pp. 99-112.

Foster, H.L., Laird, J., Keith, T.E.C., Cushing, G.W., and Menzie, W.D., 1983. Preliminary geologic map of the Circle quadrangle, Alaska. USGS Open-File Report No. 83-170-A.

Fournier, R.O., 1981. Application of water geochemistry to geothermal exploration and reservoir engineering. In: L. Rybach and L. J. P. Muffler (Editors), Geothermal Systems: Principles and Case Histories. Wiley & Sons, New York, pp. 3-31.

Galanis, S.P., Jr., and Williams, C.F., in preparation. An Updated Map and Database of Heat Flow Measurements in Alaska. USGS Open-file report.

Gault, H.B., Killean, P.L., West, W.S., 1953. Reconnaissance for Radioactive Deposits in the Northeastern Part of the Seward Peninsula, Alaska, 1945-47 and 1951. ADDGS Report No. C-250.

Ghiassi-Nejad, M., Beitollahi, M.M., Fallahian, N., and Saghirzadeh, M., 2005. New findings in the very high natural radiation area of Ramsar, Iran. International Congress Series, 1276: 13-16

Giggenbach, W.F., 1988. Geothermal Solute Equilibria: Derivation of Na-K-Mg-Ca geoindicators. Geochimica et Cosmochimica Acta, 52: 2749-2765.

Gomes, A.J., and Hamza, V.M., 2005. Geothermal Gradient and Heat Flow in the State of Rio de Janeiro. Revista Brasileira de Geofisica, 23(4): 325-347.

Herreid, G.H., 1969, Geology and geochemistry, Sithylemenkat Lake area, Bettles Quadrangle, Alaska: Alaska Division of Mines and Geology Geologic Report 35, 22 p., 1:50,000 map, 1 sheet.

Henley, R.W., Truesdell, A.H. and Barton, P.B.J., 1984. Chemical Geothermometers for Geothermal Exploration. Reviews in Economic Geology, 1: 31-43.

Hudson, T., 1979. Igneous and Metamorphic Rocks of the Serpentine Hot Springs Area, Seward Peninsula, Alaska. USGS Professional Paper No. 1079.

Hudson, T., and Arth, J.G., 1983. Tin-granites of Seward Peninsula, Alaska. Geological Society of America Bulletin, 94: 768-790.

Jones, B.R., and Forbes, R., 1976. Uranium and Thorium in Granitic and Alkaline Rocks in Western Alaska. Fairbanks, Alaska: M.S. Thesis, University of Alaska Fairbanks Department of Geology and Geophysics.

Kennedy, B.M., Lynch, M.A., Reynolds, J.H., and Smith, S.P., 1985. Intensive sampling of noble gases in fluids at Yellowstone: I. Early overview of the data; regional patterns. Geochimica et Cosmochimica Acta, 49 (5): 1251-1261.

Kennedy, B.M., and Truesdell, A.H., 1996. The Northwest Geysers high-temperature reservoir: evidence for active magmatic degassing and implications for the origin of the Geysers geothermal field. Geothermics, 25 (3): 365-387.

Kennedy, B.M. and van Soest, M.C., 2005. A helium isotope perspective on the Dixie Valley, Nevada hydrothermal system. Geothermics, 35: 26-43.

Kennedy, B.M. and van Soest, M. C., 2007. Flow of mantle fluids through the ductile lower crust: helium isotope trends. Science, 318: 1433-1436.

Kinnaird, J.A., Batchelor, J.E., Whitley, J.E., and Mackenzie, A.B., 1985.Geochemistry, mineralization and hydrothermal alteration of the Nigerian high heat-producing granites. In: High heat production (HHP) granites, hydrothermal circulation and ore genesis, Institution of Mining and Metallurgy, London, UK, pp. 169-198.

Kolker, A., Newberry, R., Larsen, J., Layer, P., and Stepp, P., 2007. Geologic Setting of the Chena Hot Springs Geothermal System, Alaska. Stanford 32nd Workshop on Geothermal Reservoir Engineering, Stanford University, Palo Alto, CA.

Kolker, A., Newberry, R., Larsen, J., and Layer, P., *in press*. Geologic Setting of the Chena Hot Springs, Alaska: A Fault-related Geothermal System Hosted by an Anomalously Radioactive Pluton. Journal of Volcanology and Geothermal Research.

Liss, S.A., Robinson, M.S., Burns, L.E., and Nye, C.J., 1993. Land Selection Unit 32 (Shungnak, Hughes, and Melotzina Quadrangles): Geochemistry, Major Oxides, Sample Locations, and Reference Data. ADGGS Public-data File 93-32.

Liss, S.A., Reifenstuhl, R.R., Clautice, K.H., Bundtzen, T.K., Newberry, R.J., Dover, J.H., and Blodgett, R.B., 1998. Rock geochemistry from the Manley mining district. ADGGS Public Data File 98-39, 41 pp., 1 disk.

Lockhart, A., and Kienle, J., 1981. Deep Seismic Refraction Profile in the Pilgrim River and Gravity Survey of the Central Seward Peninsula. In: E.M. Wescott, & D. L. Turner (Editors), Geothermal Reconnaissance Survey of the Central Seward Peninsula, Alaska. Fairbanks, AK, University of Alaska Fairbanks, Geophysical Institute Report No. UAG R-284.

Marjaniemi, D.K., and Basler, A.L., 1972. Geochemical Investigations of plutonic rocks in the western United States for the purpose of determining favorability for vein-type uranium deposits. U.S. Atomic Energy Commission Report No. GJO-912-16.

Matzco, J.J., and Freeman, V.L., 1955. Summary of Reconnaissance for Uranium in Alaska, 1955. Contributions to Economic Geology of Alaska: USGS Bulletin, 1155: 33-49.

Miller, T. P., 1972. Potassium-Rich Alkaline Intrusive Rocks of Western Alaska. Geological Society of America Bulletin, 83: 2111-2128.

Miller, T.P., Barnes, I., and Patton, W.W., 1973. Geologic Setting and Chemical Characteristics of Hot Springs in Central and Western Alaska. USGS Open-file Report No. 575.

Miller, T.P. and Bunker, C.M., 1975. U, Th, and K Analyses of Selected Plutonic Rocks from West-Central Alaska. ADGGS Open-file Report No. 75-216.

Miller, T.P. and Finch, W.I., 1976. Preliminary Report on Uranium-, Thorium-, and Rare-Earth-Bearing Rocks Near Golovin, Alaska. UGSS Open-file Report No. 76-71.

Miller, T.P., and Johnson, B.R., 1978. An occurrence of parsonite, a secondary uranium mineral, in alaskite of the Wheeler Creek Pluton, Alaska. ADGGS Open-file Report No. 78-315.

Miller, T., 1994. Geothermal Resources of Alaska. In: G. Plafker, and Berg, H. (Editor), The Geology of North America, Vol. G-1, The Geology of Alaska. The Geological Society of America, Boulder, CO.

Motyka, R.J., Forbes, R.B. and Moorman, M., 1980. Geochemistry of Pilgrim Springs Thermal Waters, University of Alaska Fairbanks, Geophysical Institute Report No. UAG R-271.

Motyka, R.J., Moorman, M.A., and Liss, S.A., 1983. Geothermal resources of Alaska. ADGGS Miscellaneous Publication 8, 1:2,500,000 map, 1 sheet.

Newberry, R.J., Wiltse, M.A., Queen, L.K., and Pinney, D.S., 1994. Geochemical major-oxide and trace-element data for rock samples collected in the Circle mining district, June 1993. ADGGS Public Data File No. 94-32A, 1:63,360 map, 1 sheet.

Newberry, R.J., Layer, P.W., Solie, D.N., and Burleigh, R.E., 1998. New $^{40}Ar/^{39}Ar$ Dates for Intrusions and Mineral Prospects in the Eastern Yukon-Tanana Terrane, Alaska--Regional Patterns and Significance. In: J.E. Gray and J.R. Riehle (Editors), Geologic studies in Alaska by the U.S. Geological Survey. USGS Professional Paper No. 1595.

Newberry, R.J., 2000. Mineral deposits and Associated Mesozoic and Tertiary Igneous Rocks within the Interior Alaska and adjacent Yukon portions of the 'Tintina Gold Belt': A Progress Report. University of Alaska, Fairbanks, Fairbanks, AK.

Nicholson, K., 1993. Geothermal Fluids: Chemistry and Exploration Techniques. Springer-Verlag, New York, 223 pp.

Oxburgh, E.R., and O'Nions, R.K., 1987. Helium loss, tectonics and the terrestrial heat budget. Science, 237: 1583–1588.

Page, R.A. and G. Plafker, 1995. Block rotation in east-central Alaska: A framework for evaluating earthquake potential? Geology, 23: 629-632.

Plant, J.A., O'Brien, C., Tarney, J., Hurdly, J., 1985. Geochemical criteria for the recognition of heat production granites. In: High Heat Production (HHP) Granites, Hydrothermal Circulation and Ore Genesis. Institute of Mining and Metallurgy, London, England, pp. 263–285.

Poreda, R.J., Jeffrey, A.W., Kaplan, I.R. and Craig, H., 1988. Magmatic helium in subduction-zone natural gases. Chemical Geology, 71: 199–210.

Ratchkovski, N. and Hansen, R., 2002. New Constraints on Tectonics of Interior Alaska: Earthquake Locations, Source Mechanisms, and Stress Regime. Bulletin of the Seismological Society of America, 92 (3): 998-1014.

Redfield, T.F., Scholl, D.W., Fitzgerald, P.G., Beck, M.E. Jr., 2007. Escape tectonics and the extrusion of Alaska: Past, present, and future. Geology, 35 (11): 1039-1042.

Reed, B.L., and Miller, T.P., 1980. Uranium and thorium content of some Tertiary granitic rocks in the southern Alaska Range. USGS Open-File Report No. 80-1052.

Reifenstuhl, R.R., Dover, J.H., Newberry, R.J., Clautice, K.H., Pinney, D.S., Liss, S.A., Blodgett, R.B., and Weber, F.R., 1998. Geologic map of the Tanana A-1 and A-2 quadrangles, central Alaska. ADDGS Public Data File 98-37A, 1:63,360 map, 1 sheet.

Rinehart, C.D., Light, T.D., and Shew, N.B., 1997, Petrography and Radiometric Ages for Selected Rocks from the Livengood Quadrangle, Alaska, Open-File Report 97-484-D, Alaska Division of Geologic and Geophysical Surveys, 24 pp.

Roy, R.F., Blackwell, D.D., and Birch, F., 1968. Heat generation of plutonic rocks and continental heat flow provinces. Earth and Planetary Science Letters, 5: 1-31.

Rybach, L., 1981. Geothermal Systems, Conductive Heat Flow, Geothermal Anomalies. In: L. Rybach and L. J. P. Muffler (Editors), Geothermal Systems: Principles and Case Histories. New York, Wiley and Sons, pp. 3-31.

Sainsbury, C.L., Hudson, T., Rachadoorian, R., and Richards, T., 1970. Geology, Mineral Deposits, and Geochemical and Radiometric Anomalies, Serpentine Hot Springs Area, Seward Peninsula, Alaska. Contributions to Economic Geology, Geological Survey Bulletin: 1312-H.

Saltus, R.W., Riggle, F.E., Clark, B.T., and Hill, P.L., 1999. Merged aeroradiometric data for Alaska; a web site for distribution of gridded data and plot files. USGS Open File Report No. 99-16.

Solie, D.N., Buntzen, T.K., Bowman, N.D., and Cruse, G.R., 1993a. Land Selection Unit 16 (Selawik, Candle, Norton Bay, Unalakleet, Kateel River, and Nulato Quadrangles): References, DGGS Sample Locations, Geochemical and Major Oxide Data. ADGGS Public-data File No. 93-32.

Solie, D.N., Wiltse, M.A., Gilbert, W.G., and Kline, J.T., 1993b. Land Selection Unit 17 (Nulato Quadrangle): References, DGGS Sample Locations, Geochemical and Major Oxide Data. ADGGS Public-data File No. 93-17.

Solie, D.N., Buntzen, T.K., Bowman, N.D., and Cruse, G.R., 1993c. Land Selection Unit 18 (Melotzina, Ruby, Nulato, and Kateel River Quadrangles): References, DGGS Sample Locations, Geochemical and Major Oxide Data." ADDGS Public-data File No. 93-18.

Solie, D.N., Wiltse, M.A., Harris, E. E., and Roe, J. T., 1993d. Land Selection Unit 34 (Shungnak, Hughes, and Melotzina Quadrangles): Geochemistry, Major Oxides, Sample Locations, and Reference Data. ADGGS Public-data File No. 93-34.

Sorey, M.L., Kennedy, B.M., Evans, W.C., Farrar C.D., and Suemnicht G.A., 1993. Helium isotope variations associated with crustal unrest in Long Valley Caldera, California, in 1989-1992. Journal of Geophysical Research, 98: 15871-15889.

Stone, M., and Exley, C. S., 1985. High heat production granites of southwest England and their associated mineralization: a review. In: High heat production granites, hydrothermal circulation, and ore genesis. London, UK: Institution of Mining and Metallurgy, pp. 571-593.

Torgerson, T., 1993. Defining the role of magmatism in extensional tectonics: Helium 3 fluxes in Extensional Basins. Journal of Geophysical Research, 9 (B9): 16257-16269.

Turner, D.L., and Forbes, R.B., 1980. A geological and geophysical study of the geothermal energy potential of Pilgrim Springs, Alaska. University of Alaska Fairbanks, Geophysical Institute Report No. UAG R-271.

Turner, D.L., and Swanson, S.E., 1981. Continental rifting - a new tectonic model for geothermal exploration of the central Seward Peninsula. In: E. Wescott and D.L. Turner (Editors), Geothermal reconnaissance survey of the central Seward Peninsula. University of Alaska Fairbanks, Geophysical Institute Report UAG-R 284, pp. 7-36.

U.S. Geological Survey (USGS), 2007. Geothermal Database for Alaska.

Wallace, A.R., 1979. Occurrence of Uranium in Rocks of the Ekiek Creek Complex, Western Alaska. ADGGS Open-file Report No. 79-1653.

Wedow, H., and White, M.G., 1949. Reconnaissance for Radioactive Deposits in East-Central Alaska, 1949. USGS. circular 385.

Welhan, J. A., Poreda, R. J., Rison, W., & Craig, H. 1988. Helium isotopes in geothermal and volcanic gases of the western United States, I. Regional variability and magmatic origin. Journal of Volcanology and Geothermal Research, 34: 185-199.

Wescott, E., and Turner, D., 1981a. A Geological and Geophysical Study of the Chena Hot Springs Geothermal Area, Alaska. University of Alaska Fairbanks, Geophysical Institute Report No. UAG-R-271.

Wescott, E. and Turner, D., 1981b. Geothermal Reconnaissance Survey of the Central Seward Peninsula, Alaska. University of Alaska Fairbanks, Geophysical Institute Report No. UAG R-284.

West, W.S., 1948. Reconnaissance for Radioactive Deposits in the Darby Mountains, Seward Peninsula, Alaska, 1948. USGS Circular 300.

White, M.G., West, W.S., and Matzco, J.J., 1968. Reconnaissance for Radioactive Deposits in the Vicinity of Teller and Cape Nome, Seward Peninsula, Alaska, 1946-47. USGS Circular 244.

Wilson, F.H., Dover, J. H., Bradley, D. C., Weber, F. R., Bundtzen, T. K., and Haeussler, P. J., 1998. Geologic Map of Central (Interior) Alaska. 1:63,360 map, 1 sheet.

Wiltse, M.A., Queen, L.K., and Pinney, D.S., 1994. Geochemical trace-element data for rock samples collected in the Circle mining district, June 1993. ADGGS Public Data File 94-31A, 1:63,360 map, 1 sheet.

Wisian, K.W., and Blackwell, D.D., 2004. Numerical modeling of Basin and Range geothermal systems. Geothermics, 33 (6): 713-741

Wood, C.A., and Kienle, J. (Editors.), 1990. Volcanoes of North America. Cambridge, U.K: Cambridge University Press, 354 pp.

Appendix 2.A: U, Th concentration data for CAHSB plutons.

Hot Springs name	Sample	U (ppm)	Th (ppm)	Pluton name	Reference
Serpentine	AK100	13	65.6	Serpentine	Hudson and Arth, 1983
Serpentine	AK101	33.8	53.8	Serpentine	Hudson and Arth, 1983
Serpentine	-	20	62	Serpentine	Hudson and Arth, 1983
Serpentine	77AH3B	30.7	27.6	Serpentine	Hudson and Arth, 1983
Serpentine	77AH3A	32.6	32.1	Serpentine	Hudson and Arth, 1983
Granite Mtn	2323	62.3	117	Granite Mtn	Jones and Forbes, 1976
Granite Mtn	2163	95.8	116	Granite Mtn	Solie et al., 1993a
Granite Mtn	2164	198	129	Granite Mtn	Solie et al., 1993a
Granite Mtn		7.28	36.21	Granite Mtn	Solie et al., 1993a
Granite Mtn		16.36	58.11	Granite Mtn	Miller 1975
Granite Mtn		9.49	39.16	Granite Mtn	Miller 1975
Granite Mtn		5.29	10.94	Granite Mtn	Miller 1975
Granite Mtn		5.5	24.3	Granite Mtn	Miller 1975
Granite Mtn		4.24	21.71	Granite Mtn	Miller 1975
Kwiniuk, Clear Ck., Lava Ck.		7.3	27.3	Darby	Miller 1975
Kwiniuk, Clear Ck., Lava Ck.		17.2	33.9	Darby	this study
Kwiniuk, Clear Ck., Lava Ck.		7.92	55.18	Darby	this study
Kwiniuk, Clear Ck., Lava Ck.		10.29	51.9	Darby	Miller and Bunker, 1975
Kwiniuk, Clear Ck., Lava Ck.		15.89	83.75	Darby	Miller and Bunker, 1975
Kwiniuk, Clear Ck., Lava Ck.		17.33	68	Darby	Miller and Bunker, 1975
Kwiniuk, Clear Ck., Lava Ck.		10.36	64.65	Darby	Miller and Bunker, 1975
Kwiniuk, Clear Ck., Lava Ck.		13.58	50.76	Darby	Miller and Bunker, 1975
Kwiniuk, Clear Ck., Lava Ck.		8.81	48.77	Darby	Miller and Bunker, 1975
Kwiniuk, Clear Ck., Lava Ck.		6.18	54.89	Darby	Miller and Bunker, 1975
Kwiniuk, Clear Ck., Lava Ck.		7.82	53.16	Darby	Miller and Bunker, 1975
Kwiniuk, Clear Ck., Lava Ck.		13.71	66.58	Darby	Miller and Bunker, 1975
Kwiniuk, Clear Ck., Lava Ck.		8.33	68.58	Darby	Miller and Bunker, 1975
Kwiniuk, Clear Ck., Lava Ck.		9.32	40.94	Darby	Miller and Bunker, 1975
Kwiniuk, Clear Ck., Lava Ck.		14.6	52.92	Darby	Miller and Bunker, 1975
Kwiniuk, Clear Ck., Lava Ck.		7.3	55.9	Darby	Miller and Bunker, 1975
Kwiniuk, Clear Ck., Lava Ck.		5.9	37.1	Darby	Forbes and Jones, 1976
Battleship Mt.		4.06	36.09	Kachauik	Forbes and Jones, 1976
Battleship Mt.		12.46	34.28	Kachauik	Forbes and Jones, 1976
Battleship Mt.		4.69	30.68	Kachauik	Miller and Bunker, 1975
Battleship Mt.		6.1	19.59	Kachauik	Miller and Bunker, 1975
Battleship Mt.		4.33	18.69	Kachauik	Miller and Bunker, 1975
Division, South, Hawk		8.9	36	Purcell mts	Miller and Bunker, 1975
Division, South, Hawk		7.9	43	Purcell mts	Miller and Bunker, 1975
Division, South, Hawk		10	30	Purcell mts	Solie et al., 1993b
Division, South, Hawk		10	28	Purcell mts	Solie et al., 1993b
Division, South, Hawk		11	26	Purcell mts	Solie et al., 1993b

Hot Springs name	U (ppm)	Th (ppm)	Pluton name	Reference
Division, South, Hawk	11	55.8	Purcell mts	Solie et al., 1993b
Division, South, Hawk	4.4	13	Purcell mts	Solie et al., 1993b
Division, South, Hawk	7.5	42	Purcell mts	Solie et al., 1993b
Division, South, Hawk	11	46	Purcell mts	Solie et al., 1993b
Division, South, Hawk	2.9	12	Purcell mts	Solie et al., 1993b
Division, South, Hawk	3.7	12	Purcell mts	Solie et al., 1993b
Division, South, Hawk	3.5	23	Purcell mts	Solie et al., 1993b
Division, South, Hawk	28	50.1	Purcell mts	Solie et al., 1993b
Division, South, Hawk	4.4	26	Purcell mts	Solie et al., 1993b
Division, South, Hawk	11	49	Purcell mts	Solie et al., 1993b
Division, South, Hawk	12	38	Purcell mts	Solie et al., 1993b
Division, South, Hawk	8.8	22	Purcell mts	Solie et al., 1993b
Division, South, Hawk	7.1	23	Purcell mts	Solie et al., 1993b
Division, South, Hawk	11	29	Purcell mts	Solie et al., 1993b
Division, South, Hawk	3.5	10	Purcell mts	Solie et al., 1993b
Division, South, Hawk	1.8	5.3	Purcell mts	Solie et al., 1993b
Division, South, Hawk	2.1	6.3	Purcell mts	Solie et al., 1993b
Division, South, Hawk	12	20	Purcell mts	Solie et al., 1993b
Division, South, Hawk	9.1	22	Purcell mts	Solie et al., 1993b
Division, South, Hawk	8.3	22	Purcell mts	Solie et al., 1993b
Division, South, Hawk	17	41	Purcell mts	Solie et al., 1993b
Division, South, Hawk	7.6	15	Purcell mts	Solie et al., 1993b
Division, South, Hawk	12	19	Purcell mts	Solie et al., 1993b
Division, South, Hawk	1470	56.5	Purcell mts	Solie et al., 1993b
Division, South, Hawk	564	110	Purcell mts	Solie et al., 1993b
Division, South, Hawk	2000	5000	Purcell mts	Solie et al., 1993b
Division, South, Hawk	6.9	16	Purcell mts	Solie et al., 1993b
Division, South, Hawk	12	36	Purcell mts	Solie et al., 1993b
Division, South, Hawk	6.3	50	Purcell mts	Solie et al., 1993b
Division, South, Hawk	14.4	52.3	Wheeler Ck'	Solie et al., 1993b
Division, South, Hawk	13.4	45.2	Wheeler Ck'	Solie et al., 1993b
Division,Sun Mtn.	62.8	191	ZaneH:Boston Ridge	Barker, 1991
Division,Sun Mtn.	26.5	178	ZaneH:Boston Ridge	Barker, 1991
Division,Sun Mtn.	188	499	ZaneH:Boston Ridge	Barker, 1991
Division,Sun Mtn.	89.9	350	ZaneH:Boston Ridge	Barker, 1991
Division,Sun Mtn.	32.7	121	ZaneH:Boston Ridge	Barker, 1991
Division,Sun Mtn.	32.9	120	ZaneH:Boston Ridge	Barker, 1991
Division,Sun Mtn.	139	3281	ZaneH:SantaMaria	Barker, 1991
Division,Sun Mtn.	54.7	1161	ZaneH:SantaMaria	Barker, 1991
Division,Sun Mtn.	955	374	ZaneH:SantaMaria	Barker, 1991
Division,Sun Mtn.	176	5073	ZaneH:SantaMaria	Barker, 1991
Division,Sun Mtn.	23.3	746	ZaneH:SantaMaria	Barker, 1991
Division,Sun Mtn.	27.4	531	ZaneH:SantaMaria	Barker, 1991

Hot Springs name	Sample	U (ppm)	Th (ppm)	Pluton name	Reference
Division,Sun Mtn.		59.8	1619	ZaneH:SantaMaria	Barker, 1991
Division,Sun Mtn.		17.1	429	ZaneH:SantaMaria	Barker, 1991
Division,Sun Mtn.		25	766	ZaneH:SantaMaria	Barker, 1991
Division,Sun Mtn.		51.9	1574	ZaneH:SantaMaria	Barker, 1991
Division,Sun Mtn.		56.3	637	ZaneH:SantaMaria	Barker, 1991
Division,Sun Mtn.		217	3821	ZaneH:SantaMaria	Barker, 1991
Division,Sun Mtn.		52.4	1804	ZaneH:PotatoSaddle	Barker, 1991
Division,Sun Mtn.		147	4741	ZaneH:PotatoSaddle	Barker, 1991
Division,Sun Mtn.		167	4032	ZaneH:PotatoSaddle	Barker, 1991
Division,Sun Mtn.		224	5201	ZaneH:PotatoSaddle	Barker, 1991
Division,Sun Mtn.		5.9	25	ZaneH:PotatoSaddle	Barker, 1991
Division,Sun Mtn.		87.8	2078	ZaneH:PotatoSaddle	Barker, 1991
Division,Sun Mtn.		55.8	140	ZaneH: Border	Barker, 1991
Div+Sun Mtn.		2.3	3.2	Zane Hills	Solie et al., 1993b
Div+Sun Mtn.		2	4.7	Zane Hills	Solie et al., 1993b
Div+Sun Mtn.		97.3	2910	Zane Hills	Solie et al., 1993b
Div+Sun Mtn.		53.8	1220	Zane Hills	Solie et al., 1993b
Div+Sun Mtn.		29	401	Zane Hills	Solie et al., 1993b
Div+Sun Mtn.		37	602	Zane Hills	Solie et al., 1993b
Div+Sun Mtn.		10	45	Zane Hills	Solie et al., 1993b
Div+Sun Mtn.		11	47	Zane Hills	Solie et al., 1993b
Div+Sun Mtn.		64.4	1940	Zane Hills	Solie et al., 1993b
Div+Sun Mtn.		7.9	16	Zane Hills	Solie et al., 1993b
Div+Sun Mtn.		1.1	3	Zane Hills	Solie et al., 1993b
Div+Sun Mtn.		2.3	8.6	Zane Hills	Solie et al., 1993b
Div+Sun Mtn.		1	3.6	Zane Hills	Solie et al., 1993b
Div+Sun Mtn.		3.7	1.3	Zane Hills	Solie et al., 1993b
Div+Sun Mtn.		7.7	22	Zane Hills	Solie et al., 1993b
Div+Sun Mtn.		39	29	Zane Hills	Solie et al., 1993b
Sun Mtn.	3255	24	140	Sun Mt.	Solie et al., 1993c
Sun Mtn.	3292	5.2	20	Sun Mt.	Solie et al., 1993c
Sun Mtn.	3294	2.5	12	Sun Mt.	Solie et al., 1993c
Sun Mtn.	3295	7.3	32	Sun Mt.	Solie et al., 1993c
Sun Mtn.	3296	14	97.2	Sun Mt.	Solie et al., 1993c
Sun Mtn.	3324	39	100	Sun Mt.	Solie et al., 1993c
Sun Mtn.	3325	39	78.9	Sun Mt.	Solie et al., 1993c
Sun Mtn.	31938	39	160	Sun Mt.	Solie et al., 1993c
Sun Mtn.	31940	33	106	Sun Mt.	Solie et al., 1993c
T. Lake HS, Pocahontas		5.8	26	Indian Mt?	Solie et al., 1993d
T. Lake HS, Pocahontas		6.3	26	Indian Mt?	Solie et al., 1993d
T. Lake HS, Pocahontas		2.6	7.8	Indian Mt?	Solie et al., 1993d
T. Lake HS, Pocahontas		39	29	Indian Mt?	Solie et al., 1993d
T. Lake HS, Pocahontas		10	31	Indian Mt?	Solie et al., 1993d

Hot Springs name	Sample	U (ppm)	Th (ppm)	Pluton name	Reference
T. Lake HS, Pocahontas		4.9	14	Indian Mt?	Solie et al., 1993d
T. Lake HS, Pocahontas		5.1	18	Indian Mt?	Solie et al., 1993d
Dulbi Crk.		7.4	52	Kokrines Hills	Solie et al., 1993d
Kanuti	AK07-KHS-24	7.2	22.7	Kanuti	this study
Kanuti	AK07-KHS-22	8.3	32.3	Kanuti	this study
Kanuti	AK07-KHS-21B	12.2	33.2	Kanuti	this study
Kanuti	AK07-KHS-21A	4.9	7.9	Kanuti	this study
Kanuti	AK07-KHS-21B	4.6	7.8	Kanuti	this study
Kanuti	AK07-KHS-21A	8.1	42.3	Kanuti	this study
Kanuti	AK07-KHS-19	9.8	50.6	Kanuti	this study
Kanuti	AK07-KHS-11	12	26.2	Kanuti	this study
Kanuti	AK07-KHS-09A	8.3	24.2	Kanuti	this study
Kanuti	AK07-KHS-015	19.1	35.5	Kanuti	this study
Kanuti	AK07-KHS-05A	7.8	37.7	Kanuti	this study
Kanuti	AK07-KHS-02	6	35.1	Kanuti	this study
Kanuti	AK07-KHS-24B	4.1	32.1	Kanuti	this study
Kanuti	AK07-KHS-23	4.7	37.6	Kanuti	this study
Kanuti	AK07-KHS-20	6.8	28.4	Kanuti	this study
Kanuti	AK07-KHS-18	19.5	39	Kanuti	this study
Kanuti	AK07-KHS-16	18.2	39.1	Kanuti	this study
Kanuti	AK07-KHS-13	6.1	28.7	Kanuti	this study
Kanuti	AK07-KHS-08	9.1	25.1	Kanuti	this study
Kanuti	AK07-KHS-03	3.2	8.5	Kanuti	this study
Kanuti	KHS-03(duplicate)	3	10.1	Kanuti	this study
Kanuti	AK07-KHS-27	4.9	20.4	Kanuti	this study
Kanuti	AK07-KHS-25	4.7	12.6	Kanuti	this study
Kanuti	AK07-KHS-06F	8.2	25	Kanuti	this study
Tolovana	AK07-THS-03	5.5	23.9	Tolovana	this study
Tolovana	AK07-THS-01A	5.5	22.6	Tolovana	this study
Tolovana	AK07-THS-10	3.5	9.8	Tolovana	this study
Tolovana	AK07-THS-09	3	9.2	Tolovana	this study
Tolovana	AK07-THS-07	5.9	20.9	Tolovana	this study
Tolovana	AK07-THS-06	3.2	21	Tolovana	this study
Tolovana	AK07-THS-05	5.5	26.4	Tolovana	this study
Tolovana	AK07-THS-04	4.8	16.7	Tolovana	this study
Tolovana	AK07-THS-02B	4.4	18.2	Tolovana	this study
Tolovana	AK07-THS-02A	11.5	21.1	Tolovana	this study
Tolovana	AK07-THS-12	4.1	23	Tolovana	this study

Hot Springs name	Sample	U (ppm)	Th (ppm)	Pluton name	Reference
Tolovana	AK07-THS-11	5.6	19.4	Tolovana	this study
Tolovana	AK07-THS-08	2.5	14.5	Tolovana	this study
Circle	1013	9	57.9	Circle	Wiltse et al., 1994
Circle	1014	32	66.7	Circle	Wiltse et al., 1994
Circle	1015	14	64.4	Circle	Wiltse et al., 1994
Circle	1042	7.2	45	Circle	Wiltse et al., 1994
Circle	1043	11	68	Circle	Wiltse et al., 1994
Circle	1044	10	57.8	Circle	Wiltse et al., 1994
Circle	1053	14	53	Circle	Wiltse et al., 1994
Circle	1054	10	50.3	Circle	Wiltse et al., 1994
Circle	1055	9.2	50	Circle	Wiltse et al., 1994
Circle	1067	12	41	Circle	Wiltse et al., 1994
Circle	1080	52	87.7	Circle	Wiltse et al., 1994
Circle	1082	16	56	Circle	Wiltse et al., 1994
Circle	1099	5.3	31	Circle	Wiltse et al., 1994
Circle	1133	32	27	Circle	Wiltse et al., 1994
Circle	1752	10	32	Circle	Wiltse et al., 1994
Circle	1781	15	20	Circle	Wiltse et al., 1994
Circle	1796	11	38	Circle	Wiltse et al., 1994
Circle	2971	21	32	Circle	Wiltse et al., 1994
Circle	2972	30	50.7	Circle	Wiltse et al., 1994
Circle	4581	13	18	Circle	Newberry et al., 1994
Circle	4582	24	73	Circle	Newberry et al., 1994
Circle	4583	12	62	Circle	Newberry et al., 1994
Circle	4601	26	43	Circle	Newberry et al., 1994
Circle	4602	12	63	Circle	Newberry et al., 1994
Circle	4606	4.1	43	Circle	Newberry et al., 1994
Circle	4608		71	Circle	Newberry et al., 1994
Circle	4609	12	29	Circle	Newberry et al., 1994
Circle	4621	7.6	52.5	Circle	Newberry et al., 1994
Circle	4653	10	18	Circle	Newberry et al., 1994
Circle	4654	17	29	Circle	Newberry et al., 1994
Circle	4655	11	33	Circle	Newberry et al., 1994
Circle	4691	9.3	70.2	Circle	Newberry et al., 1994
Circle	4692	15	65.9	Circle	Newberry et al., 1994
Circle	4723	16	37	Circle	Newberry et al., 1994
Circle	1797A	7.8	44	Circle	Wiltse et al., 1994
Circle	1798A	19	74	Circle	Wiltse et al., 1994
Circle	CH61	23	78.8	Circle	Wiltse et al., 1994
Chena	056	10	40	Chena	Kolker et al., in press
Chena	CHS056	12	43	Chena	Kolker et al., in press
Chena	057-CHS		48	Chena	Kolker et al., in press
Chena	CHS057		44	Chena	Kolker et al., in press

Hot Springs name	Sample	U (ppm)	Th (ppm)	Pluton name	Reference
Chena	058-CHS	11	45	Chena	Kolker et al., in press
Chena	CHS058	13	46	Chena	Kolker et al., in press
Chena	061-CHS	12	41	Chena	Kolker et al., in press
Chena	CHS061	14	39	Chena	Kolker et al., in press
Chena	06CHS058B	11	46	Chena	Kolker et al., in press
Chena	07NO41B	14	46	Chena	Kolker et al., in press
Chena	07RN184C	8	32	Chena	Kolker et al., in press
Chena	07AK75	8	33	Chena	Kolker et al., in press
Chena	CHS062A	15	39	Chena	Kolker et al., in press
Chena	94rn05	16	44	Chena	Kolker et al., in press
Chena	08RN05A	12	21	Chena	Kolker et al., in press
Chena	08RN06A	10	20	Chena	Kolker et al., in press
Chena	08RN07A	16	23	Chena	Kolker et al., in press
Chena	08RN08A	10	23	Chena	Kolker et al., in press
Chena	08RN09A	9	25	Chena	Kolker et al., in press
Melozi		7.5*	30	Kokrines Hills	Chapman and Patton, 1978
Melozi		7.5*	30	Kokrines Hills	Chapman and Patton, 1978
Melozi		12.5*	50	Kokrines Hills	Chapman and Patton, 1978
Melozi		7.5*	30	Kokrines Hills	Chapman and Patton, 1978
Melozi		7.5*	30	Kokrines Hills	Chapman and Patton, 1978
Melozi		12.5*	50	Kokrines Hills	Chapman and Patton, 1978
Melozi		12.5*	50	Kokrines Hills	Chapman and Patton, 1978
Melozi		17.5*	70	Kokrines Hills	Chapman and Patton, 1978
Melozi		12.5*	50	Kokrines Hills	Chapman and Patton, 1978
Ray River	4236	11.4	41	Ray Mtns.	Chapman and Patton, 1978
Ray River	4239	8.1	29	Ray Mtns.	Chapman and Patton, 1978
Ray River	2961	10.3	37	Ray Mtns.	Solie et al., 1993d
Ray River	4501	8.3	30	Ray Mtns.	Solie et al., 1993d
Ray River	4502	15.6	56.2	Ray Mtns.	Solie et al., 1993d
Ray River	4503	16.9	60.6	Ray Mtns.	Solie et al., 1993d
W of Kilo	4543	38	175.6	Ray Mtns.	Solie et al., 1993d
W of Kilo	4545	7.4	34.2	Ray Mtns.	Solie et al., 1993d
W of Kilo	4166	2.6	12.0	Ray Mtns.	Solie et al., 1993d
W of Kilo	4087	7.1	32.8	Ray Mtns.	Solie et al., 1993d
W of Kilo	4088	28	129.4	Ray Mtns.	Solie et al., 1993d
W of Kilo	4155	4.7	21.7	Ray Mtns.	Solie et al., 1993d
W of Kilo	4165	9.4	43.4	Ray Mtns.	Solie et al., 1993d
W of Kilo	4156	29	134.0	Ray Mtns.	Solie et al., 1993d
W of Kilo	4157	3.4	15.7	Ray Mtns.	Solie et al., 1993d
W of Kilo	4105	23	106.3	Ray Mtns.	Solie et al., 1993d
W of Kilo	4085	17	78.6	Ray Mtns.	Solie et al., 1993d
W of Kilo	4086	10	46.2	Ray Mtns.	Solie et al., 1993d
W of Kilo	4547	17	78.6	Ray Mtns.	Solie et al., 1993d

Hot Springs name	Sample	U (ppm)	Th (ppm)	Pluton name	Reference
W of Kilo	4548	18	83.2	Ray Mtns.	Solie et al., 1993d
E of Kilo	2995	40	184.8	Ray Mtns.	Solie et al., 1993d
E of Kilo	2996	65.9	304.5	Ray Mtns.	Solie et al., 1993d
E of Kilo	2997	73	337.3	Ray Mtns.	Solie et al., 1993d
E of Kilo	2998	61.1	282.3	Ray Mtns.	Solie et al., 1993d
E of Kilo	2999	58	268.0	Ray Mtns.	Solie et al., 1993d
E of Kilo	4092	50.8	234.8	Ray Mtns.	Solie et al., 1993d
E of Kilo	4094	17	78.6	Ray Mtns.	Solie et al., 1993d
E of Kilo	4095	31	143.3	Ray Mtns.	Solie et al., 1993d
E of Kilo	4096	60.8	281.0	Ray Mtns.	Solie et al., 1993d
E of Kilo	4097	1.7	7.9	Ray Mtns.	Solie et al., 1993d
E of Kilo	4171	1.1	5.1	Ray Mtns.	Solie et al., 1993d
E of Kilo	4158	50	231.1	Ray Mtns.	Solie et al., 1993d
E of Kilo	4159	28	129.4	Ray Mtns.	Solie et al., 1993d
E of Kilo	4160	39	180.2	Ray Mtns.	Solie et al., 1993d
E of Kilo	4522	42	194.1	Ray Mtns.	Solie et al., 1993d
E of Kilo	4551	41	189.5	Ray Mtns.	Solie et al., 1993d
E of Kilo	4552	30	138.6	Ray Mtns.	Solie et al., 1993d
E of Kilo	4553	38	175.6	Ray Mtns.	Solie et al., 1993d
E of Kilo	4554	29	134.0	Ray Mtns.	Solie et al., 1993d
E of Kilo	4555	46	212.6	Ray Mtns.	Solie et al., 1993d
E of Kilo	4556	31	143.3	Ray Mtns.	Solie et al., 1993d
E of Kilo	4557	47	217.2	Ray Mtns.	Solie et al., 1993d
E of Kilo	4558	20	92.4	Ray Mtns.	Solie et al., 1993d
E of Kilo	4559	32	147.9	Ray Mtns.	Solie et al., 1993d
E of Kilo	4560	38	175.6	Ray Mtns.	Solie et al., 1993d
E of Kilo	4561	61.5	284.2	Ray Mtns.	Solie et al., 1993d
E of Kilo	4562	56.4	260.6	Ray Mtns.	Solie et al., 1993d
E of Kilo	4563	58.1	268.5	Ray Mtns.	Solie et al., 1993d
E of Kilo	4564	42	194.1	Ray Mtns.	Solie et al., 1993d
E of Kilo	4565	31	143.3	Ray Mtns.	Solie et al., 1993d
E of Kilo	4240	74.5	344.3	Ray Mtns.	Solie et al., 1993d
Manley	97RR168B	40	164.8	Manley	Liss et al, 1998
Manley	97SL229A	10	41.2	Manley	Liss et al, 1998
Manley	97KC049A	10	41.2	Manley	Liss et al, 1998
Manley	97SL052C	10	41.2	Manley	Liss et al, 1998
Circle	4607	8.576515	38	Circle	Newberry et al, 1994
Circle	4608	16.07045	71	Circle	Newberry et al, 1994

*Indicates estimated value from local U:Th ratio.

CHAPTER 3:

Geothermal Development at Hot Springs in Central Alaska: A Potential Sustainable Energy Source for Remote Communties[3]

Abstract

Small-scale geothermal energy development may be a potential solution to the problems caused by diesel power generation in some remote Alaskan communities. This study examines whether similar geothermal development is sustainable for the 15 communities in Western and Central Alaska relatively close to low-temperature hot springs similar to Chena Hot Springs. Sustainable production of geothermal energy ensures the renewability of the energy supply, minimizes environmental impacts, and enhances the social-ecological resilience of its users. It is therefore an interdisciplinary problem requiring a combined geoscientific and socio-economic approach. We use geologic, geochemical, and hydrologic methods to assess the power production capacity of hot springs close to potential users in Western and Central Alaska and to evaluate the performance of the power extraction system at Chena Hot Springs from a resource perspective. We then develop an economic model for comparing the costs and benefits of geothermal vs. diesel generation that includes up-to-date cost assumptions as well as quantitative treatment of market externalities operating in this system. The cost analysis model is run under three scenarios with respect to renewable energy development in Alaska. Future fuel prices, heating benefits, financial incentives for renewable

[3] Prepared for submission in Geothermics.

development, and fuel-related subsidies for CAHSB communities have the largest impact on the cost analysis. Other components (carbon taxes, greenhouse benefits, fuel spill costs) have a lesser impact. This combined geoscientific/socio-economic approach is unconventional but extremely valuable in its comprehensive treatment of the concept of sustainability. In addition, it provides clear guidance with respect to decision-making about long-term energy supply. Several policy recommendations are given that would promote the sustainability of energy production from low-temperature geothermal resources and enhance the resilience of rural Alaskan social-ecological systems.

3.1. Introduction

> "Although the earth is an immense source of heat, most of this heat is either buried too deeply or too diffuse to be exploited economically. However, in some places the heat is concentrated as a result of certain geological and hydrological processes, and it is in these geothermal regions that conditions sometimes occur which allow the heat to be extracted through drill-holes sunk to modest depths in the earth's crust." (Lumb, 1981)

Geothermal energy resources in many parts of Alaska hold potential for displacing diesel fuel, reducing and stabilizing energy costs, stimulating local economic development, reducing fuel spills, and decreasing air pollution and greenhouse gas emissions (REAP, 2006). In 2007, electricity in rural Alaska was almost invariably produced by diesel generators. This is unsustainable, especially as the costs of fossil resources continue to increase. Between 2002 and 2007, the median price of diesel fuel increased by 72% to $0.71/l ($2.70/gal) in rural communities (Crimp et al., 2007). The sharp increase has had a profound impact on rural communities (Haley and Saylor, 2007).

High diesel prices are a serious economic problem statewide, as the state subsidizes electricity production in remote communities (the state currently pays over $15M in energy subsidies to rural utilities and faces pressure to increase that amount). Reliance on diesel also generates carbon emissions, increases the risk of fuel spills, and perpetuates reliance on politically tenuous subsidies.

Recent small-scale geothermal development at Chena Hot Springs, Alaska (CHS) has demonstrated many benefits of geothermal energy use in rural Alaska, such as: lowering diesel fuel costs, providing local jobs, boosting tourism, producing fresh vegetables from geothermally-heated greenhouses, among others. The hot springs at Chena are the lowest temperature geothermal fluids ever tapped for power generation in the world. This technological innovation has opened up many possibilities for utilizing Alaska's low-temperature resources, which were previously eliminated as potential sites for power generation. Chena Hot Springs lies in the eastern part of the Central Alaskan Hot Springs Belt (CAHSB), a vast low temperature geothermal resource with several hot springs located relatively close to population centers.

Despite the proven existence of high-potential reservoirs, geothermal resources in Alaska remain largely unexploited. A major problem has been the distance between high-grade geothermal resources and potential users. This has changed now that Alaska's low-grade geothermal resources are candidates for development. Another problem has also been the high risk of investing in resources about which relatively little is known.

The purpose of this study is to determine whether small-scale geothermal development is sustainable for remote communities in Central and Western Alaska. This

study investigates the capacity of geothermal resources near communities in the CAHSB and investigates the sustainability of energy production from these resources.

3.2. Background and Previous Work

3.2.1. Geothermal energy from hydrothermal systems

Geothermal heat is usually exploited for energy via hydrothermal systems. In hydrothermal systems, geothermal heat is transferred to groundwater primarily by convection, though some conductive heat transfer can occur (Duffield and Sass, 2003). In high-temperature systems (<250 °C), almost all of the heat transfer is convective. The relative importance of convection vs. conduction is more complex for low-temperature systems (Rybach, 1981). Whatever the mechanism of heat transfer is at depth, hydrothermal fluids are always transported via convection to earth's surface. Hence, hydrothermal systems have three components: 1) a heat source; 2) circulating groundwater; and 3) a 'plumbing system' of sub-vertical permeability (fractures or faults) that enables groundwater to efficiently convect through or around the heat source. The heat source can be shallow (magma or shallow hot rock) or deep (crustal depths of 4 km or greater).

Geothermal energy can be used for a range of applications, from indirect use (electric power generation) to direct use (heat applications). In low- to moderate-temperature geothermal areas (fluids <150 °C), energy is extracted via *binary-cycle* or Organic Rankine Cycle (ORC) power plants. In binary plants, hydrothermal fluid and a

secondary ("binary") fluid with a boiling point lower than water pass through a heat exchanger. Heat from the hydrothermal fluid causes the secondary fluid to flash to vapor, which then drives the turbines. The binary unit at Chena Hot Springs utilizes 80 °C fluids and operates at approximately 8.5 % efficiency to generate a net 350-400 kW. Actual power produced is partially dependent upon the cooling source and temperature. Water at 40-50 °C is used for cooling during summer months, and in the winter the system is switched to run off an air-cooled condenser system that can achieve higher than rated efficiency and output during the cold winter months. Spent geothermal fluid is reinjected into the system to maintain reservoir integrity.

Low-temperature hydrothermal fluids and/or spent fluids from electric plants can also be used to provide direct heat for buildings, greenhouses, food processing, absorption chilling, and a variety of other applications (Barbier, 2002).

3.2.2. Sustainable development, resilience, and geothermal energy production

One of the principal benefits of geothermal power is sustainable development (Kagel, 2006; USDOE, 2005). Sustainable development is defined by the World Commission on Environment and Development as "*development that meets the needs of the present without compromising the ability of future generations to meet their own needs"* (Brundtland Commission, 1987). Geothermal development is generally considered sustainable because it provides renewable energy production that is reliable over multi-generational timescales (via secure, domestic, baseload power) as well as long-term benefits to users (such as near zero fuel costs, near-zero air emissions and

associated health impacts, and stable jobs) and the economy (via development stimulated by the availability of low-cost power) (Kagel, 2006).

Geothermal is consistently available, but geothermal reservoirs must be managed properly in order to ensure resource sustainability, and thus, geothermal plants have potential resource availability concerns (Kagel, 2006). Sustainable production of a geothermal resource ensures the renewability of the energy supply. In sustainably produced geothermal fields, energy extracted from a resource is replaced by an equal additional amount of energy on the same time scale (Stefansson, 2000). Production declines in geothermal fields, such as the Geysers and Larderello, have been attributed to unsustainable energy production (overproduction and/or improper re-injection). In contrast, many geothermal fields have sustained relatively constant energy production (23.5 MW) for more than three decades (e.g., Matsukawa, Japan: Hanano, 2003; Laugarnes, Iceland: Axelsson and Steffanson, 2003).

Determination of the sustainability of production from a given hydrothermal resource depends on both geoscientific and economic factors, and these factors can, in principle, all be determined (Wright, 1998). For the CAHSB resource, many geoscientific parameters (the available amount of heat in the system, the rate of resupply by conduction, fluid recharge from depth) are not known, so our approach is deductive: we assume 1) necessary parameters can be estimated from available surface and near-surface data; and 2) the performance of the geothermal development at Chena Hot Springs (CHS) can be used as a proxy, since it is analogous to the rest of the CAHSB springs (Kolker et al., in preparation).

Measuring social sustainability is much more difficult than measuring resource sustainability. Minimizing the environmental impact of development is one way of augmenting social sustainability, so we examine the impact of the CHS development in the context of potential development elsewhere in the CAHSB. To measure social sustainability, we draw from resilience theory. Resilience is a property of linked social-ecological systems (SESs), which are complex systems with countless variables at play but only a few key controlling variables. There are also exogenous drivers, which control the system but are not variables within the system, such as climate change, national policy, etc. If rapid changes (perturbations) occur with respect to one or more of these key variables or exogenous drivers the system can cross a *threshold*, which kicks the entire system into a new state. One definition of resilience, then, is the maintenance of fundamental properties of a system in the face of perturbations (www.resalliance.org). An SES is resilient if it can absorb perturbations without crossing a threshold and is vulnerable when it is close to a threshold (Chapin et al., 1996).

3.2.3. Geothermal resources of the Central Alaska Hot Springs Belt (CAHSB)

The availability of a geothermal resource is highly site-specific, and restricted to small areas relative to other energy sources such as solar, wind, and hydro. Alaska possesses substantial geothermal resources but few are well-characterized (Kolker et al., 2007). Most exploratory geothermal work in Alaska occurred during the period 1970-1985, driven by the energy crisis of the 1970's. Preliminary exploration studies were started for the Central Alaskan Hot Springs Belt (CAHSB) during this period but never

completed. Motyka et al. (1983) surveyed 111 known hot springs and other geothermal manifestations in the state, and recorded temperature, flow rate, fluid chemical composition, and other data for selected sites. Several more detailed studies took place at individual hot springs sites (e.g., Wescott and Turner, 1981; East, 1982).

The CAHSB stretches from the Seward Peninsula to the Yukon Territory. Hot springs in the CAHSB are lower-temperature resources (<100 °C) than elsewhere in Alaska, but in many cases they are closer to population centers than high-temperature resources. Fifteen communities in Central and Western Alaska are located within 45 miles of a geothermal resource. These communities are: Elim, Golovin, White Mountain, Koyuk, Buckland, Kobuk, Shungnak, Hughes, Huslia, Ruby, Tanana, Minto, Manley, Circle, and Central. Many of these communities suffer extremely high costs of power. These 15 communities are likely candidates for geothermal development and thus are the subject of this study.

The low temperature geothermal resource of the Central Alaska Hot Springs Belt is poorly understood and is commonly attributed to deep circulation of meteoric water along faults and fractures. Kolker et al. (2007) proposed an alternative heat source model as the driver of geothermal activity in the CAHSB: radiogenic heating from high-heat-producing granites. Regardless of the heat source model, CAHSB resources are remarkably similar in fluid chemistry, temperature, and geologic setting (Miller et al., 1973) and hence almost certainly originate from a similar geologic mechanism. In this sense, the resource can be considered as one regime.

The geothermal power plant at Chena Hot Springs resort (CHS) is the only location in the CAHSB where power is currently being produced. The binary plant was installed in 2006 and has a capacity of 400 kW via two modular units of 200 kW each. Prior to the installation of the geothermal power plant, diesel generators supplied all power to CHS at a cost of 30 ¢ per kWh. The CHS power plant utilizes geothermal fluids of approximately 80 °C (176 °F) extracted from wells with maximum depths of <300m (<1000 ft). These fluids are a mix between deep thermal fluids and shallow groundwater (Kolker et al., in press) and are therefore probably not the hottest fluids in the system. Geothermal drilling also occurred at Pilgrim Hot Springs in the 1970's, but also to shallow depths (<300m). and the deep thermal source was never penetrated. Hence, the deep ("reservoir") characteristics of the CAHSB resource remain unknown despite the shallow drilling at CHS.

3.2.4. Energy economics in Alaska

Most of the economic growth in Alaska since 1969 has been caused by recycling of oil revenues from state government into the state's economy (Jorgensen, 1990). Since the 1970s, over 80% of Alaska state annual revenue has consistently come from oil industry taxes and royalties; in 2007 it was 88% (FY08 Summary of Appropriations, 2007). Because state income is almost solely a function of oil revenues, the state economy has experienced several major fluctuations in recent decades. For example, the collapse of the oil prices in the mid-1980s caused a drop in employment of 9.4% between 1986 and 1988, and between 1990 and 2005 the Alaska economy moved into a period of

slower growth because petroleum production has been in decline (Goldsmith, 2005). However, the rapid increase in crude oil prices since 2005 has brought billions of dollars of new revenue to the state treasury.

Ironically, Alaskans usually pay more for petroleum products than consumers in other states despite the fact that Alaska is rich in fossil fuels. This is because some refining occurs outside of the state, and resources are commonly located hundreds of miles over roadless terrain from potential users. Financial assistance is provided to electric utilities in most rural Alaska communities that rely on diesel fuel for power generation through the state's Power Cost Equalization (PCE) program. The PCE program is designed to pay a portion of the electric generation costs for a basic level of service for rural customers and community facilities. The state legislature appropriates approximately $15 million of state funds for the PCE program each year. Even so, rural utility customers often pay twice as much as urban consumers for their electricity (Goldsmith, 1998).

As is the case for other renewables, the dominant costs for geothermal energy projects in Alaska are up-front, or "capital" costs (Crimp et al., 2007). For example, the power plant at Chena Hot Springs cost ~$2 million to build, whereas a diesel generation system with equal output costs under ~$200,000. However, over a 20-year period, the diesel generation plant was estimated to have cost approximately 4 times as much as the geothermal plant, assuming no increase in fuel prices since 2005 (Gwen Holdmann, pers. comm). Many of the benefits of renewable energy generation are difficult to quantify, such as boosting local economies, creating jobs, diversifying the electricity market

(thereby reducing consumer dependence on fuel imports), and shielding consumers from fluctuations in market prices. These benefits therefore fall into the category of market externalities. Externalities are effects that are typically not taken into account in establishing the market price of goods or materials. A growing body of literature is attempting to accurately quantify such externalities, and the studies almost always show that investing in renewable technologies produces net benefits for society in the long term (Sison-Lebrilla and Tiangco, 2005; Clemmer et al., 2001). Renewable energy projects in Alaska can qualify for several grant and loan programs through the federal government such as Production Tax Credits (PTC), which provide tax benefits for the first ten years of a renewable energy facility's operation; Tribal Energy grants, and cost-share programs to facilitate exploration and development of renewables. Additionally, a 'renewable energy project fund' was created in April 2008 by the Alaska state legislature and provides grants and loans for renewable energy projects in the state.

For small-scale geothermal plants, initial costs per kW of capacity are even higher than for large-scale geothermal plants because economies of scale work against small plants. This is especially true in Alaska, where the resources are relatively unexplored so exploration and drilling costs are necessary for all projects. These essentially fixed costs have a major impact on electricity costs for small plants (Gawlik and Kutcher, 2000). Geothermal plants have the highest projected rated capacity factor (CF) of any renewable facility, making them competitive with other fuel sources (EIA). CF measures the amount of energy that a facility produces related to its rated capacity over time.

Difficult-to-quantify market externalities operating with respect to diesel fuel use play an important role in stifling renewable energy development as well. For example, the Denali commission, a federal-state partnership that provides cost-shared infrastructure projects across the state through federal funds, spends millions annually on diesel fuel-related projects such as bulk fuel storage, diesel plant installations and maintenance, etc. (www.denali.org). Funds are also provided through the Denali commission for electrical transmission projects. Another subsidy is available to offset the costs of heating fuel through the Alaska Division of Public Assistance's Heating Assistance Program (HAP). Finally, cleanup funds for fuel spills are appropriated through the state's Oil and Hazardous Substance Release and Response Fund.

A standard cost template for estimating the costs and benefits of renewable energy projects has not yet emerged. Several recent studies assessing the economic impacts of renewable energy policies have noted that more work is needed to explicitly treat the public benefits of renewable energy in energy economic analyses, including the fossil fuel hedge value of renewable energy and the benefits of reduced carbon emissions, employment and economic development impacts, etc. (Chen et al., 2007). Crimp et al. (2007) assessed the economics of small utility-scale hydroelectric, wind-diesel, and biomass-fired combined heat and power systems in rural Alaska under a range of future oil price assumptions. Geothermal power was not assessed in that study due to lack of consistent resource data, despite the fact that it "holds promise as an energy source in numerous locations" (Crimp et al., 2007 p. 2).

3.3. Methods

3.3.1. Assessing geothermal capacity for CAHSB communities

Whether geothermal energy production is a cost-effective or sustainable technology for a given community is, to a large extent, a function of the available resource potential. Unfortunately, the critical data needed—reservoir temperature and flow rate (Fig. 3.1)—are available for none of the hot springs. There is no way to determine these master parameters except by extensive drilling and pumping. Even at Chena Hot Springs (CHS), drilling has only occurred to maximum depths of 300m and has not hit "reservoir" fluids yet. In the absence of such parameters, we provide very rough estimates of resource capacity based on a combination of available data (surface temperature, fluid chemical composition and flow rate) combined with a 'standardization factors' created from the CHS data. In this section we examine the CHS system with regards to such standardization and then apply it to the other systems.

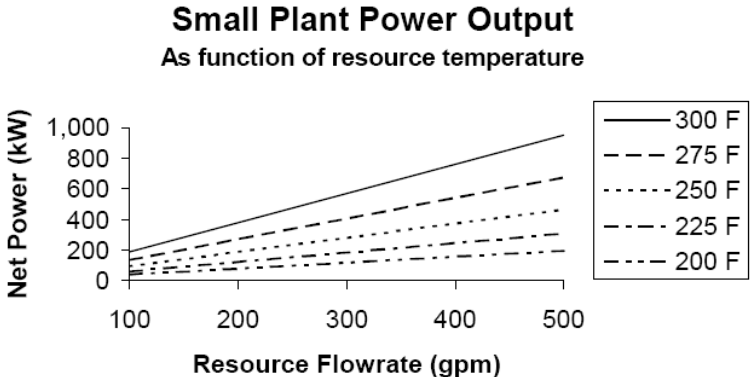

Figure 3.1. Net power plant output as a function of resource temperature and flow rate. Based on empirical data from 143 hot springs. Assumes 10% efficiency and a heat sink of 15° C. From Gawlik and Kutcher, 2000.

According to the Geothermal Resources of Alaska map (Motyka et al., 1983) 15 communities in Central and Western Alaska are located within 45 miles of a hot springs site. The individual resources proximal to these communities were assessed for capacity in terms of heat and electricity. Surface temperature, flow rate, chemical composition, and predicted reservoir temperature (by chemical geothermometry) data were compiled for the hot springs proximal to those 15 communities. These data were evaluated in the context of empirical data from the geothermal development at Chena Hot Springs. Available water volume for each of the springs was estimated via a scaling factor for natural flow rate vs. pumped capacity based on Chena Hot Springs production.

The binary Organic Rankine Cycle (ORC) unit at CHS uses fluids at <80 °C (<176 °F – well below boiling) and operates at approximately 8.5 % efficiency to generate a net 350-400 kW. These are the lowest temperature geothermal fluids used for electrical power generation in the world. That is why the efficiency of power generation is so low; however, the advantage is that the production fluids at Chena Hot Springs come from relatively shallow depths (100-270 m; 300-700 ft), reducing drilling costs. The extremely low-temperature fluids used at CHS represent a mixture of deep thermal fluids and shallow groundwater (Kolker et al., in press). Hence, they are *not* the hottest temperature of the system. Conventionally, geothermal resources are drilled to depths that reach the hottest fluids – or *nearly* the hottest – in a given system (often called "reservoir fluids"). For the purposes of this study, we assume that reservoir fluids will be utilized from depths greater than 1000 m (3000 ft).

Reservoir fluid temperatures can be indirectly estimated from regional heat flow patterns and/or geochemical methods. Regional heat flow patterns are uncertain for the CAHSB, so we relied on geothermometry: reservoir temperature estimates based on the chemical composition of surface fluids. Geothermal fluid geothermometry is based on the principle that fluids cool faster as they rise than they chemically re-equilibrate, so they retain their reservoir chemical characteristics. Some fluid characteristics are useful 'indexes' of the most recent temperature of equilibration between fluids and rocks because they are a direct function of reservoir fluid temperature. The two most widely used geothermometers involve silica concentration and relative amounts of Na, Ca, and K. The first is based on the principles that 1) quartz solubility is a function of temperature and 2) the kinetics of quartz precipitation are relatively slow, so that fluids upon cooling will become oversaturated with respect to quartz. The other major technique involves equilibration between Ca, Na, and K (alkalis) in fluid and in feldspar-bearing rocks. In practice, the choice and interpretation of geothermometer data by exploration geochemists is highly variable (Henley et al., 1984).

Of all the various chemical geothermometer methods, Kolker et al. (in press) argued that the chalcedony geothermometer was most appropriate for CAHSB fluids due to their low temperature and host rock characteristics. Hence, where silica concentration data was available, we used reservoir temperature estimates from chalcedony geothermometer methods after Fournier (1981). Where silica concentration data was not available, we used the average reservoir temperature for CAHSB fluids (92 °C).

The exact relationship between natural flow rates in geothermal systems and extractable volume of fluids for energy production is somewhat variable. It is a function of many factors, one of the most important of which is injection scheme, which varies widely from field to field. In some cases, such as at Balcova, Turkey, geothermal fluids are pumped at over ten times their natural flow rate without any observed decline in the resource (Serpen, 2004). In other cases, such as at Pauzhetsky, Russia, reservoir declines were observed when fluids were extracted at approximately 3 times their natural flow rate, but the resource has stabilized since fluid extraction was reduced to approximately twice the natural flow rate (Kiryukhin and Yampolsky, 2004). At CHS, geothermal fluids are extracted at approximately 4.5 times their natural flow rate (natural flow rate = 850 LPM; extraction rate = 3785 LPM), with no observed declines to the system. This rate is the total for all energy extraction, including power production and direct uses.

Due to this variability, we present two different estimates for the pumped capacity of CAHSB fluids. The first is based on the minimum ratio between natural flow rate and sustainable production rate (2:1) and the second is based on the ratio between natural flow rate and production rate at CHS (approximately 4.5:1). These two ratios were used as scaling factors to determine the fluid production rate for CAHSB springs.

We then compared the available generation capacity to the generation capacity required by CAHSB communities. Required generation capacity comes from converting consumption data to average electrical demand, then calculating peak by multiplying this by 2. No consumption data was available for the village of Ruby so we used the average kWh/capita for CAHSB communities and multiplied it by the population of Ruby.

3.3.2. Sustainability analysis of geothermal development at Chena Hot Springs

Hydrothermal systems require recharge in terms of both water and heat. Even in hydrothermal systems that are produced for geothermal energy, water recharge should keep the system in a state of dynamic equilibrium wherein the geothermal reservoir is continually recharged by re-injecting spent fluids into the geothermal reservoir (Nicholson, 1993). The geothermal production at CHS provides a useful empirical study of whether exploitation rates are sufficiently lower than regeneration/recharge rates, and by extension, whether CAHSB geothermal systems can sustain energy production at the scale of CHS.

Empirical data from the geothermal development at Chena Hot Springs was examined to identify and characterize any changes in the resource. These data include: 1) Downhole temperature and pressure data from wells at CHS between 2005 (prior to the installation of the power plant) and 2008, as measured by staff at Chena Hot Springs resort using a Kuster gauge; 2) Temperatures of the production fluids between 2006 and 2008, as recorded by staff at Chena Hot Springs resort; and 3) Temperatures of the cooling fluids over a two-month period in 2006, as recorded by staff at Chena Hot Springs resort.

Finally, we examined the probability and severity of potential environmental impacts from the geothermal development being investigated in the CAHSB, following a model created by Rybach (2003). The environmental impact of geothermal development varies by project type, but the potential environmental impacts of geothermal projects

include: air pollution, surface water pollution, underground pollution, land subsidence, high noise levels, well blowouts, conflicts with cultural/archaeological features, socioeconomic problems, and solid waste disposal (Rybach, 2003).

3.3.3. External benefits of geothermal energy

Effects that are typically not taken into account in establishing the market price of goods or materials are known in economics as "externalities." These factors, not necessarily apparent at first, directly impact the levelized cost of power over the long and short term. For example, the fossil fuel industry receives almost 80% of the subsidies supplied to the energy industry in the U.S. – this translates into billions of dollars each year (Kagel, 2006). In Alaska, subsidies for fossil fuel use in remote communities are strong disincentives to renewable energy development; however, positive externalities such as energy security and reliability are rarely explicitly accounted for in economic analyses of energy projects.

Where appropriate, we monetized externalities operating in this system in terms of benefits of geothermal development (avoided costs of diesel use). Where possible, we followed methods used in the literature; in other cases we developed our own methodology. Electrical load, population size, generation system (load size, operator, etc.) fuel use, and fuel cost data for each community comes from the Alaska Energy Authority (AEA) Power Cost Equalization program (PCE) statistics for 2007.

3.3.3.1. Quantifiable external benefits

Some quantifiable external benefits from geothermal energy production include: 1) elimination of fuel-related subsidies for electricity generation; 2) savings on heating fuel and elimination of emergency assistance for heating fuel costs; 3) benefits to the community from greenhouse production; 4) avoided fuel spills; and 5) avoided CO_2 emissions.

To quantify the amount of fuel-related subsidy dollars for electrical generation that geothermal development would reduce, we used FY07 PCE data from the Alaska Energy Authority, in dollar disbursements to each community per year, and expenditure data from the Denali commission for bulk fuel and power plant upgrade projects, reduced to statewide averages per community per year.

To quantify the savings in heating fuel and the reductions in emergency assistance for heating fuel costs, we assumed that the avoidable cost of heating oil would be $1 per gallon higher than the price of utility diesel fuel based on historical patterns in remote rural Alaska communities (Crimp et al, 2007). For heating fuel use, we assumed an average consumption of 1000 gal/household/yr for Interior and Western Alaska, considering the extremely cold winters in those regions. Household size was computed based on the most recent U.S. census bureau data on average household size for Interior and Western Alaska. Heating assistance disbursements per household come from the Alaska Heating Assistance Program (HAP, see description above). We assumed the $2795 maximum for low-income household assistance (ADHSS, 2007). Computations were performed assuming no escalation in fuel prices.

Costs of the geothermal heating system come from Rafferty (1998) and include the assumptions given in Table 3.1. Well costs (drilling, casing, cementing, and drill rig mobilization) are excluded as they are covered by the power plant analysis. The efficiency of a binary geothermal generation plant is typically around 10%, meaning that some 10 kW of heat (kWt) are required to generate 1 kWe of electricity. Hence, we assumed average available heat was 3 MWt (10X the average kWe capacity of 300 kWe).

Table 3.1. Geothermal direct heating system assumptions.

Peak Load: 3000 kWt = : 1E+07 Btu/hr
Load Factor: 0.25
Temp: 160 F
Flow: 500 gallons per minute
Capital costs: Pump & wellhead equipment $ 84,606
Annual maintenance costs: Pump maintenance = 60% of capital cost in 5-year intervals + One pump replacement + well head equipment maintenance = 1.5% of capital cost

Costs based on Rafferty (1998) and adjusted from 1998 by a 2.5% inflation rate.

To quantify the benefits provided by geothermal greenhouses, we used revenue calculations for the geothermal greenhouses at Chena Hot Springs from Mager et al. (2008). That study calculated the potential annual income for the optimal greenhouse from vegetable sales (projected yearly revenue minus yearly operating and maintenance costs such as labor, materials, repairs, etc.) as $146,755. This is probably a minimum since other studies (e.g. USDOE, 2005, for geothermal greenhouses in New Mexico) estimated the annual income for geothermal greenhouses of a similar size over twice that amount. These calculations assumed total initial (one-time up-front) cost for the greenhouses at $144,303, based on the Chena Hot Springs experience. These include costs for a 60ft x 72ft greenhouse kit (including structure, ventilation system, and

shipping), growing equipment, labor and equipment costs to erect the greenhouse, heating and lighting system, and piping costs. Well costs (drilling, casing, cementing, and drill rig mobilization) are excluded as they are covered by the power plant analysis. To these costs we added costs for on site warehouse and packaging plant, ($16,600); and piping costs ($84,000/mile, after Rafferty, 1998 and escalated to reflect 2008 costs) for each individual project. It is unclear whether the optimal greenhouse site is at the location of the hot springs (with road access) or in town (with fluids piped to town), so we present calculations for both scenarios.

To quantify the cost of avoided fuel spills, we used data from the Alaska Department of Environmental Conservation (ADEC) summary for 1995-2005. The study divided Alaskan communities into subareas; we used data from the subareas of Interior and Western Alaska. There are a total of 31 villages in the Western Alaska subarea and 57 villages in the Interior Alaska subarea. Our values for spills per community were generated from an average of the gallons spilled per subarea over 10 years and from estimates from ADEC. The most important factors in determining the cost of cleaning up fuel spills are location, total spill amount, and fuel type, which dictates cleanup method (Etkin, 1999). The average size of a spill is approximately 114 gallons (ADEC, 2007).

Totals for Interior and Western subareas was divided by the number of communities to obtain averages per community. These averages were used to calculate cleanup costs to the state per CAHSB community. There are ten subareas and therefore the Interior and Western subareas would be allocated approximately 2.2 million annually for cleanup costs. Hence, the average cost of cleaning up spills of this type is $25,000.

Our study excludes costs associated with oil transportation and production as well as private sector costs for cleaning up spills in the villages.

Finally, to quantify the costs of carbon (CO_2) emissions, we calculated emissions in lbs/yr per community using a value of 21.5531 lbs CO_2 per gallon of diesel fuel. Fuel use data comes from the FY07 PCE dataset compiled by the Alaska Energy Authority for electricity generation. The methodology for calculating costs of carbon emissions is highly variable at the present time so we develop different scenarios in section 3.3.

3.3.3.2. Non-quantifiable benefits

Geothermal energy production (power and heat) provide many benefits that are extremely difficult to quantify. In this section we identify benefits and specify which could potentially apply to particular CAHSB communities, but we do not monetize them. Energy security, heating security, food security, and price stabilization cannot be quantified but are undeniably important in a rural Alaskan setting. Another benefit is job creation from power plant operation and greenhouse operation; however, we did not attempt quantify this in dollars for the following reasons: it is unclear how many jobs geothermal may potentially displace, how geothermal jobs would affect the subsistence economy, and how many jobs per kW or per project are realistic for Alaskan geothermal projects.

3.3.4. Scenarios affecting renewable energy development in Alaska

The future costs of conventional generation as well as renewable generation are both uncertain. Such uncertainty can be evaluated, to a degree, through the use of scenario analysis. Three groups of scenarios were developed in order to explore how future developments would affect the economics of geothermal projects. A scenario is a coherent, internally consistent, and plausible description of a possible future state of the world. A scenario is not a *forecast*; each scenario is one alternative image of how the future can unfold (Carter and La Rovere, 1994). By offering insight into uncertainties and the consequences of current and possible future actions, scenarios support more informed and rational decision-making in situations of uncertainty. The critical assumptions that went into each scenario are given in Table 3.2.

Three major cost variables affect geothermal development in Alaska. These are (1) future diesel prices; (2) future costs of carbon emissions; (3) economic incentives available for renewable energy development. To develop realistic scenarios we examined the fuel price projections conventionally accepted by Alaska state agencies and projections developed by external studies, several pieces of legislation pertaining to renewable energy incentives for Alaska, and bills that would regulate carbon emissions which are currently pending before the U.S. Congress as well as published studies.

Data and information about economic incentives come from the U.S. Department of Energy's Database of State Incentives for Renewable Energy (DSIRE). Until 2006, federal cost-shares for particular aspects of geothermal development (typically drilling and/or transmission) were available for geothermal projects. That cost share is no longer

available, but U.S. Congress is presently considering a bill that would reinstitute such a program. This cost-share is assumed in our mid-range and favorable scenarios. In addition, funding has recently become available for renewable energy projects through the Alaska Renewable Energy project fund (RE fund), which was created in 2008 by the Alaska state legislature. Utility-scale renewable energy projects around Alaska would be eligible for both funds, though due to its very recent passage the award amount is not defined. For the mid-range scenario, we assume the award will consist of a state match to any federal awards; for the favorable scenario we assume the award will consist of half the transmission costs or $5 million, whichever is less.

In conventional economic analysis of projects, a discount rate is applied to determine the present value of a future asset. When this is done for the relatively long time periods of interest in sustainability, the present value of future geothermal production becomes very small. For example, the present value of $1,000 available 30 years hence discounted at a rate of 10% is $57. If discounted over 100 years, the same $1,000 is worth a mere $0.07 today. Using a discount rate this high there is little economic incentive for a developer to manage a resource in a sustainable way (Wright, 1998). Hence, we assume three different discount rates corresponding to each scenario.

Table 3.2. Critical assumptions used in scenarios presented in this study.

Critical Assumptions	**Scenario 1: Unfavorable to RE development**	**Scenario 2: Mid-range**	**Scenario 3: Favorable to RE development**
Fuel prices through 2030	Projection based on $73/bbl crude and dropping (U.S. Energy Information Administration)	Projection based on $110/bbl crude and holding (Alaska Energy Authority)	Projection based on current prices of $150/bbl crude and holding (this study)
Carbon taxes through 2030	None	$12/tonne CO_2 + 5% above inflation starting 2010 (Bingaman-Specter, 2007)	$32/tonne CO_2 + 4% above inflation starting 2015 (MIT, 2007)
Financial incentives	None	PTC (1.9¢/kWh) + minimum tribal grant award + federal cost-share for non-transmission capital costs + state match	PTC (1.9¢/kWh) + maximum tribal grant award + federal cost-share for non-transmission capital costs + state award of half transmission costs or $5M, whichever is less
Discount rate	5%	3%	0%

RE = Renewable Energy. Bbl=$Billions/barrel. PTC = production tax credit. References for particular assumptions are given in parentheses; details are discussed below.

3.3.4.1. Unfavorable

For this scenario we used projections from the U.S Department of Energy, Energy Information Administration Annual Energy Outlook (EIA, 2007) for crude oil and assuming that the cost to refine and deliver fuel to *individual* rural communities would follow historical patterns. This case assumes a $72.77/bbl crude oil cost, dropping over time to $58.66 in 2030 in inflation-adjusted dollars. The basic projection was adjusted by adding $0.05/gal to account for the long run price premium associated with ultra-low sulfur diesel fuel anticipated to be required in rural Alaska going forward from 2010 (Hayley and Saylor, 2007). This scenario assumes zero cost of carbon, that is, that carbon emissions in Alaska will not be subject to penalties imposed by the federal government in the near future. This scenario assumes that renewable energy projects will receive neither

grant funding nor financing incentives (loans, etc.) to assist with capital costs, nor tax credits to offset costs over time. This scenario assumes that fuel-related subsidies will continue to be available to rural communities following historical patterns. Finally, a real discount rate of 5% was chosen because it is consistent with the state's investment rates (it is the benchmark for what the Permanent Fund can earn).

3.3.4.2. Mid-range

This scenario follows the fuel price projections accepted by the Alaska Energy Authority (2008) of $110/bbl for crude oil from 2008-2030, assuming that the percent multiplier cost to refine and deliver fuel to *individual* rural communities would follow historical patterns. This scenario adds CO_2 emission fees based on the Bingaman-Specter Low Carbon Economy Act of 2007 (United States Senate, 2007). This bill adds the technology accelerator payment (TAP) of $12 per tonne of CO_2 equivalent escalated at 5% above inflation. This adds $0.029/l ($0.11/gal) in 2008 rising to $0.053/l ($0.20/gal) in 2020. This scenario assumes that geothermal energy projects will receive some financial incentives from the federal government in the near future, but that they will only be funded at the minimum levels available. The minimum funding available to Alaskan geothermal projects from federal sources includes the USDOE's Renewable production tax credit (PTC) program, and grant funding through USDOE's Tribal Energy Program. Production Tax Credits (PTC) provide tax benefits for the first ten years of a renewable energy facility's operation. This PTC provides a 1.9 cent tax credit for each kWh of power produced by an eligible facility as adjusted annually for inflation (Kagel, 2006).

USDOE's Tribal Energy Program provides a minimum of $500,000 of grant funding for renewable energy projects. We also consider funding opportunities via federal cost shares in this scenario. The last available cost share for geothermal development was 80% of the capital cost or $4,000,000, whichever was lower (Gawlik and Kutcher, 2000). Though that cost share is no longer available, the U.S. Congress is presently considering a bill that would reinstitute such a program (HR2304, The Advanced Geothermal Energy Research and Development Act of 2007). Since the present cost share ratio is unknown, our scenario assumes the last available cost-share subsidy of 80% of the capital cost or $4,000,000, whichever is lower. We assume the state will match federal funds through the RE fund. Finally, a real discount rate of 3% was assumed because it treats future generations with more equality with respect to present generations (Nordhaus, 2006).

3.3.4.3. Favorable

This scenario assumes fuel price projections based on a cost of $150/bbl for crude oil from 2008-2030, assuming that the percent multiplier cost to refine and deliver fuel to *individual* rural communities would follow historical patterns. In this scenario, we assumed the carbon tax price projection from the MIT Future of Coal study, which starts with a $32 per tonne of CO_2 equivalent escalated at 4% above inflation beginning in 2015. This adds $0.066/l ($0.25/gal) in 2015 rising to $0.122/l ($0.46/gal) in 2030. This scenario assumes that geothermal energy projects will receive financial incentives from the state and/or federal government at the maximum level available. For this scenario we used the same pieces of legislation as in the mid-range scenario, but assumed maximum

levels. The PTC rate is the same as in the mid-range scenario (2¢/kWh as of FY08). The maximum award from the Tribal Energy grants program is $500,000 or 25% of project costs. We apply the same cost share assumptions as in the mid-range scenario to this scenario, but instead of assuming a state match, we assume that the state will cost-share transmission costs with a cap at $5M through the RE Fund. Finally, for the favorable scenario, no discount rate was used (that is, future generations are treated with total equality with respect to present generations).

3.3.5. Cost comparison of geothermal versus diesel cases

We used a spreadsheet model to compare costs of geothermal energy generation vs. diesel generation for CAHSB communities. We used a lifetime of 22 years because most fuel price projections and carbon cost frameworks operate only through 2030; however geothermal plants typically last well beyond 22 years (Kagel, 2006). We present cost analyses operating under the three scenarios identified in section 3.3.

The cost analysis is presented both with and without inclusion of the quantifiable externalities identified in section 3.2. Externalities are included on a case-by-case basis: for example, PCE and other fuel-related subsidies (remote power system upgrades and bulk fuel storage upgrades) are included in the cost calculations for diesel generation only if a community is slated to receive such upgrades in the future. Fuel spill costs are included in the costs of diesel generation.

3.3.5.1. Geothermal cost assumptions

Three cost components characterize geothermal development: (1) resource exploration and confirmation costs, including exploratory drilling (temperature gradient slimholes); (2) power production and transmission; and (3) operations and maintenance costs. We generated costs in $/kW for resource exploration, confirmation, and power production by averaging a number of costs from the literature and from the Chena Hot Springs project (Table 2.3). Data for capital costs (excluding transmission costs) comes from the Chena Hot Springs project (Gwen Holdmann, pers. comm.); other industry quotes; the U.S. government (USDOE, 2005; Hance, 2005); and independent studies of geothermal development in the U.S. (Sison-Lebrilla and Tiangco, 2005; Kagel, 2006; Gawlik and Kutcher, 2000). If a range was given, the high end was used. Costs of exploratory/thermal gradient drilling are included in exploration and confirmation category, but production drilling costs are included in their own category since they are highly variable (highly dependent on resource depth)

Unfortunately, many of the costs embedded in published sources are highly variable and required further examination for Alaska. For example, transmission and drilling costs are typically higher for Alaska due to the cost of mobilization in remote and rugged conditions. Production drilling costs were calculated from an empirical relationship given in GeothermEx (2004) multiplied by the "Alaska factor" of 2x, yielding a value of $5,212/kW. We added this cost to averages from the other studies to generate an estimated total capital cost for a small geothermal plant in the CAHSB (Table 3.3). This table does not include transmission costs.

Table 3.3. Capital costs of geothermal power production, from 7 different sources.

Cost	**(1)**	**(2)**	**(3)**	**(4)**	**(5)**	**(6)**	**(7)**	**Average****
Exploration & confirmation	$332	$200	$150	-	-	-	-	$175
Production costs: Drilling	$5,212	-	-	-	-	-	-	$5,212
Production costs: Plant	$1,900	-	-	$1,350	$3,100	$3,616	$2,400	-
Production costs: Total	-	$2,770	$2,770	-	-	-	-	$2,473
Totals	$7,444	$2,970	$2,920	$1,350	$3,100	$3,616	$2,400	**$7,860****

All costs expressed in $/kW. Sources: (1) GeothermEx, 2004; (2) Hance, 2005; (3) Kagel, 2006; (4) Holdmann, pers. comm; (5) Sison-Lebrilla, 2005; (6) Gawlik & Kutcher, 2000; (7) Ormat, 2006. **Includes production drilling. Transmission costs not included.

Based on these considerations, the total capital cost of geothermal plant installation in the CAHSB is assumed to be $7860.18/kW. With that rate applied to the Chena Hot Springs power plant installation, the total cost computes as $3.1 million. Compared to the actual cost (approximately $2 million in 2006), this appears to be a reasonable number, considering that the wells drilled at Chena are substantially shallower (~300 m / 1000 ft.) than the deep wells assumed for this study (~1000 m / 3000 ft.). These numbers can therefore be considered a maximum cost. Operations and maintenance costs for the geothermal plant were assumed to be $0.026/kW, also based on averages from the Chena experience, the literature and industry standards.

Transmission distances are only approximate since the hottest subsurface resource (the geothermal “reservoir”) may or may not be located very close to the surface expression (hot springs). Distances were estimated on a case-by-case basis for each of the communities. Transmission costs include electric lines and road access for the entire

distance between the community and the hot springs, and should be considered maximum since existing roads and power lines were not accounted for. An exception is Shungnak and Kobuk, which share an electrical generation and distribution system. In that case, transmission is considered only to one community. Transmission costs are assumed to be $850,000/mile ($350,000/mile for transmission line + $500,000/mile for road access).

3.3.5.2. Other assumptions

Electrical load for each community (kWh/yr) is based initially on the last published PCE statistics for 2006, then assumed to increase by 1.5 % per year (after Crimp et al., 2007). Diesel capital costs were not included since they are sunk costs. Operations and maintenance costs were assumed to be 0.2 ¢/kWh (after the mean given in Crimp et al, 2007). We added the costs of bulk fuel storage upgrades and power system upgrades into the costs for diesel generation ($3 million; Mark Foster, pers. comm.).

3.4. Results

3.4.1. Assessing geothermal capacity for CAHSB communities

Reservoir temperatures are unknown for all the CAHSB hot springs, so Table 3.4 presents approximate energy production capacity for the based on estimated reservoir temperatures from chemical geothermometry and measured flow rates. The energy needs of proximal communities are also presented for comparison.

Table 3.4. Estimated electrical generation capacity of CAHSB hot springs vs. electrical generation requirements of CAHSB communities.

Hot Springs	**Communities within 45 miles**	**Est. Res. T. (°C)**	**Est. Res. T. (°F)**	**Natural flow rate (GPM)**	**kW capacity***	**kW capacity required**
Battleship Mtn.	Golovin, White Mtn	92*	223*	18	<100	160, 178
Circle	Circle, Central	103	243	407	600-800	80, 101
Clear Creek	Elim, White Mountain, Golovin	92*	223*	232	400-600	258, 178, 160
Division	Kobuk-Shungnak	92*	223*	547	600-1000	485
Dulbai	Huslia	92*	223*	-	-	225
Granite Mtn.	Buckland, Koyuk	91	221	431	550-750	325, 295
Hornor	Ruby	47	142	132	<100	-
Kwiniuk"Elim"	Elim, Golovin	67	178	22	<100	129, 80
Little Melotzina	Tanana	97	232	95	150-350	325
Manley	Manley, Minto	88	216	349	450-650	63, 140
Melozi	Ruby	96	230	375	500-700	-
Pocohontas	Hughes	92*	223*	-	-	71
South	Huslia	86	212	357	450-650	225
Sun Mtn.	Huslia	92*	223*	-	-	225
T. Lake	Hughes	92*	223*	-	-	71

Est. Res. T. = Estimated reservoir temperatures from chalcedony geothermometer methods (see Kolker et al., in press). Starred values indicate hot springs for which SiO_2 data is not available, in which case the average temperature estimate for the CAHSB was used. Flow rates measured by Motyka et al. (1983). The range in output capacity accounts for two different pumped capacity assumptions. The low end assumes 2X natural flow rate (conservative) and the high end assumes 4.5x natural flow rate (Chena Hot Springs pumping rate). Electrical consumption in kWh/yr data from AEA, 2007.

Table 3.4 shows that only eight out of the fifteen hot springs of interest are eligible for geothermal energy generation due to resource constraints. Those are: Clear Creek (17 miles from Elim and ~40 miles from Koyuk); Granite Mountain (~40 miles from Buckland and Koyuk); South (~40 miles from Huslia) Circle (3 miles from Central and ~15 miles from Circle); Manley (2 miles from Manley, ~25 miles from Minto, and ~40 miles from Tanana, respectively). The rest of the hot springs are either too cool or

have too low water flow to provide energy adequate to meet the needs of the community, or they are missing required data for such a determination.

There is some overlap between communities and the closest hot springs resource. For example, geothermal power development at Clear Creek hot springs could benefit the communities of Golovin, Koyuk, Elim, and/or White Mountain, and development at Manley Hot Springs could benefit the communities of Manley and/or Minto (Table 3.5).

Table 3.5. Potential shared projects from a single geothermal resource.

Hot springs	**Communities**	**Combined energy needs (kW)**	**Resource capacity match need?**	**Approximate distance (miles)**
Granite Mountain	Buckland	620	Y	40
	Koyuk			40
Circle	Central	180	Y	3
	Circle			15
Clear Creek	Elim	596	Maybe	17
	White Mountain			30
				30
	Golovin			30
South	Huslia	112	Y	40
Division	Kobuk	485	Y	40
	Shungnak			40
Manley	Manley	203	Y	2
	Minto			25
Little Melotzina	Tanana	325	Y	40
Melozi	Ruby	171*	Y	35

*Starred values estimated from average consumption per capita in the CAHSB.

Most of the hot springs in Table 3.5 can probably sustain production for more than one community. One exception may be Clear Creek hot springs which is within 30 miles of three communities but may not contain enough energy to meet the needs of all those communities.

3.4.2. Sustainability analysis of geothermal development at Chena Hot Springs

Fig. 3.2 presents the total geothermal fluid uses at CHS. Geothermal fluids are extracted from two shallow (<300 m) wells at a combined rate of 1000 GPM. 700 GPM of these fluids goes to power production, and 250-300 GPM goes to direct uses such as district heating, absorption chilling of the Ice Museum, greenhouses, and other uses such as laundry, pool heating, showers, etc. Because the chilling of the Ice Museum is only necessary in summer and the district heating system is only necessary in winter, there is little seasonal variation in direct use needs. 70% of spent fluids are reinjected at CHS. These fluids are reinjected into 3 wells at the eastern end of the system: W1 (reinjected at ~300 ft. depth); TG7 (reinjected at ~720 ft. depth); and W0 (reinjected at ~90 ft. depth).

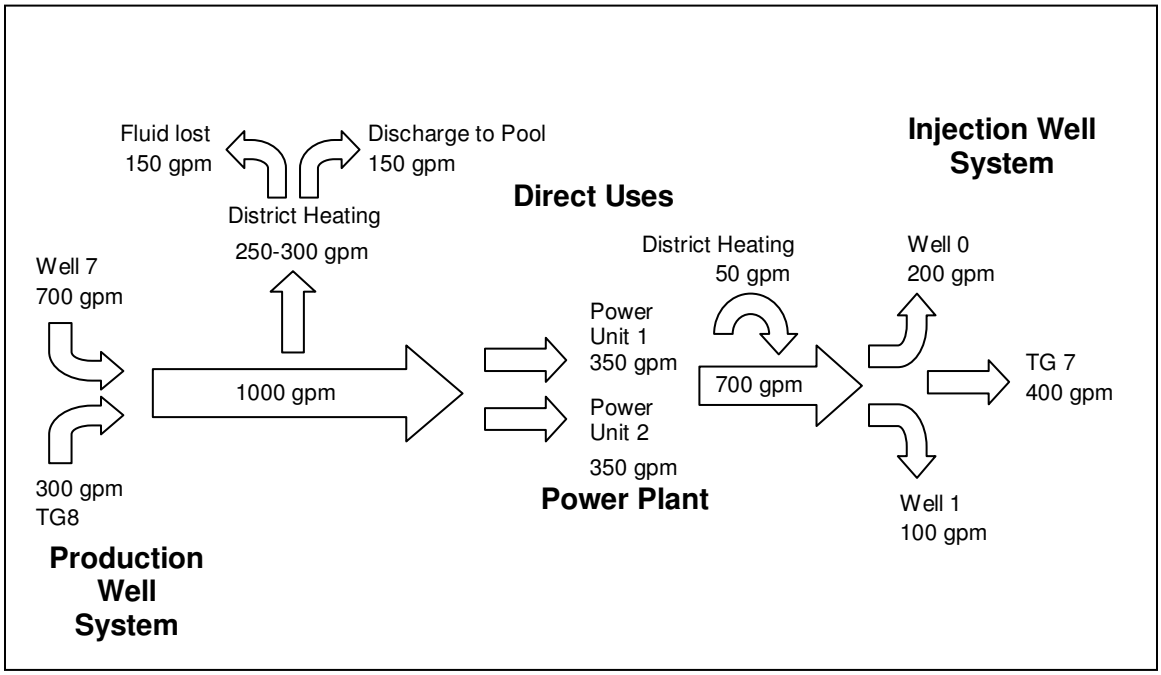

Figure 3.2. Cartoon of geothermal fluid uses at Chena Hot Springs, showing flow rate in gallons per minute (GPM) and production and injection wells. Figure courtesy of Gwen Holdmann.

Bottom hole temperature and pressure data from 17 wells at CHS are presented in Figs. 3.3 and 3.4. Data comes from one to four downhole measurements taken between 2005 (prior to the installation of the power plant) and 2008 (after two years of production). Seasonal effects are reported not to effect system performance since small pressure declines in the winter are offset by small rises in fluid temperatures (Gwen Holdmann, pers. comm.).

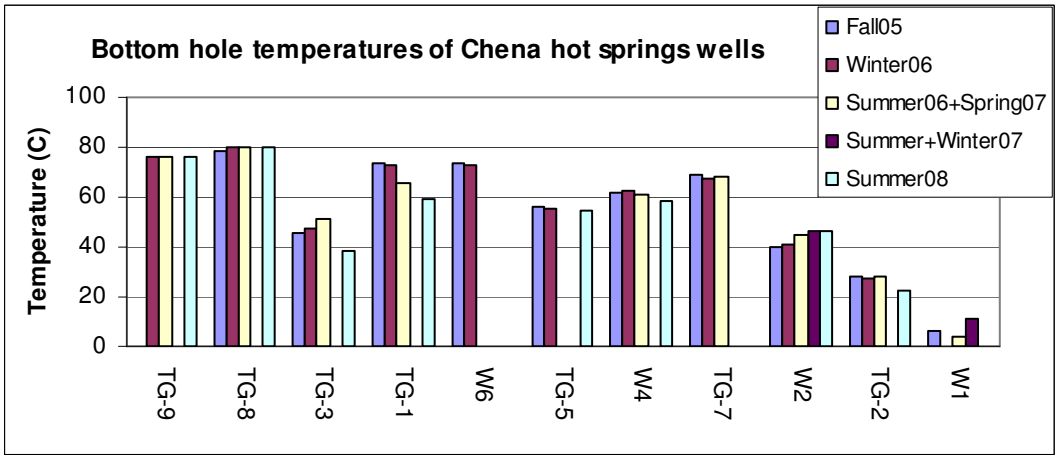

Figure 3.3. Bottom hole temperatures measured in CHS wells 2005-2007, arranged from west to east.

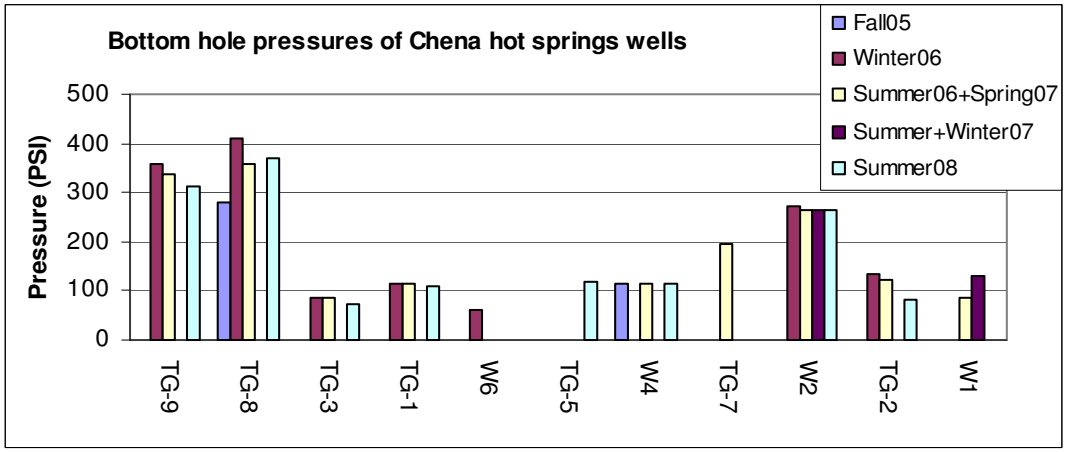

Figure 3.4. Bottom hole pressures measured in CHS wells 2005-2007, arranged from west to east.

Figs. 3.3 and 3.4 show that the geothermal wells have experienced some fluctuation in temperatures and pressures since the power plant system began operations in 2006. Temperatures have dropped in some geothermal wells but have risen in others, with a net temperature drop of 2.1°C (3.7 °F). Pressures have dropped in all wells, for a net pressure drop of 18.4 psi (Table 3.6).

Table 3.6. Change in temperatures and pressures of CHS wells, 2005-2008.

Well	**Fall05**		**Winter06**		**Summer/Spring07**		**Smmer2008**		**Net**	
	Temp (°C)	**Press. (psi)**	**Temp (°F)**	**Press. (psi)**	**Temp (°C)**	**Press. (psi)**	**Temp (°C)**	**Press. (psi)**	**Temp. Δ(°C)**	**Press. Δ(psi)**
TG-9	-	-	76.1	358.7	76.2	338.9	-	314.3	0.07	-44.4
TG-8	78.1	279.4	80.1	411.7	80.3	355.8	-	368.3	2.11	***elim***
TG-3	45.6	-	47.3	85.9	51.6	83.6	-	72.7	-7.07	-13.3
TG-1	73.4	-	72.5	114.8	65.9	113.0	-	110.1	-14.2	-2.9
W6	73.7	-	72.5	62.6	-	-	-	-	-1.26	-
TG-5	56.2	-	55.1	-	-	-	-	116.5	-1.81	-
W4	62.0	-	62.2	-	60.8	113.2	-	111.8	-3.42	-2.8
TG-7	69.1	-	67.2	-	67.7	197.2	-	-	-1.39	-
W2	39.8	-	41.0	270.8	44.8	263.6	46.8	264.4	6.48	-6.4
TG-2	27.8	-	27.4	134.1	27.7	123.2	-	82.3	-5.25	-40.9
W1	6.7	-	-	-	4.0	87.1	11.5	-	4.81	***elim***
Average	**-2.1**		**-18.4**							

Note that pressures in wells TG8 and W1 (the production well and reinjection wells, respectively) were eliminated from the average calculations.

It is not surprising that temperatures and pressures in individual wells should change somewhat, since pumping and injection of fluids will inevitably alter the dynamics of the system. Since the fluids used for power generation at CHS are not reservoir fluids but mixtures of reservoir fluids and cold groundwater, fluctuations due to mixed-aquifer phenomena (such as well drawdown followed by immediate recompensation by groundwater inflow) should be expected. In a simple case of reservoir re-equilibration, there should be minimal changes to the overall system (net

drops or increases in temperature and pressure). However, CHS appears to have experienced a net pressure drop of 18.4 PSI and a net temperature drop of 2.1 °C (3.4 °F). A temperature drop has also been observed in the geothermal fluids entering the power plant, but here it is a drop of ~3.3 °C (~6 °F) (Fig. 3.5).

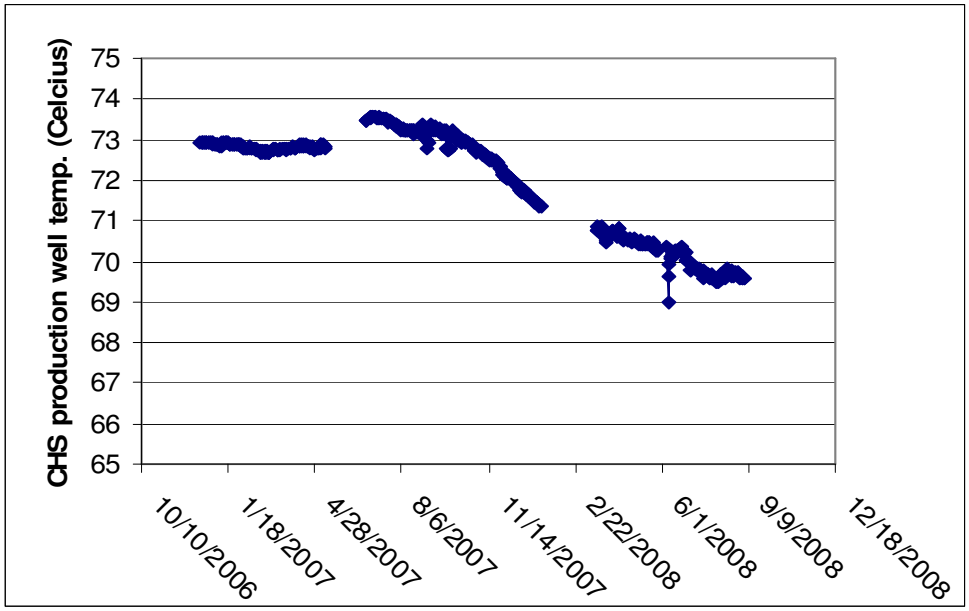

Figure 3.5. Temperature of CHS geothermal production fluids over time. Production fluids = fluids entering the binary power plant. Note that drops in fall 2007 and early summer 2008 are due to system shutdowns and not to resource dynamics. The cause for the data gap between April and July 2007 is unknown.

Actual power produced from a geothermal generation unit is partially dependent upon the cooling source and temperature. Water at 4-10 °C (40-50 °F) is used for cooling during summer months, and in the winter the system is switched to run off an air-cooled condenser system which can achieve higher than rated efficiency and output during the cold winter months. The heat sink, or cooling system, for the Chena Hot Springs power

plant is an infiltration gallery that utilizes cold water from a nearby creek. The condenser uses 1600 GPM of creek water for one unit for a 3200 GPM total water usage when two generators are running parallel. Unfortunately, we were only able to obtain data from August 10 to October 11, 2006. The production fluid temperature remained constant during this period, and the average drop in temperature between entry fluid and spent fluid was 17.4 °C (~31 °F). The cooling water experienced an average gain in temperature of 4.8 °C (8.64 °F). The generator units at Chena Hot Springs have a capacity of 200 kW but sometimes, especially in the summer months where cooling fluid temperatures are higher, produce less than capacity. In addition, fluids are pumped from depths in geothermal production wells, which causes a considerable parasitic load on the system. The average pump load is ~20 kW, so the net electric power available for use from a single generator unit at Chena Hot Springs was, on average, ~170 kW for the period Aug.-Oct. 2006 (Table 3.7).

Table 3.7. Data from the CHS power system, Aug.-Oct. 2006.

ΔT-Cooling water	**ΔT-Geothermal fluid**	**Generated kW**	**Pump kW**	**Net kW power**
4.8 °C (8.6 °	-30.9 (17.4 °C)	189.3	19.7	169.6

ΔT = Average change in temperatures of cooling water and geothermal fluids; generated kW = power output, pump kW = parasitic pumping load; net kW power = output – parasitic pumping load.

The net power output experienced fluctuations during the period Aug.-Oct. 2006, including a system shutdown for two discrete periods (Fig. 3.6).

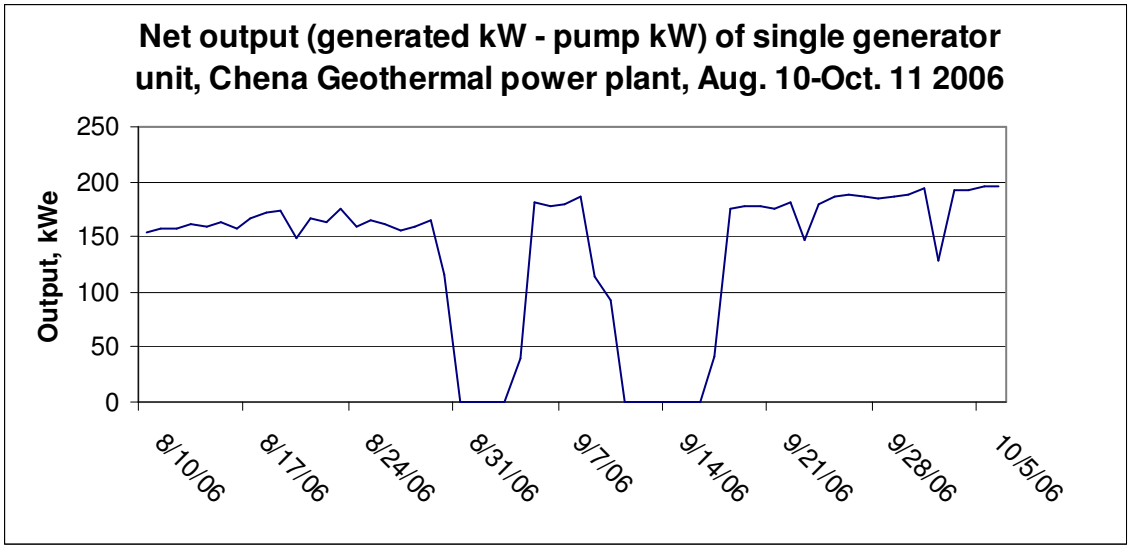

Figure 3.6. Net kW output for Chena Hot Springs geothermal power plant, 2006. Net output is the generated output minus the parasitic load taken by the pumping system (Table 3.7). Data is from August – October 2006. Note system shutdown for about a week in early September and about a week in mid-September.

The geothermal power plant at CHS has not totally displaced diesel use, due to shutdowns (as shown above) and also due to the need for an alternative power source during the generation process. The system was designed to use a battery bank for storage and to provide power to the induction motor; however, at the time of writing the battery bank was not operational. Nonetheless, the geothermal generation has displaced nearly all diesel use. In 2007, the 400kW geothermal power plant displaced 101,060 gallons of diesel fuel which translated to a fuel savings of $243,555 for the year. This is despite a 5 week shutdown caused by a fire in the building not associated with the power plant but which caused damage to control and electrical wiring.

All of the small-scale geothermal plants investigated by this study would utilize binary technology. This closed-loop system would produce no emissions, noise pollution,

solid waste or underground contamination (USDOE, 2005; Gawlik and Kutcher, 2000); hence these are eliminated from possible impacts of geothermal development in the CAHSB (Table 3.8). The probability of occurrence of most of the remaining potential impacts is quite low, providing spent fluids are properly reinjected.

Table 3.8. Potential environmental impacts from CAHSB geothermal projects.

Impact	**Probability of Occurrence**	**Severity of Consequence**
Surface water discharge	medium	low to medium
Land subsidence	Low if fluids are reinjected	low to medium
Well blowouts	very low	low to medium
Conflicts with cultural/archeological features	low to medium	medium to high
Social economic problems	low	low
Chemical or thermal contamination	low if fluids reinjected	medium

Probability and severity of potential impacts after Rybach, 2003. Only impacts that would apply to small, low-temperature, binary plants in Alaska are presented in this table.

3.4.3. External benefits of geothermal energy

3.4.3.1. Quantifiable benefits.

Elimination of subsidies for diesel electricity generation.

In 2007, the PCE program allocated $26.7 million dollars to rural communities that rely on power through diesel generation (AEA, 2008). CAHSB communities received a total of $1.49 million, with an average disbursement of $99,267 per community (Table 3.9). In addition, rural Alaskan utilities receive two other important fuel-related subsidies, in the form of Denali commission expenditures for bulk fuel

storage upgrades (BFU) and remote power system upgrades (RPSU). These projects are administered by AEA via a priority list of remote communities in need, or they are administered the Alaska Village Electric Cooperative (AVEC). Many CAHSB communities have already received this service as of 2007; others are on the priority list slated to receive this service in the next decade. The total cost of fuel-related subsidies for electricity generation for CAHSB communities through 2030 will be over $82 million, with a mean of $5.3 million per community.

Table 3.9. Electricity generation subsidies CAHSB communities will receive through 2030.

Community	**PCE (2007) ($thousands)**	**PCE 2008-2030 ($millions)**	**RPSU ($millions)**	**BFU ($millions)**	**Total subsidies through 2030 ($millions)**
Buckland	$ 77	$ 1.8	*Completed*	*Completed*	$ 1.8
Central	$ 77	$ 1.8	$ 3 (AEA#3)	$ 3 (AEA#3)	$ 7.8
Circle	$ 34	$ 0.8	-	-	$ 0.8
Elim	$135	$ 3.1	*Completed*	*Completed*	$ 3.1
Golovin	$ 87	$ 2.0	*Completed*	*Completed*	$ 2.0
Hughes	$54	$ 1.2	*Completed*	*Completed*	$ 1.2
Huslia	$187	$ 4.3	$ 3 (AVEC)	$ 3 (AVEC)	$ 10.2
Kobuk	$ 25	$ 0.6	$ 3 (AEA #9)	$ 3 (AEA #9)	$ 6.6
Koyuk	$ 160	$ 3.6	*Completed*	*Completed*	$ 3.7
Manley	$41	$ 0.9	$ 3 (AEA #47)	$ 3 (AEA #47)	$ 6.9
Minto	$ 137	$ 3.1	$ 3 (AVEC)	$ 3 (AVEC)	$ 9.2
Ruby	$ 57	$ 1.3	$ 3 (9)	$ 3 (9)	$ 7.3
Shungnak	$ 130	$ 3.0	$ 3 (AVEC)	$ 3 (AVEC)	$ 9.0
Tanana	$ 174	$ 4.0	$ 3 (AEA #43)	$ 3 (AEA #43)	$ 10.0
White Mtn.	$ 115	$ 2.6	*Completed*	*Completed*	$ 2.6
Mean	*$99*	*$2.2*	*$3.0*	*$3.0*	*$ 5.3*
Totals	**$1.5**	**$34.2**	**$24**	**$24**	**$82.2**

PCE = Power Cost Equalization allocations, based on 2007 disbursements; RPSU = Denali commission expenditures for remote power system upgrades. Priority number and administrative entity given in parentheses (AEA = Alaska Energy Authority; AVEC = Alaska Village Electric Cooperative); BFU = Denali commission expenditures for bulk fuel storage upgrade projects; HAP= Heating fuel assistance provided to CAHSB communities, calculated from HAP data on the number of recipient households in each community multiplied by the maximum assistance amount for 2007.

Heating cost savings, elimination of emergency assistance for heating costs.

The total minimum avoided cost in heating fuel for CAHSB communities is ~ $84 million. This is a minimum because it assumes present rates with zero escalation. The minimum amount that CAHSB communities will receive through 2030 in emergency assistance for heating fuel is ~ $18 million. The total costs of geothermal heating for CAHSB communities is ~ $38 million. Hence, geothermal heating could save CAHSB communities a minimum of $27 million, which could eliminate ~$18 million in emergency assistance by the state of Alaska. The cost-benefit ratio of geothermal heating projects vs. heating with fuel oil is <1 in all cases, despite the costs of piping geothermal fluids (Table 3.10). Note that Golovin, Hughes, and Ruby were eliminated from the analysis because the resource is not adequate to support development (see Table 3.4).

Table 3.10. Potential benefits of geothermal heating in CAHSB communities 2008-2030.

Community	Geothermal heating costs	Avoided heating fuel	HAP costs	Savings	CB ratio
Buckland	$4.7	$8.4	$2.2	$3.7	1.78
Central	$0.9	$2.7	$1.5	$1.8	3.01
Circle	$1.7	$2.6	$1.5	$0.9	1.54
Elim	$2.2	$4.8	$1.7	$2.6	2.16
Golovin	$3.7	$3.5	$1.6	-$0.2	0.95
Huslia	$5.2	$10.1	$2.0	$4.9	1.93
Kobuk	$4.7	$5.0	$2.3	$0.3	1.06
Koyuk	$4.7	$5.6	$1.6	$0.9	1.18
Manley	$0.9	$2.1	$0.9	$1.2	2.36
Minto	$3.2	$5.9	$1.0	$2.7	1.84
Ruby	$4.2	$6.0	$1.8	$1.8	1.42
Shungnak	$5.2	$10.0	$2.3	$4.7	1.93
Tanana	$5.2	$10.1	$1.3	$4.8	1.93
White Mtn.	$3.7	$5.0	$1.8	$1.3	1.35
Mean	*$3.6*	$5.8	*$1.7*	*$2.2*	*1.75*
Totals	**$49.2**	**$79.2**	**$22.9**	**$30.0**	

Benefits in $millions.Abbreviations: HAP = Heating Assistance Program allocations to CAHSB communities, based on disbursements for 2007.

Benefits to communities from greenhouse production.

The total cumulative profit for geothermal greenhouses in the CAHSB is presented in Table 3.11, using values from Mager et al. (2008). Since it is unclear whether the optimal greenhouse site would be at the location of the hot springs (with road access) or in town (with fluids piped to town), we present computations for both scenarios (Table 3.11). Note that this analysis does not consider any engineering limitations on piping hot fluids long distances from hot springs. The communities of Golovin, Hughes, and Ruby were eliminated from the greenhouse analysis because the resource at those communities is not adequate to support development. That is, because the resource at those communities is not adequate to support power production (see Table 3.4), geothermal greenhouse costs would be substantially elevated and thus uneconomic.

Table 3.11. Potential geothermal greenhouse profits for CAHSB communities 2008-2030.

Community	**Approx. distance to hot springs (miles)**	**Total profit through 2030 yrs: onsite greenhouse ($million)**	**Total profit through 2030 yrs: in-town greenhouse ($million)**
Buckland	40	$ 3.1	*NEG*
Central	3		$2.9
Circle	15		$2.1
Elim	17		$1.6
Huslia	45		*NEG*
Kobuk	40		*NEG*
Koyuk	40		*NEG*
Manley	2		$2.9
Minto	25		$0.6
Tanana	45		*NEG*
Shungnak	45		*NEG*
White Mtn.	40		*NEG*

NEG = In-town greenhouse is unprofitable; primarily due to the high costs of piping over 25 miles. Revenue estimates from Mager et al. (2008) and piping costs from Rafferty (1998). Onsite greenhouse assumes only 300 ft. of piping, whereas in-town greenhouses account for piping costs for the distance between hot springs and communities.

If greenhouses are built at the hot springs site and accessed by roads, the total profit to CAHSB communities would be approximately $3.1 million through 2030 (Table 3.11). If greenhouses were to be built in town utilizing hot fluids piped from the hot springs, Table 3.11 shows that the total profits through 2030 would range from $0.6 to $2.9 million for communities <25 miles from hot springs. 'In-town' greenhouses do not appear to be economical for communities more than 25 miles from hot springs due to piping costs. Note also that the greenhouse will require ~62kW of electric power, primarily for lighting, 16 hours per day (Mager et al., 2008).

Avoided fuel spills.

Between the years of 1995 and 2005, 431 fuel spills were reported for Western Alaska, resulting in 87,132 gallons of fuel spilled; and 1,296 fuel spills were reported for Interior Alaska, resulting in 236,161 gallons of fuel spilled (ADEC, 2007). The approximate cost to the state during the period 2008-2030 for cleanup for spills in CAHSB communities would be over $15 million (Table 3.12).

Table 3.12. Fuel spills in the CAHSB region, 1995-2005.

DEC Subarea	**Fuel spills/10yrs**	**gal/10yrs**	**Cost through 2030**
Western AK	431	87,132	$764,677 (per community)
Interior AK	1,296	236,161	$1,250,526 (per community)
Total			*$15. 3 M (all communities)*

Future cost to the state from fuel spills in these communities is based these numbers and on the conservative assumption of $25,000 cleanup cost per spill for remote communities.

Avoided CO_2 emissions.

Based on 2007 data, the amount of CO_2 emitted by CAHSB communities varies widely, from <1 x 10^6 lbs./yr to nearly 5 x 10^6 lbs/yr (Fig. 3.7). The total amount of CO_2 emitted by CAHSB communities was approximately 41 million lbs. in 2007. Because the costs of CO_2 emissions are highly uncertain at this time, those are treated separately in the scenarios section of this study.

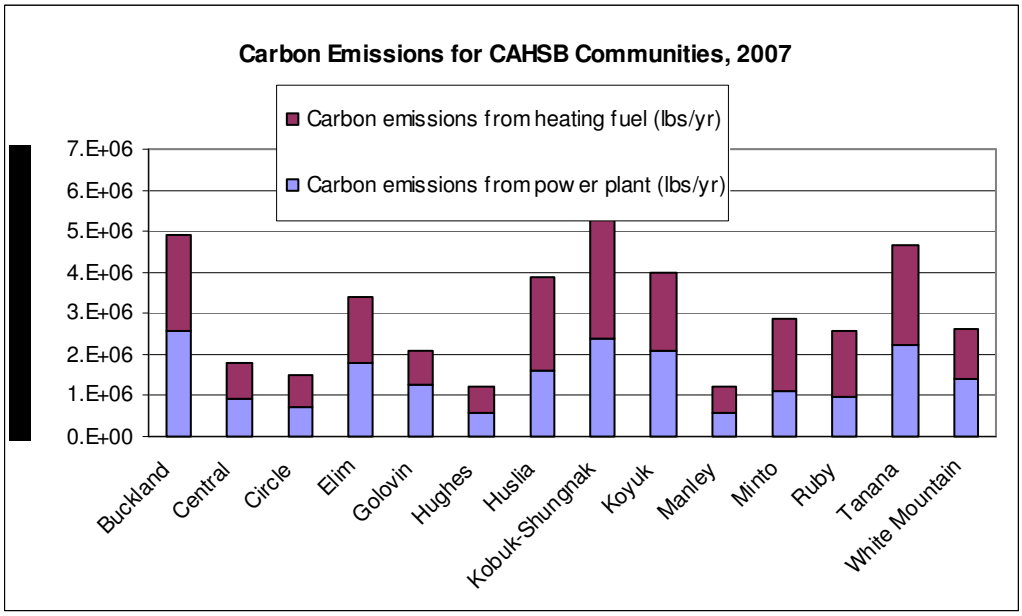

Figure 3.7. Carbon emissions per CAHSB community, in lbs/yr. Based on PCE data for diesel fuel consumption for power generation and assuming heating fuel consumption of 1000 gal/yr for CAHSB communities.

3.4.3.2. Non-quantifiable benefits

Several studies have shown that geothermal investment stimulates economic development in the local area. However, we chose not to quantify this for CAHSB communities due to concerns about qualities particular to Alaska (displacement of diesel-related jobs, subsistence economies, etc.) Economic activity and job creation within the

geothermal industry impact the following areas: utility, government, power plant operators and maintenance staff mechanical equipment and metal suppliers, general consultants and contractors, drilling and well services firms, environmental services firms, developers and/or independent power producers, and other professions. Geothermal greenhouse development at Chena Hot Springs provides two full-time jobs (Mager et al., 2008). Geothermal greenhouses in New Mexico have created about 250 jobs with an estimated payroll of $3.7 million per year (USDOE, 2005). This translates to 3-9 jobs that would potentially be created by geothermal development in the CAHSB, including power plant and greenhouse jobs. However, at least some of these jobs would replace existing jobs (such as powerhouse operation, fuel transit, etc.) so we do not quantify these as jobs created for CAHSB communities.

Finally, another difficult-to-quantify benefit of geothermal energy is food security. Food security is also a big issue in Alaska with the impact of climate change on subsistence food sources and the impact of rising fuel prices on food shipments to rural communities. Food security benefits include locally grown produce; absorption chilling; aquaculture/agriculture opportunities, and other benefits. The greenhouses at CHS provide produce year-round. A particularly attractive option for many CAHSB communities could be the utilization of geothermal fluids for absorption chilling for fish processing applications. The resort at Chena Hot Springs uses geothermal heat for chilling their ice museum via refrigeration provided by an absorption chiller similar to one used in a propane refrigerator for an RV (http://www.chenahotsprings.com/).

3.4.4. Scenarios affecting renewable energy development in AK

The cumulative fuel costs through 2030 for power generation and heating fuel are presented in Table 3.13, under three scenarios.

Table 3.13. Fuel cost projections through 2030 for CAHSB communities.

Community	Fuel use (power, gal/yr)	Fuel use (heat, gal/yr)	Fuel costs (power): low ($M)	Total fuel costs: low ($M)	Fuel costs (power): mid ($M)	Total fuel costs: mid ($M)	Fuel costs (power): high ($M)	Total fuel costs: high ($M)
Buckland	118,708	108,500	7.7	16.9	11.6	24.3	14.6	29.8
Central	43,572	38,800	2.3	5.1	2.8	6.0	3.1	6.6
Circle	32,998	36,000	1.9	4.8	3.3	7.6	4.4	9.7
Elim	83,192	75,500	4.0	9.2	5.6	12.1	6.8	14.4
Golovin	59,237	37,500	4.0	7.4	5.8	10.2	7.1	12.3
Hughes	27,956	27,600	2.6	5.8	3.9	8.1	4.8	9.9
Huslia	73,631	106,000	5.5	15.6	9.1	24.1	14.6	30.5
Kobuk-Shungnak	109,965	155,600	8.8	24.3	13.0	34.1	16.1	41.5
Koyuk	97,261	87,500	5.0	11.3	7.0	15.1	4.4	18.0
Manley	27,217	29,600	1.6	3.8	2.6	5.9	6.8	7.5
Minto	51,643	80,800	3.0	9.3	5.3	15.1	7.1	19.4
Ruby	45,514	74,000	3.8	11.5	6.1	17.4.	7.9	21.8
Tanana	104,243	112,400	7.1	17.0	7.6	15.1	10.0	20.4
W. Mountain	65,676	56,000	4.9	10.2	8.4	18.8	10.1	23.9
Mean	*62,721*	*73,271*	*4.4*	*10.8*	*6.6*	*16.1*	*8.8*	*19.9*
Totals	**940,813**	**1,025,800**	**62.2**	**162.5**	**92.7**	**241.6**	**131.4**	**298.2**

Using 2007 consumption rates and assuming no increase through 2030, the carbon costs (from combustion for both power and heating) for individual communities range from a mean of $0.58 million to $0.91 million; total costs for CAHSB carbon taxes range from $8.8 million to $13.7 million. Financial incentives (grants and tax credits) for geothermal development for individual communities range from a mean of $0.65 million to $8.1 million (Table 3.14).

Table 3.14. Carbon taxes and financial incentives for renewable energy development through 2030 for CAHSB communities.

Community	**2007 CO_2 production (tons)**	**CO_2 taxes thru 2030: Mid case ($millions)**	**CO_2 taxes thru 2030: Favorable case ($millions)**	**Incentives: Mid case ($millions)**	**Incentives: Favorable case ($millions)**
Buckland	2449	$1.4	$4.3	$4.7	$6.7
Central	888	$0.5	$1.6	$1.7	$3.5
Circle	744	$0.4	$1.4	$1.7	$3.5
Elim	1710	$1.0	$3.0	$3.2	$5.4
Golovin	1042	$0.6	$1.8	$3.1	$5.4
Hughes	599	$0.3	$1.1	$2.1	$5.4
Huslia	1936	$1.8	$3.7	$3.7	$6.1
Kobuk-Shungnak	1883	$1.6	$5.4	$4.7	$6.7
Koyuk	1991	$1.2	$3.5	$1.8	$4.7
Manley	612	$0.3	$1.1	$1.9	$4.7
Minto	1427	$0.8	$2.7	$4.9	$6.8
Ruby	1288	$0.7	$2.5	$2.9	$5.9
Tanana	2335	$1.3	$4.3	$3.2	$5.4
White Mountain	1311	$0.7	$2.3	*$3.0*	*$5.4*
Mean	*1371*	***$0.8***	***$2,8***	*$3.0*	*$5.4*
Totals	**20,564**	**$11.8**	**$38.6**	**$42.65**	**$75.76**

The range of assumptions for these scenarios are given in Table 3.2. The low case assumes zero carbon taxes and zero incentives so it is not presented in this table.

3.4.5. Cost analysis of geothermal versus diesel cases.

Cost comparisons between geothermal and diesel power generation, operating under the three scenarios described above, are presented below (Figs. 8-14). Five separate sets of externalities are 'internalized' in a step-wise fashion to examine how each individual item impacts the cost analysis.

3.4.5.1. Cost analysis under 3 scenarios: no externalities included.

If no externalities are considered, the number of cost-effective geothermal projects ranges from 0-5 out of 13 possible projects, depending on the scenario (Fig. 3.8).

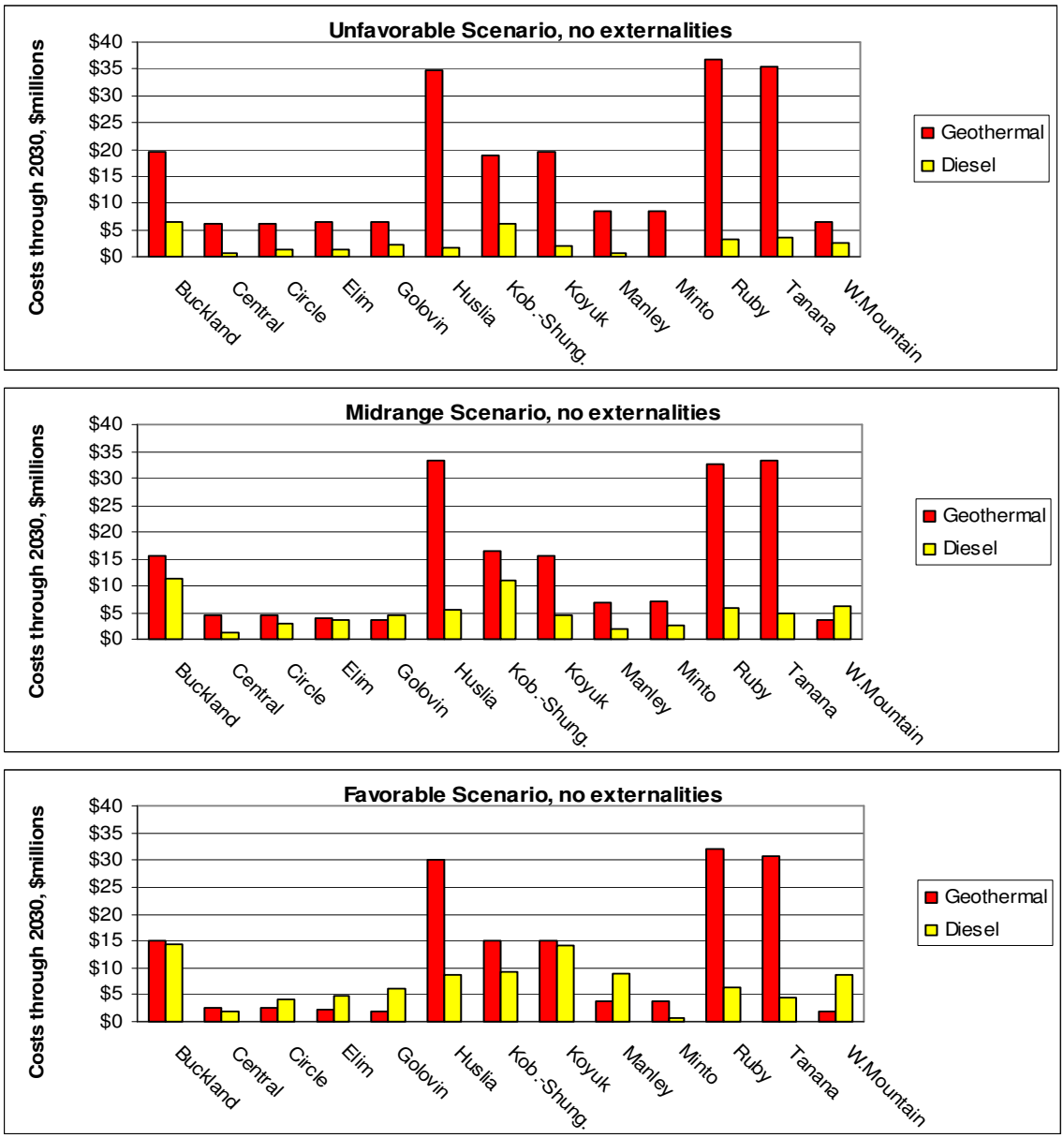

Figures 3.8a, b and c. Cost comparison between geothermal and diesel generation, 2008-2030, no externalities. No externalities = not including any of the externalities described in section 4.2. Cost comparisons operate under 3 scenarios described in section 4.3.

3.4.5.2. Cost analysis: internalizing PCE subsidies.

If the costs of PCE subsidies are considered, the number of cost-effective geothermal projects ranges from 0-9 out of 13, depending on the scenario (Fig. 3.9).

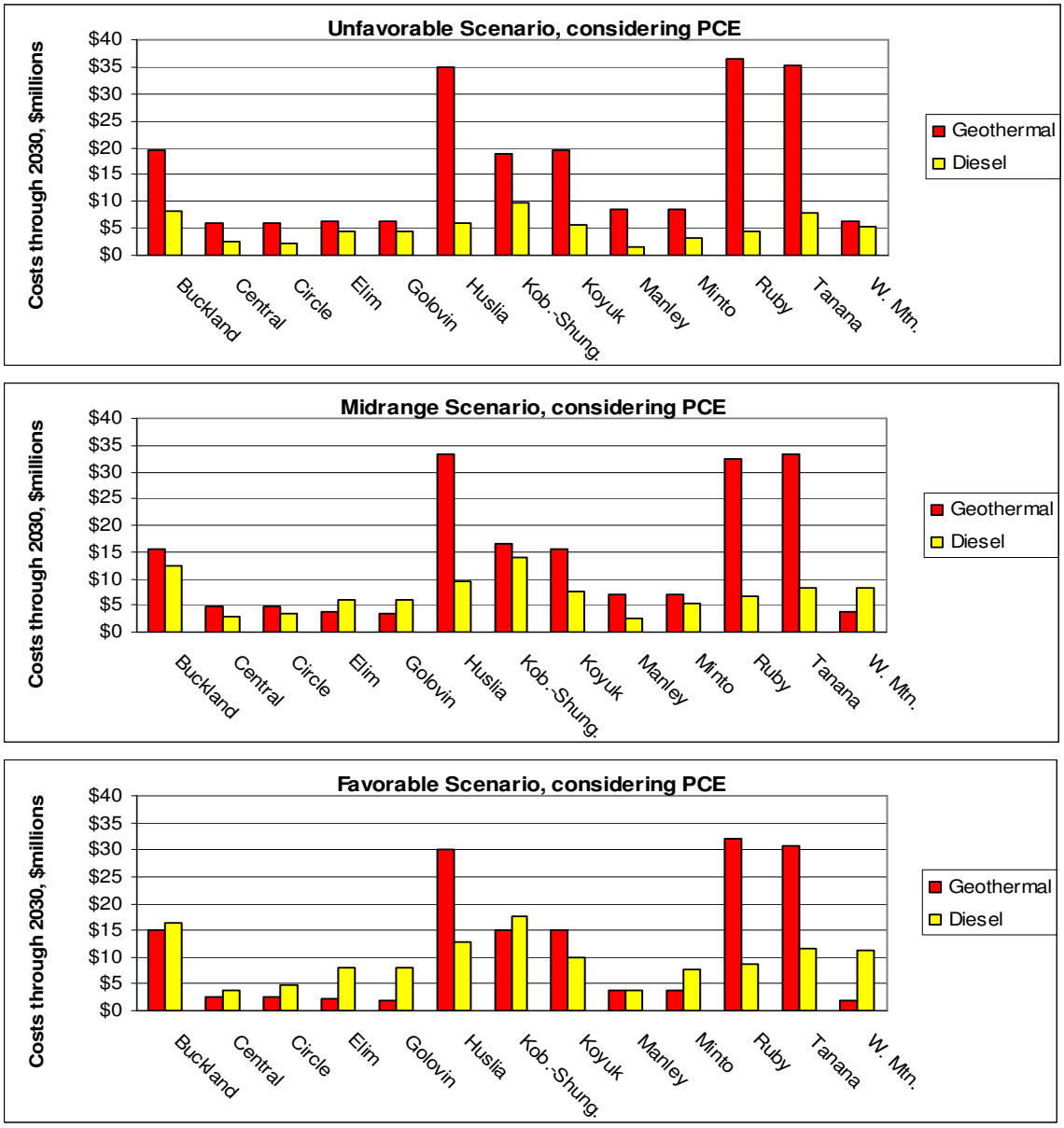

Figures 3.9a, b and c. Cost comparison between geothermal and diesel generation, 2008-2030, considering PCE. PCE = Power Cost Equalization externality described in section 4.2. Cost comparisons operate under 3 scenarios described in section 4.3.

3.4.5.2. Cost analysis: internalizing all fuel-related subsidies.

If the costs of planned upgrades are added, the number of cost-effective geothermal projects ranges from 2-9 out of 13, depending on the scenario (Fig. 3.10).

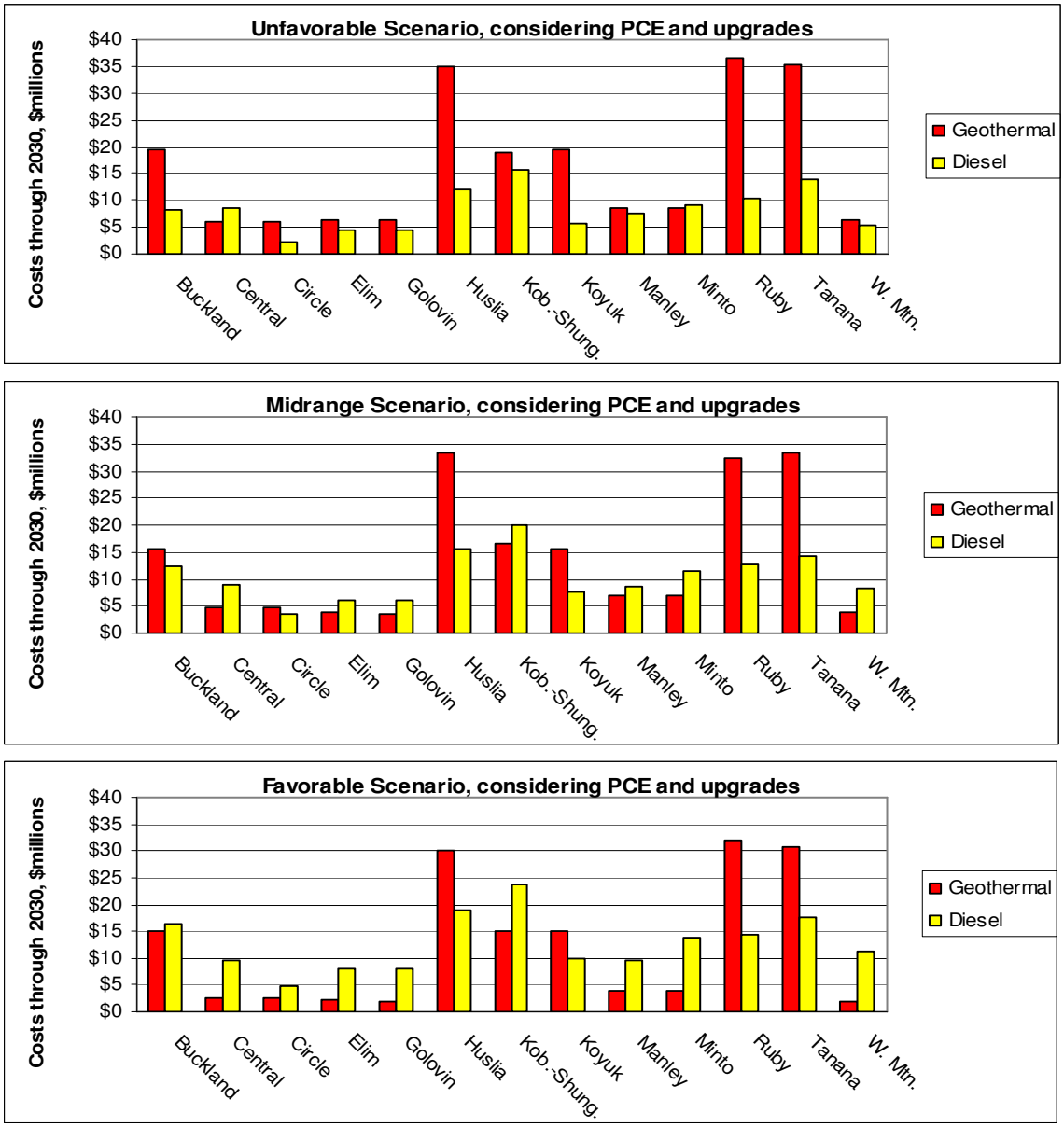

Figures 3.10a, b and c. Cost comparison between geothermal and diesel generation, 2008-2030, considering PCE and upgrades. PCE and upgrades = costs of all fuel-related subsidies described in section 4.2. Cost comparisons operate under 3 scenarios described in section 4.3.

3.4.5.2. Cost analysis: internalizing subsidies + direct use benefits.

If the benefits of geothermal direct use are added, the number of cost-effective geothermal projects ranges from 6-11 out of 13, depending on the scenario (Fig. 3.11).

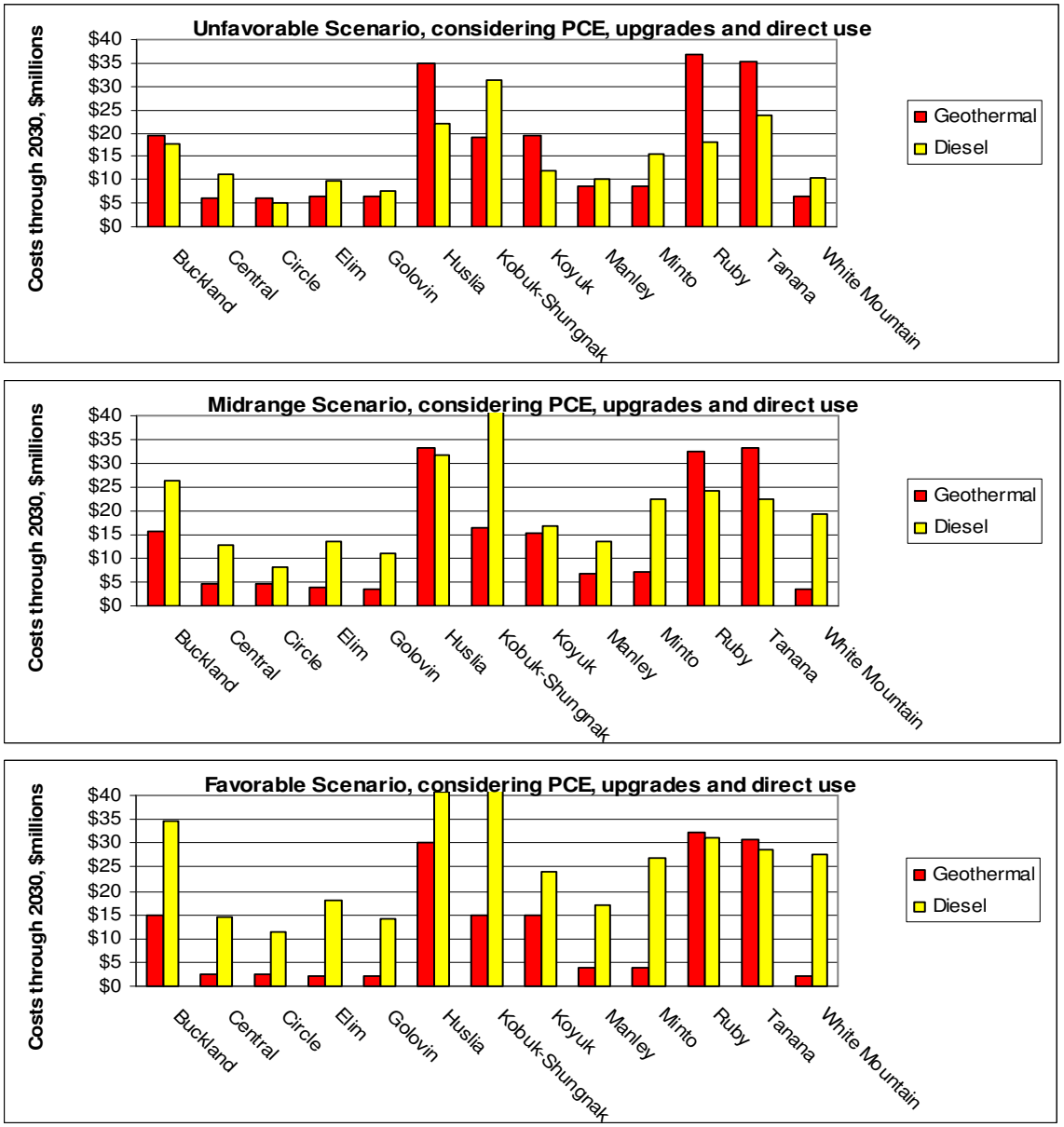

Figures 3.11a, b and c. Cost comparison between geothermal and diesel generation, 2008-2030, considering PCE, upgrades, and direct use. PCE, upgrades and direct use externalities described in section 4.2. Cost comparisons operate under 3 scenarios described in section 4.3.

3.4.5.2. Cost analysis: considering subsidies, direct use benefits, and fuel spill costs.

Finally, if the costs of fuel spills are added, the number of cost-effective geothermal projects ranges from 8–12 out of 13, depending on the scenario (Fig. 3.12).

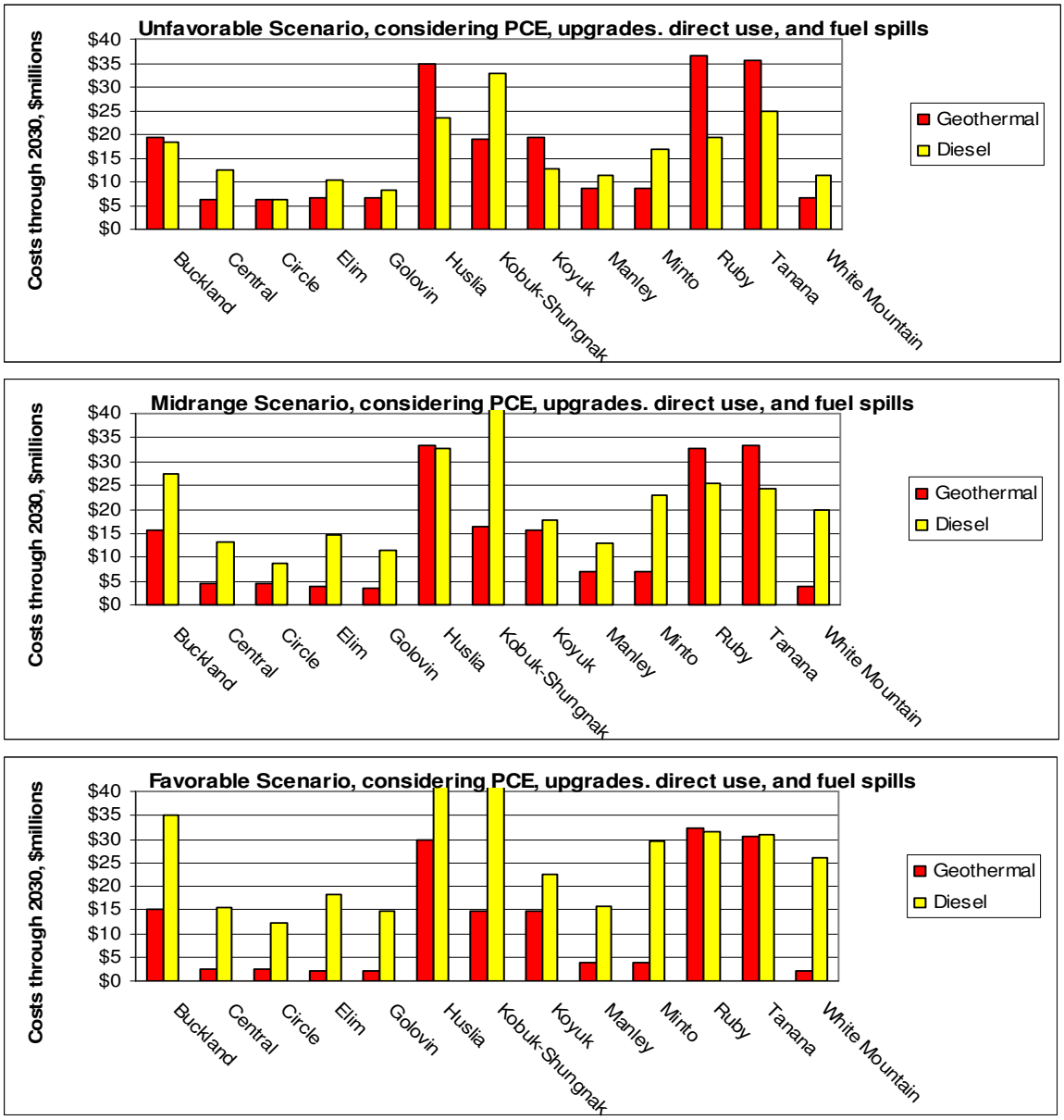

Figures 3.12a, b and c. Cost comparison between geothermal and diesel generation, 2008-2030, considering PCE, upgrades, direct use, and fuel spills. PCE, upgrades, direct use, and fuel spill externalities described in section 4.2. Cost comparisons operate under 3 scenarios described in section 4.3.

3.5. Discussion

3.5.1. Resource potential/capacity of CAHSB hot springs.

No discussion about geothermal development in Alaska can begin without adequate examination of the resource potential. Unfortunately, there is a noticeable lack of exploration data for most of Alaska's geothermal resources – and often what little data exists is not publicly available. The exploration data that exists is almost exclusively from the 1970's and early 1980's. Many basic geothermal assessment techniques that have been applied to the continental U.S. over the last few decades have not been applied to Alaska; for example, Alaska lacks a high-resolution heat flow map such as those that have been generated for most states in the U.S. from borehole data – despite the fact that abundant data of this type exist for Alaska. In the absence of such assessments, our preliminary evaluation based on empirical data from Chena Hot Springs implies that many of the hot springs near CAHSB communities can in fact be utilized for power production and direct use similar to the development at Chena Hot Springs. However, our evaluation relies not upon solid geological and geophysical data but upon assumptions and guesswork; it should not be used to replace true geoscientific exploration.

Our analysis assumes that the "reservoir" fluids – or the hottest fluids in the system – will be used for power production. In reality, this may or may not be the case if such fluids are prohibitively deep in terms of drilling. In the case of Chena Hot Springs, the hottest ("reservoir") fluids are clearly not the ones being used for power production (Kolker et al., in press). The geothermal power plant at Chena Hot Springs is able to use

such low-temperature fluids due to the availability of an extremely cold heat sink (creek water from a nearby creek). If such a heat sink is unavailable and/or if higher efficiency is desired, the hottest fluids should be used.

In general, the silica geothermometers used in this study probably underestimate reservoir temperatures, because (a) at lower temperature the form of silica equilibrating with fluid is uncertain, and (b) geothermal fluid dilution by groundwater will create waters with silica concentrations diluted from their reservoir concentrations.

3.5.2. Sustainability

Geothermal resources must be managed properly in order to ensure sustainability (that is, the renewability of the energy supply). The CHS system has experienced a net drop in both overall system temperatures and in the temperatures of production fluids. This could be due to several (possibly interrelated) factors: (1) addition of cooler fluids into the production supply; (2) changes in pumping rate over time; (3) reinjection of cooler fluids directly into the shallow thermal source. The net pressure drop of 18.4 PSI could also be the result of several factors: (1) insufficient reinjection of fluids into the deep system; leading to a decline in reservoir pressures, (2) drawdown at the wellhead; or other factors. It is difficult to favor or rule out any of these possibilities since none of the geothermal wells at CHS have penetrated the presumed deep reservoir. The ‘fluid loss’ of 150 GPM could be a factor in the observed pressure decline.

These data confirm the importance of penetrating a deeper, unmixed reservoir. In addition, water recharge to the system should be maximized by maximum reinjection into

the presumed reservoir. The deep reservoir was not drilled at Chena primarily due to budget constraints. Many instances of geothermal reservoir decline have occurred in places where reinjection has been non-existent or unsuccessful. If the pressure drop is indicating a reduction in the source thermal fluids, a large temperature drop would be expected to follow throughout the lifetime of the energy system.

The rapidity of the resource change is somewhat alarming because it usually takes a longer period of time for problems to become evident. For example, at the Geysers geothermal field in California, the generation system was operational for nearly two decades before the resource decline was apparent (Axelsson and Steffanson, 2003). However, that system is not analogous to CAHSB systems. It is orders of magnitude larger and hotter, and is steam-dominated (which makes it much more precarious than liquid dominated resources). The CAHSB low-temperature resource is likely to behave quite differently, and it may be that low-temperature systems such as these are inherently more dynamic. The only way to know is through careful monitoring of system pressures and temperatures over a longer period of time.

The power plant at CHS has experienced multiple shutdowns since inception. Many of these have been explained by factors unrelated to the geothermal resource, such as an electrical fire in the plant building (Gwen Holdmann, pers. comm.). However, it is unknown whether some of the shutdowns are due at least in part to resource issues. This too would have to be examined before the sustainability of the CHS system can be fully evaluated. If system shutdowns are inevitable, this would seriously compromise the

possibility of using CAHSB resources for remote power generation in off-grid communities.

Theoretically, a scale of <1MWe power output appears to be reasonable for the CAHSB resources being considered for geothermal power development. In general, recoverable energy and reservoir longevity are both highest at small production rates. Hanano et al. (1990) showed that system longevity for a 1 Mwe plant was almost 200 times greater than for a 100 MWe plant, and the recoverable electric energy from 1 MWe steady production is twice as large as that of 100 MWe. Six factors strongly influence longevity -- (1) output power, (2) well density, (3) injection strategy, (4) initial reservoir pressure, (5) initial fluid temperature, and (6) permeability in and around the reservoir. Management of the first three factors at Chena Hot Springs provides a useful dataset to design such engineering strategies for future development. The last three are fixed by nature and are specific to the area, and will need to be analyzed at a detailed individual scale if geothermal development is to proceed.

3.5.3. Economics and externalities

Economic influences have profound consequences on geothermal resource utilization and capacity (Wright, 1998). Table 3.15 summarizes the outcome of the fifteen cost analysis models run in section 3.4.4. Our cost comparison shows that internalizing several factors that are typically treated as externalities has a profound impact on the overall cost analysis of geothermal development (Table 3.16).

Table 3.15. Results of different models shown in Figs. 3.8-3.12. Number is out of thirteen possible projects.

Externality	**Number of cost-effective geothermal projects: Unfavorable scenario**	**Number of cost-effective geothermal projects: Mid-range scenario**	**Number of cost-effective geothermal projects: Favorable scenario**
None	0/13	2/13	5/13
PCE subsidies	0/13	3/13	9/13
PCE, RPSU &BFU subsidies	2/13	7/13	9/13
PCE, RPSU &BFU subsidies + direct use projects (heating and greenhouses)	7/13	10/13	12/13
PCE, RPSU &BFU subsidies, direct use projects, and fuel spills	8/13	10/13	12/13

Table 3.16. Relative impacts of the cost components considered in the analysis.

Cost component / externality	**Impact on overall cost**
Fuel price acceleration	Highest
Direct use projects (heating) (e)	High
Financial incentives for renewable development	Medium high
RPSU and BFU subsidies (e)	Medium high
PCE subsidies (e)	Medium
Carbon taxes	Medium
Direct use projects (greenhouses) (e)	Medium low
Fuel spill costs (e)	Low

(e) = externality.

By a large margin, the greatest influence on the cost analysis is the choice of future fuel price projections. Our scenarios utilize three distinctly different forecasts for fuel price projections. Our low-end forecast projects that fuel prices will *drop* over the next twenty years (Fig. 3.13). We believe this is unrealistic; after all, USDOE's own researchers found that the EIA has consistently under-forecast fuel prices since 2000 (Wiser and Bolinger, 2004). That study found that their '*High Fuel Price Scenario'* was in fact reasonable if not conservative, based on current oil and natural gas prices and other externally generated forecasts and scenarios. Moreover, present-day prices are

substantially higher than that prediction (Fig. 3.13). Hence, we believe that our mid-range and high-end forecasts of $110/bbl and $150/bbl and holding are more realistic. According to the World Energy Assessment, two global developments will likely put upward pressure on fuel prices. The first is the increasing volume of energy that will be demanded in the first half of the 21st century. The second is the increased cash flows required by the international oil industry to sustain enhanced investment in the initial large-scale exploitation of rapidly increasing volumes of unconventional oil and gas (Rogner et al, 2005).

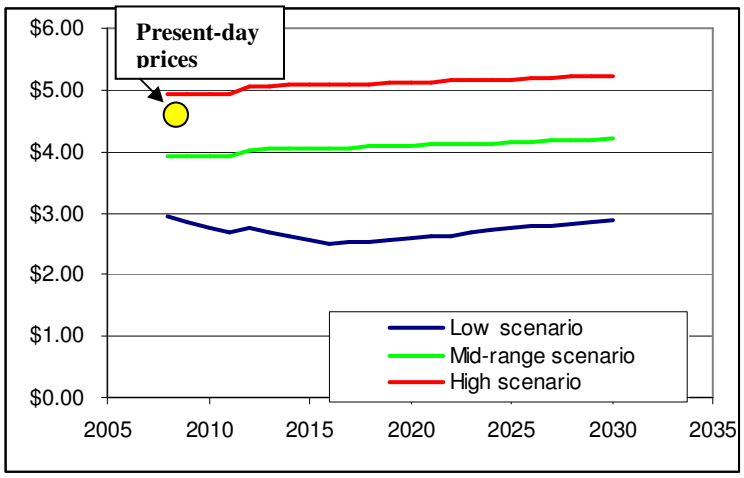

Figure 3.13. Fuel price projections cited by this study, using the village of Buckland as an example. Fuel prices are after PCE. Note that present-day prices are consistent with the mid-range and high scenarios, but not with the low scenario.

Relatedly, the next most important cost component is whether direct use of the geothermal fluids for heating purposes is included in a potential installation. This is because heating fuel costs are even higher than the costs of fuel for power generation, and are also likely to increase in the coming years. Heating is an issue that should be treated with special attention as it is a matter of survival for most of the year in remote parts of

Alaska. In 2008, not only were heating fuel prices at a record high but several villages actually ran out of oil, and had to pay more than double the going price to restock (Stapleton, 2008). The district heating system at CHS has resulted in savings of almost $300,000 in 2007. It should be noted that while our study included reliable cost assumptions for piping hot fluids long distances, we did not examine the technical feasibility of such a feat in sub-Arctic conditions. However, geothermal heating is likely to be technically feasible for most if not all the communities considered in this study, considering that geothermal fluids are transported for heating purposes up to 38 miles in Iceland (Karlsson, 1982). Nonetheless, this potential benefit is somewhat uncertain and requires additional consideration.

The next most important cost component are the financial incentives available to mitigate the high capital costs of geothermal projects. The incentives employed by our scenarios are only the ones either available at the time of writing or ones very likely to be implemented in the near future. However, there is significant reason to believe that even more incentives will be available in the future for Alaskan projects. These could include funding for research and development (R&D), which would offset exploration costs; net metering, which allows independent producers to sell their energy back to the utility; Renewable Portfolio Standards (RPS), which mandate that utilities generate some percent of their electricity from renewable sources; and other policies that have been employed by other U.S. states. To date, 22 states in the U.S., along with the District of Columbia, have adopted RPS policies, and such policies are being considered on a federal level by the U.S. Congress (REAP, 2006).

The next most important cost components are the fuel-related subsidies presently available to Alaskan communities. These subsidies depend on highly variable sources of funding. For example, the PCE funding levels for FY06 were paid at the reduced level of 81% for the first four months, 78% for the next three months, and at 100% for the remaining five months of the program year (AEA, 2007). Should any of these subsidies become less available in the future, this would greatly impact the feasibility of geothermal generation.

Carbon emissions are a good example of a market externality that has been quantitatively internalized – via taxes and other methods – by a number of studies. In our system, the impact of carbon taxes is minimal when compared to the factors described above. Benefits from greenhouse development and the costs of fuel spill costs have an even lesser impact on overall costs. Incidentally, those components contain the most uncertainty (monetary benefits of greenhouses assume commercialization of produce; and costs of fuel spill cleanup are highly variable).

This has profound implications for decision making in terms of choices of future energy supplies and investments. For example, most conventional cost-benefit analyses neglect market externalities such as carbon emissions, long-term benefits of renewable energy sources, and other factors. Hence, most CBAs fail in assessing the true costs and benefits of different energy supplies. Traditional methods of economic analysis were inherited from an era when the carrying capacities of the earth's natural systems were assumed to be large compared with the demands being made upon them. Today, this is no

longer the case, and new methods of economic analysis are badly needed in this new era of documented resource limitation and conservation need (Wright, 1998).

We quantified external benefits in terms of dollars. Profits, however, are probably not appropriate measures of some benefits of geothermal development to CAHSB communities, such as greenhouses. The most important benefits of geothermal development are probably those that cannot be quantified, such as energy security, food security, health improvements, and other benefits.

3.5.4. Energy, resilience, and vulnerability of the rural Alaskan SES

While resource sustainability is one aspect of energy sustainability in Alaska, there is a social aspect of sustainability that is difficult to measure. Assessing the sustainability of rural Alaskan communities is particularly problematic since they are not 'static' systems. The majority of residents in most of the rural Alaskan communities in this study are Alaska Natives groups who, prior to being forced to settle around schools, were essentially nomadic in pursuit of mobile resources – and in this sense are in constant transition. Perhaps a better way to frame the problem, then, is whether geothermal development would enhance the resilience of rural Alaskan communities.

Resilience is a property of linked social-ecological systems (SESs). Resilience theory recognizes the importance of changes in a system (Folke, 2006), and that systems can have multiple alternative states (Walker & Salt, 2006). The first step in a resilience-based approach to a social-ecological problem is to identify the boundaries of the system,

isolate its critical components, key variables, and cross-scale influences (Resilience Alliance, 2007).

Social-ecological systems (SES) in rural Alaska today are inextricably linked to energy consumption. Table 3.17 presents boundaries, critical components, key variables, and cross-scale influences for the rural Alaskan SES with respect to energy use.

Table 3.17. The rural Alaskan SES with respect to energy use.

System	**Boundaries**	**Critical components**	**Key variables**	**Cross-scale influences**
Communities near hot springs in Interior and Western Alaska	Spatial scale: regional (Interior AK, Western AK)	Energy use and flow (diesel fuel)	Fuel-related subsidies	State-local interactions
				Federal-local interactions
	Temporal scale: 20-30 years		Subsistence and cash economies	Ecosystem changes
				Demographic and cultural dimensions
				Global fuel markets and costs
				Food and energy supply/ availability
			Ecological impacts of fuel use (spills, emissions, etc.)	Ecosystem characteristics

After Resilience Alliance, 2007.

In resilience-based approaches to social-ecological problems, understanding the *interactions* between component pieces of a system is as important as identifying the components themselves (Resilience Alliance, 2007). Fig. 3.14 presents a model of the Alaskan SES with respect to energy, showing the interconnectedness between exogenous factors (such as global energy market forces), fast variables (such as the costs of fuel),

slow variables (local cash and subsistence economies), and outcomes (system health, sustainability and resilience) in a rural Alaskan social-ecological system.

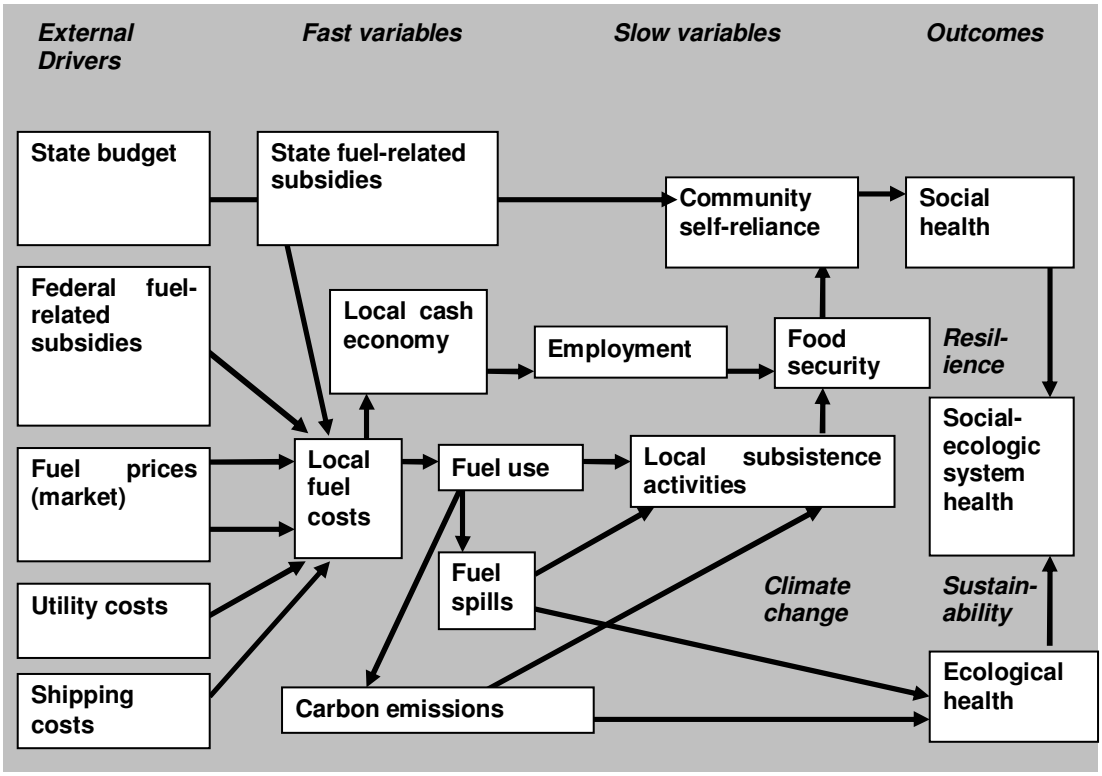

Figure 3.14. Model of the rural Alaskan SES with respect to energy. SES = social-ecologic system.

One of the central tenets of resilience theory is that only a few key variables control SES system behavior. Rapid change of any of the key variables in a system can trigger a threshold change, at which point the system will undergo a major transformation. The resilience of a system can be measured by its distance from a threshold. Reliable, affordable energy has been an intrinsic part of Alaskan SES's for a long time. But Alaskan SES's are in transition. Escalating fuel prices, rapid resource decline, changing climate, urban migration, and other rapid changes are creating

vulnerability in the present Alaskan rural SESs. This model highlights the fact that many of the system's vulnerabilities are related to the interconnectedness of exogenous drivers (federal budget, global energy market forces) and Alaska's socio-economic structure. By *vulnerability,* we mean the likelihood that the system will experience harm as a result of exposure to a hazard (Chapin et al., 2006).

One important threshold in this SES is some unknown tipping point wherein fuel prices are just too high for Alaskan residents to survive. Alaska's heavy reliance on fossil fuels makes the state highly vulnerable to price fluctuations as well as supply shortages and interruptions. Another is the amount of federal expenditures into the state of Alaska. Alaska currently receives more in federal expenditures per capita than any other state. The national economy is currently in a period of slow growth that is having several effects on the Alaska economy (Goldsmith, 2005).

Since many of the key variables within the rural Alaska SES are in a state of rapid change, it appears that the SES is very close to – if not squarely *at* – a threshold. Hence, resilience of most rural Alaskan SES's is low; meaning they are highly vulnerable.

Application of resilience theory can also be helpful for formulating a long-term plan to reduce the vulnerability of rural Alaskan SES's. Encouraging adaptation and diversity of capital and opportunities within an SES is one method for reducing vulnerability. Another way to reduce vulnerability is to manage so that thresholds are avoided. Policies emphasizing innovation/learning mechanisms, and redundancy within an SES would also enhance resilience (Walker and Salt, 2006). However, several political and economic factors are preventing these systems from generating such

qualities. One factor is the political lock-in trap of fuel-related subsidies. Another factor in the lock-in trap that discourages adaptation is related to the abundance of diesel generation infrastructure, subsidies, and expertise. Diesel generation is perceived as the 'tried-and-true' method for electricity and heat production in rural Alaska, and this drives many decisions about energy supply for rural communities. Lastly, fuel-related subsidies are highly political, and few Alaska legislators are willing to risk votes by proposing changes to the PCE or other programs. Hence, several policy recommendations can be drawn from the evaluation of community resilience in the context of energy consumption and supply.

3.5.4.1. Emphasizing the avoidance of thresholds by removing disincentives for alternative energy development

Management that emphasizes the avoidance of thresholds would suggest that rural Alaska SES's need to switch to alternate resource supplies, since diesel fuel use is pushing the system very close to a threshold. The state of Alaska could help communities avoid the threshold of energy crises by mandating or encouraging efficiency and conservation measures, and by removing (or at least reducing) existing disincentives to alternative energy development.

This study has identified two major disincentives towards geothermal energy development: 1) Lack of geothermal exploration data and/or data on geothermal resource capacity, which would reduce risk for prospective developers; 2) The availability of fuel-related subsides which encourage diesel utilization. Hence, modifying the PCE program

and other fuel-related subsides and encouraging data collection on Alaska's geothermal resources would help eliminate these disincentives. This would lead CAHSB communities away from a potentially catastrophic threshold. Modification of these subsidies would also save the state of Alaska a substantial deal of money (Fig. 3.15). For most communities these disincentives spent to maintain diesel power generation far exceed the cost of converting to geothermal power.

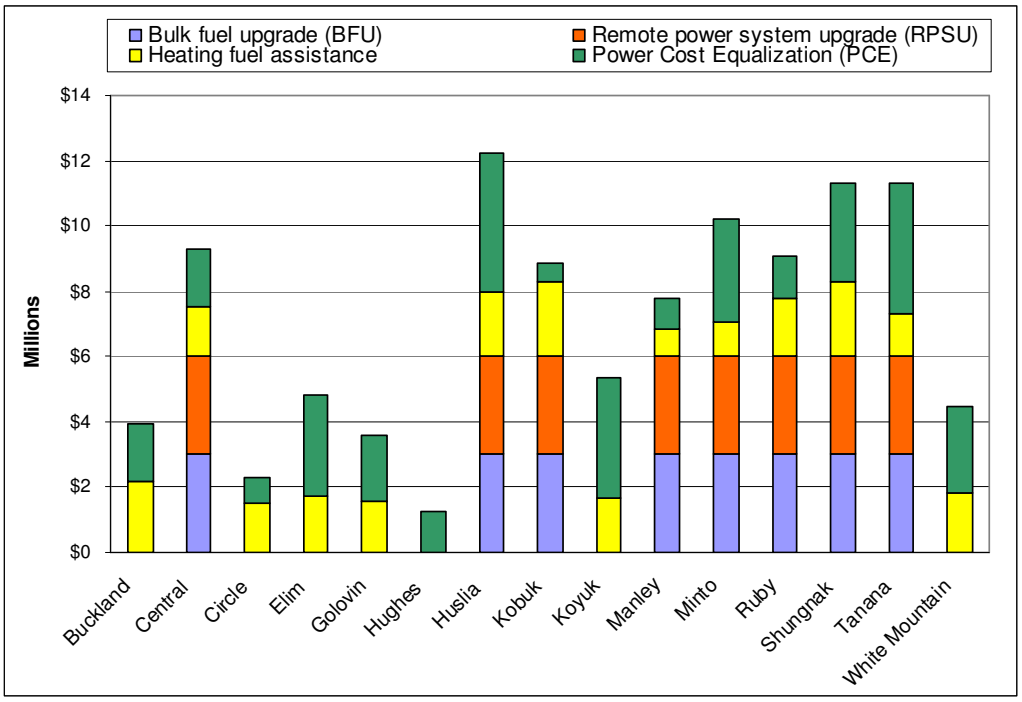

Figure 3.15. Total fuel-related subsidies CAHSB communities will receive through 2030, in $millions. For descriptions of the different subsidies, see section 3.3.

3.5.4.2. Encouraging adaptation and diversity of capital by mitigating high capital costs of geothermal development

The most important way that the state of Alaska could encourage adaptation and diversity of capital is by mitigating the high capital cost of renewable projects.

Renewable energy projects yield public benefits that will not be captured by private sector investors who need a relatively high return on their investments. Moreover, the State of Alaska – not private investors – will ultimately be responsible for the negative externalities associated with continued diesel use (carbon emissions, fuel spills, etc). To be consistent with similar development for the public good, geothermal development should be eligible for funding as capital improvement projects (CIPs). CIP's are projects for which the monetary benefits may not exceed the monetary costs – such as roads, power plant upgrades, and other basic infrastructure projects. That is, investments should be made by the state because these things contribute to the public good, not because they yield high financial returns.

One mechanism for implementing this approach could be considering transmission from renewable energy resources to users as CIP's. Transmission distances in Alaska are great, and transmission lines are often prohibitively expensive. Unfortunately, renewable energy sources are typically site-specific, so power generated by a renewable supply must often be transmitted a significant distance to users.

The other cost component specific to geothermal development in Alaska is the high cost of drilling. This too could be considered as CIP's, or at the very least cost-shared. Many federal and state cost-sharing programs have been implemented for geothermal drilling; in fact, eight out of the twelve geothermal developments of the past decade in the US were financed via cost-shares, some federally- and/or state-funded as much as 80% (Marshall Reed, personal comm.).

3.5.4.3. Facilitate innovation/learning and redundancy by encouraging combined heat-and-power projects.

This analysis shows that when geothermal power plants are combined with district heating and/or greenhouse installations, there is usually a significant monetary benefit to the community from avoided fuel costs and revenue from produce production. But perhaps more important than the monetary benefits of such projects is the non-quantifiable benefits they provide. These benefits include heating security and food security due to redundancy of supplies. Combined heat-and-power projects also facilitate innovation and learning, as the applications for geothermal heat are nearly endless. For example, this study examined greenhouses and district heating, but we did not consider uses such as aquaculture, industrial applications, and others.

3.6. Conclusions

The purpose of this study is to determine whether small-scale geothermal development is sustainable for remote communities in Central and Western Alaska. A sustainable energy resource is one which "meets the needs of present generations without compromising the needs of future generations" (Brundtland Commission, 1987). Results from this study indicate that geothermal energy – both in terms of electricity and heat – can *theoretically* be sustainably produced for community-scale (<1 MW) operations from hot springs in the CAHSB. However, our evaluation relies upon loosely constrained estimates and should not be used to replace true geoscientific exploration, which involves extensive drilling and testing of the geothermal reservoir.

In practice, it is unclear whether the energy production at Chena Hot Springs is sustainable. Examination of resource behavior since installation of the power plant reveals several potential problems that could indicate that the extraction of energy has influenced the natural process of energy circulation. These problems could possibly be mitigated with the following strategy: (1) Use of only "reservoir fluids" for power production; (2) Maximum reinjection into the "reservoir" (3) Continued levels of small output (<1 MW). Hence, sustainable production of geothermal energy from such systems would *pay careful attention* to resource dynamics by closely monitoring and evaluating reservoir pressure, fluid temperature, and reservoir permeability. Output power, well density, and injection strategy must be designed in a way that considers such resource constraints *first* before economic, engineering, and other constraints.

Whether geothermal resources can be a sustainable energy source for remote communities in the CAHSB is also a question of economics. The economic model presented in this paper includes standard cost components (capital costs, O&M, fuel prices, etc.) as well as monetized market externalities such as fuel-related subsidies, heating benefits, carbon emissions, the cost of fuel spills, and others. This model therefore captures the long-term costs and benefits of geothermal development better than conventional analyses. Our model shows that externalities are nearly as important as future fuel prices with respect to geothermal development.

The value of this study is in the framework it provides for thinking about geothermal energy development from a sustainability perspective. The actual numbers

presented are based on preliminary data and broad range of assumptions and *must* be refined before they can be the basis of any major decision.

Because the economic model presented in this paper captures the long-term costs and benefits better than conventional analyses, it could provide valuable guidance for decisions about energy supply. For example, the state of Alaska could expedite renewable development modifying such subsidies, by treating aspects of renewable energy projects, as capital improvement projects (which have certain near-term monetary costs but highly uncertain and hard-to-quantify future benefits), and other mechanisms. This is crucial, since continued diesel generation will have the ultimate effect of driving rural Alaska social-ecological systems into greater and greater states of vulnerability. Future studies should continue this work by identifying and quantifying more of the environmental, social, and political consequences of diesel dependence.

3.7. Acknowledgements

Thanks to Steve Colt, Gwen Holdmann, David Lockard, Mark Foster, Peter Crimp, Kat Keith, Chris Rose, Brian Yanity, Chris Nye, Bob Swenson, and Brent Petrie for feedback and contributions. Thanks to NSF IGERT / UAF RAP for funding.

3.8. References

Alaska Department of Environmental Conservation (ADEC), 2007. 10-Year Statewide Summary: Oil and Hazardous Substance Data, July 1, 1995 - June 30, 2005.

Alaska Department of Health and Social Services (ADHSS), 2007. Report by the State of Alaska Heating Assistance Program Division of Public Assistance Department of Health & Social Services.

Alaska Energy Authority, 2008. Statistical Report of the Power Cost Equalization Program, Fiscal Year 2007.

Axelsson, G., and Stefansson, V., 2003. Sustainable Management of Geothermal Resources. Proceedings of the 2002 Beijing International Geothermal Symposium: 667-678.

Barbier, E., 2002. Geothermal energy technology and current status: an overview. Renewable and Sustainable Energy Reviews, Vol. 6(1-2): 3-65.

Brundtland Commission, 1987. Our Common Future. UN General Assembly document No. A-42-27.

Carter, T.R. and La Rovere, E.R., 1994. Developing and applying scenarios. Intergovernmental Panel on Climate Change: Executive Summary Report.

Chapin, F.S., III, Torn, M.S., and Tateno, M., 1996. Principles of ecosystem sustainability. American Naturalist, Vol. 148: 1016-1037.

Chen, C., Wiser, R., and Bolinger, M., 2007. Weighing the Costs and Benefits of State Renewables Portfolio Standards: A Comparative Analysis of State-Level Policy Impact Projections. Lawrence Berkeley National Laboratory, Environmental Energy Technologies Division, Report # LBNL-61580.

Clemmer, S. L., Donovan, D., and Nogee, A., 2001. Clean Energy Blueprint: A Smarter National Energy Policy for Today and the Future, Phase I. Union of Concerned Scientists and Tellus Institute.

Crimp, P., Colt., S., and Foster, M., 2007. Renewable Power in Rural Alaska: Improved Opportunities for Economic Deployment. Proceedings of the 2007 Arctic Energy Summit, Institute of the North, Anchorage, AK.

Duffield, W. and Sass, J., 2003. Geothermal Energy – Clean Power from the Earth's Heat. USGS Circular 1249.

East, J., 1982. Preliminary Geothermal Investigations at Manley Hot Springs. University of Alaska Fairbanks, Geophysical Institute Report No. UAG R-290.

Etkin, D.S. 1999. Estimating Cleanup Costs for oil Spills. Oil Spill Intelligence Report, Cutter Information Corp. Proceedings of the 1999 International Oil Spill conference, Report No. 168.

Folke, C., 2006. Resilience: The Emergence of A Perspective for Social-Ecological Systems Analyses. Global Environmental Change, 16 (3): pp. 253-267.

Fournier, R.O., 1981. Application of water geochemistry to geothermal exploration and reservoir engineering. In: L. Rybach, and L.J.P. Muffler (Editors), Geothermal Systems: Principles and Case Histories. Wiley & Sons, New York, pp. 3-31.

Gawlik, K., and Kutcher, C., 2000. Investigation of the Opportunity for Small-Scale Geothermal Power Plants in the Western United States. Draft report to the National Renewable Energy Laboratory.

GeothermEx, 2004. Geothermal development costs. In: Kagel, A., 2006. A Handbook on the Externalities, Employment, and Economics of Geothermal Energy. Draft report by the Geothermal Energy Association for the USDOE.

Goldsmith, S., 1998. The Economic Significance of the Power Cost Equalization Program. Anchorage: Institute of Social and Economic Research, Report No. 947.

Goldsmith, S., 2005. Economic Projections for Alaska and the Southern Railbelt 2005-2030. Anchorage: Institute of Social and Economic Research, Report No. 1121.

Haley, S. and Saylor, B., 2007. Effects of Rising Utility Costs on Household Budgets, 2000-2006. Anchorage, AK, Institute of Social and Economic Research, Report No. 1182.

Hance, C.N., 2005. Geothermal Industry Employment: Survey Results & Analysis. US Department of Energy (USDOE), Geothermal Program Research document.

Hanano, M., Takahashi, M., Hirako, Y., Nakamura, H., Fuwa, S., and Itoi, R., 1990. Longevity evaluation for optimum development in a liquid dominated geothermal field; Effects of interaction of reservoir pressure and fluid temperature on steam production at operating conditions. Geothermics, 19 (2): pp. 199-212.

Hanano, M., 2003. Sustainable steam production in the Matsukawa geothermal field, Japan. Geothermics, 32, (3): 311-324.

Henley, R.W., Truesdell, A.H. and Barton, P.B.J., 1984. Chemical Geothermometers for Geothermal Exploration. Reviews in Economic Geology, 1: 31-43.

Jorgensen, J.G., 1990. Oil Age Eskimos. Berkeley, CA: University of California Press, 401 pp.

Kagel, A., 2006. A Handbook on the Externalities, Employment, and Economics of Geothermal Energy. Draft report by the Geothermal Energy Association for the USDOE.

Karlsson, J. 1982. Geothermal District Heating: The Iceland Experience. UNU Geothermal Training Program, University of Iceland, Reykjavik, Iceland.

Kiryukhin, A.V., and Yampolsky, V.A., 2004. Modeling study of the Pauzhetsky geothermal field, Kamchatka, Russia. Geothermics, 33 (4): 421-442.

Kolker, A., Newberry, R., Larsen, J., Layer, P. and Stepp, P., 2007. Geologic Setting of the Chena Hot Springs Geothermal System, Alaska., Stanford 32nd Workshop on Geothermal Reservoir Engineering, Stanford University, Palo Alto, CA.

Kolker, A., 2007. Geothermal Development in Alaska: A Plan. Unpublished report to the Alaska Energy Authority.

Kolker, A., Newberry, R., Larsen, J., and Layer, P. in press. Geologic Setting of Chena Hot Springs, Alaska: A Fault-Controlled Geothermal System Hosted by an Anomalously Radioactive Pluton. Journal of Volcanology and Geothermal Research.

Kolker, A., Newberry, R., and Kennedy, B., in preparation. The Central Alaskan Hot Springs Belt: Radiogenic Hydrothermal Convection Systems Driven by High Heat Producing Granites.

Lumb, J.T., 1981. Prospecting for Geothermal Resources. In: L. Rybach and L. J. P. Muffler (Editors), Geothermal Systems: Principles and Case Histories. Wiley & Sons, New York, pp. 32-65.

Mager, M., Holdmann, G., and Reynolds, D., 2008. Economics of Greenhouse Production in Alaska – Using the Greenhouse at Chena Hot Springs Resort as a Model. Unpublished report to Chena Hot Springs Resort.

Miller, T.P., Barnes, I. and Patton, W.W., 1973. Geologic Setting and Chemical Characteristics of Hot Springs in Central and Western Alaska. USGS Open-file Report No. 575.

Motyka, R.J., Liss, S.A., Nye, C.J., Moorman, M.A., 1993. Geothermal Resources of the Aleutian Arc. Alaska Division of Geological & Geophysical Surveys, Professional Paper 114, 1:1,000,000 map, 4 sheets.

Motyka , R.J., Moorman, M.A., Liss, S.A , 1983. Geothermal resources of Alaska. National Oceanic and Atmospheric Administration, pp. 1:2,500,000 scale map by NOAA National Geophysical Data Center, data compiled by Alaska Division of Geological & Geophysysical Surveys.

Nicholson, K., 1993. Geothermal Fluids: Chemistry and Exploration Techniques. Springer-Verlag, New York, 223p.

Nordhaus, W., 2006. A Review of the Stern Review on the Economics of Climate. Journal of Economic Literature, 45 (3): 686-702.

Ormat, 2006. Geothermal development costs. In: Kagel, A., 2006. A Handbook on the Externalities, Employment, and Economics of Geothermal Energy. Draft report by the Geothermal Energy Association for the USDOE.

Rafferty, K., 1998. Selected cost considerations for geothermal district heating in existing single-family residential areas. Proceedings of the Geothermal Resources Council Annual meeting, 20: 886 pp.

Renewable Energy Alaska Project (REAP), 2006. Renewable Energy Alaska Project Spring Newsletter, April 2006.

Resilience Alliance, 2007. Assessing and managing resilience in social-ecological systems: A practitioner's workbook, Vol. 1. Island Press, Washington, D.C.

Rogner, H. H., 2005. Energy Resources and Technology Options. In: World Energy Assessment: Energy and the Challenge of Sustainability. New York: United Nations Development Programme Report.

Rybach, L., 1981. Geothermal Systems, Conductive Heat Flow, Geothermal Anomalies. In: L. Rybach and L. J. P. Muffler (Editors), Geothermal Systems: Principles and Case Histories. Wiley & Sons, New York, pp. 3-31.

Rybach, L., 2003. Geothermal energy: sustainability and the environment. Geothermics, 32 (4-6): 463-470.

Serpen, U., 2004. Hydrogeological investigations on Balçova geothermal system in Turkey. Geothermics, 33 (3): 309-335.

Sison-Lebrilla, E., and Tiangco, V., 2005. Geothermal Strategic Value Analysis. Draft report to the California Energy Commission.

Stapleton, R. 2008. Alaska villages run out of heating fuel; resupplying difficult. AK Journal of Commerce, March 16, available online at: http://www.alaskajournal.com/stories/031608/hom_20080316046.shtml

Stefansson, V., 2000. The Renewability of Geothermal Energy, Proceedings World Geothermal Congress, Kyushu, Japan.

U.S. Department of Energy (USDOE), 2005. Buried Treasure: The Environmental, Economic, and Employment Benefits of Geothermal Energy.

U.S. Department of Energy, Energy Information Administration (EIA), 2007. Annual Energy Outlook 2007 With Projections to 2030. Available on-line at: http://www.eia.doe.gov/oiaf/aeo/pdf/0383(2007).pdf. Report #:DOE/EIA-0383(2007).

United States Senate, 2007. Low Carbon Economy Act of 2007. Available on-line at: http://energy.senate.gov/public/_files/END07842_xml1.pdf.

Walker, B., Salt, D., 2006. Resilience Thinking, Sustaining Ecosystems and People in a Changing World. Island Press, Washington, DC.

Wescott, E., and Turner, D., 1981. A Geological and Geophysical Study of the Chena Hot Springs Geothermal Area, Alaska. University of Alaska Fairbanks, Geophysical Institute Report No. UAG-R-268.

Wiser, R., and Bolinger, M., 2004. An Overview of Alternative Fossil Price and Carbon Regulation Scenarios. Report to the U.S. Department of Energy, Lawrence Berkeley National Laboratory.

Wisian, K.W., Blackwell, D.D. and Richards, M., 2001. Correlation of heat loss and total energy production for geothermal systems. Geothermal Resources Council Transactions, 25: 332-335.

Wright, P. M., 1998. The sustainability of production from geothermal resources, Oregon Institute of Technology Geo-Heat Center Bulletin, 19(2): 9-12.

Conclusions

No discussion about geothermal development in Alaska can begin without adequate examination of the resource potential. Unfortunately, there is a noticeable lack of exploration data for most of Alaska's geothermal resources – and often what little data exists is not publicly available. In the absence of exploration data, there is substantial uncertainty with respect to the feasibility and sustainability of geothermal energy production from most of Alaska's resources. This means that investment in Alaska's geothermal energy resources may carry considerable risk.

This study examined the geologic setting of Chena Hot Springs (CHS) and the geothermal resource characteristics, both in its natural state and in its produced state since energy extraction began in 2006. Results from that study showed that thermal fluids have circulated primarily within an anomalously radioactive granite that could be responsible for the heat anomaly driving geothermal activity. Subvertical fractures and fault planes provide the permeability pathways for circulating waters, but also allows substantial mixing between upwelling thermal sources and cold groundwater in the near-surface. The power production at CHS utilizes mixed fluids at <80 °C. The temperature of the geothermal "reservoir" fluids is probably ~100 °C, but could be as high as ~120 °C. Geothermal energy production from these mixed fluids appears to have caused a decline in temperatures and pressures in the system.

The rest of the hot springs in the CAHSB are geologically analogous to CHS, and radiogenic sources appear to be a feasible heat mechanism for driving the geothermal activity in the CAHSB. If radiogenic heat is driving the geothermal activity in the

CAHSB, that means that these hydrothermal systems must be very localized and small-scale. In that sense, the CAHSB low-temperature resource is likely to behave quite differently than most hydrothermal systems exploited for energy worldwide. For example, it may be that low-temperature systems such as these are inherently more dynamic, as seen in the behavior of well fluids at CHS.

In the absence of exploration data, we used available data on surface fluid characteristics to estimate the power output capacity of CAHSB geothermal resources. Our preliminary evaluation implies that several of the hot springs near CAHSB communities can in fact be utilized for power production and direct use similar to the development at Chena Hot Springs. However, resources must be managed properly in order to ensure sustainability. This may be accomplished by following these general guidelines: (1) Users should produce power at a scale of <1MWe output; (2) the "reservoir" fluids – that is, the hottest fluids in the system – should be used for power production, as opposed to the mixed fluids ones being used for power production at CHS; (3) the system should be engineered to obtain maximum reinjection of fluids into the deep system; (4) careful monitoring of system pressures and temperatures should occur systematically and over a long period of time. In sum, power production be designed in a way that considers resource constraints *first* before economic, engineering, and other constraints.

Our cost comparison shows that internalizing several factors that are typically treated as externalities has profound impact on the overall cost analysis of geothermal development. The greatest influence is the choice of future fuel price projections. The

next most important cost component is whether direct use of the geothermal fluids for heating purposes is included in a potential installation, followed by the financial incentives available to mitigate the high capital costs of geothermal projects. The next most important cost components are the fuel-related subsidies presently available to Alaskan communities. The impact of potential carbon taxes, greenhouse development benefits, and the costs of fuel spills are relatively minimal when compared to the factors described above. This has profound implications for decision making in terms of choices of future energy supplies and investments.

Diesel fuel use is pushing the Alaskan social-ecological system (SES) very close to a threshold in the context of escalating fuel prices, rapid subsistence resource decline, changing climate, urban migration, and other changes. This is creating vulnerability in the Alaskan SES. Management that seeks to reduce vulnerability of the system would avoid thresholds by encouraging a switch to renewable energy supplies. This would involve: 1) mitigating the high capital cost of renewable projects; 2) removing (or at least reducing) existing disincentives to alternative energy development, such as fuel-related subsides which encourage diesel utilization, and 3) facilitating data collection on Alaska's renewable resources, including geothermal.

In sum, the sustainability of geothermal production from CAHSB resources has not been proven. Immediate data collection on more geothermal resources in the CAHSB would minimize the risk to the state, private investors, and other entities presently weighing energy investment decisions. Future research activities should aim to (1) identify the subsurface location of geothermal "reservoir" fluids in CAHSB systems,

ultimately by drilling; (2) evaluate the reservoir fluids in terms of available volume, circulation patterns, and other factors vital to determining resource capacity. Another important research direction would be to investigate less expensive ways of transmitting electric power from geothermal resources to users, as that would greatly reduce costs of geothermal development.